Poznan University of Medical Sciences

Magdalena Niestrata-Ortiz

Evaluation of the retinal changes in children with type 1 diabetes mellitus by means of optical coherence tomography angiography.

PhD Thesis

Supervisor: MD PhD Marcin Stopa

Poznań, 2018

AKNOWLEDGEMENTS

Many thanks to my supervisor, Marcin Stopa, for his continued support, guidance and inspiration for this work.

Thanks to my family for their encouragement, unconditional support and understanding.

DEDICATION

Mojej ukochanej siostrze Martynie.

TABLE OF CONTENTS

ABBREVIATIONS

AAO	American Academy of Ophthalmology
AMD	Age-related macular degeneration
BDR	Background diabetic retinopathy
BG	Blood glucose measurement
BM	Bruch's membrane
BRB	Blood-retinal barrier
CI	Confidence interval
CMO	Cystoid macular oedema
D	Dioptre
DCCT	Diabetes Control and Complications Trial
DCP	Deep capillary plexus
DED	Diabetic eye disease
DM	Diabetes mellitus
DMO	Diabetic macular oedema
DR	Diabetic retinopathy
DRS	Diabetic Retinopathy Study
ETDRS	Early Treatment Diabetic Retinopathy Study
FAZ	Foveal avascular zone
FD-OCT	Fourier-domain optical coherence tomography
FFA	Fundus fluorescein angiography
GCC	Ganglion cell complex
HbA1c	Glycated haemoglobin
ICG	Indocyanine green
ILM	The inner limiting membrane
IPL	Inner plexiform layer
IRMA	Intraretinal microvascular abnormality
NFZ	Narodowy Fundusz Zdrowia
NPDR	Non-proliferative diabetic retionopathy
NVD	Neovascularisation of the disc
NVE	Neovascularisation elsewhere

NVG	Neovascular glaucoma
NVI	Neovascularisation of iris
OCT	Optical coherence tomography
OCT-A	Optical coherence tomography angiography
OPL	Outer plexiform layer
PDR	Proliferative diabetic retinopathy
PED	Pigment epithelium detachment
PPDR	Preproliferative diabetic retinopathy
PRP	Panretinal photocoagulation
Q25	25^{th} Quartile
Q75	75^{th} Quartile
ROS	Reactive oxygen species
RPE	Retinal pigment epithelium
RPE	Retinal pigment epithelium
SCP	Superficial capillary plexus
SD	Standard deviation
SD-OCT	Spectral-domain optical coherence tomography
SNR	Signal to noise ratio
SSADA	Split spectrum amplitude decorrelation angiography
SS-OCT	Swept-source optical coherence tomography
TD-OCT	Time-domain optical coherence tomography
TRP	Targeted retinal photocoagulation
UKPDS	UK Prospective Diabetes Study
V.	Version
VA	Visual acuity
VEGF	Vascular endothelial growth factor

1. INTRODUCTION

1.1. DIABETIC EYE DISEASE

Diabetes mellitus (DM) is a common disease estimated to affect 285 million people or 6.4% of the world's population as of 2010. (1) This is expected to rise to 438 million people or 7.8% of the world's population by 2030. (1) In Poland, based on the data from the National Health Fund (Narodowy Fundusz Zdrowia, NFZ) and Coalition-Diabetes Organisation, approximately 3.5 million people are affected, out of which ⅓, i.e. over a million, remain undiagnosed. (2)

Two main forms of diabetes mellitus are recognized. Type 1 (T1DM), also known as juvenile-onset or insulin-dependent diabetes, is characterized by cellular-mediated autoimmune destruction of the beta-cells in the pancreas leading to severe insulin deficiency. Type 2 diabetes mellitus (T2DM), also referred to as adult-onset or noninsulin-dependent diabetes, comprises a range of pathologies from insulin resistance with relative insulin deficiency to an insulin secretory defect combined with insulin resistance. The condition can lead to numerous eye complications termed diabetic eye disease (DED). These include:

Vascular complications:

- Diabetic retinopathy and maculopathy
- Rubeosis iridis
- Neovascular glaucoma (NVG)
- Conjunctival microangiopathy

Other complications:

- Complications of proliferative diabetic retinopathy including vitreous haemorrhage, retinal fibrosis and tractional retinal detachment
- Unstable refraction
- Recurrent styes
- Xanthelasma
- Accelerated senile cataract
- Acute-onset cataract

- Ocular motor nerve palsies
- Reduced corneal sensitivity
- Papillopathy
- Pupillary light-near dissociation
- Wolfram Syndrome (progressive optic atrophy and multiple neurological and systemic abnormalities)
- Rhino-orbital mucormycosis. (3,4)

1.2. DIABETIC RETINOPATHY

1.2.1. Epidemiology

Diabetic retinopathy (DR), the most common microvascular complication of diabetes, is the leading cause of blindness in working-age adults in the developed countries. (5,6) According to the World Health Organisation (WHO) report from 2015 diabetic retinopathy is the cause of visual impairment for 4.2 million people worldwide. (7) The reported prevalence of DR varies considerably between studies and is at approximately 40%. (3,8) It is more common in type 1 than in type 2 diabetes with sight-threatening disease occurring in up to 10%. (3) The prevalence of DR increases with the duration of diabetes. (9) After 20 years most of type 1 and more than 60% of type 2 diabetics have some degree of retinopathy. (10) Proliferative diabetic retinopathy (PDR) affects 5-10% of diabetics. Type 1 diabetics are at a particularly high risk, with an incidence of up to 90% at 30 years after the disease onset. (3) In the United Kingdom DR is responsible for 12% of registrable blindness in people aged 16 to 64 years. (11) DR is also a significant economic burden for today's societies. In Poland the medical costs of retinopathy were estimated at 780 million PLN per year as per 2002, (12) highlighting the importance of optimal screening and primary prevention.

1.2.2. Pathophysiology

Diabetic retinopathy is a microangiopathy primarily affecting pre-capillary arterioles, capillaries and post-capillary venules, which are particularly vulnerable to damage from elevated glucose levels. The principle features are microvascular occlusion and leakage. Direct hyperglycaemic effect on retinal cells has also been implicated. (3,13)

The development of DR is associated with sustained metabolic abnormalities caused by hyperglycaemia and increased levels of inflammatory cytokines. The resulting systemic inflammation leads to haemodynamic changes, blood-retinal barrier (BRB) damage, the leakage of retinal microvessels and oedema, a gradual thickening of the retinal vascular basement membrane, and a loss of pericytes. These changes result in retinal ischaemia and the release of proinflammatory and proangiogenic factors, inducing further inflammation and angiogenesis. (14)

The leakage and oedema occur as a consequence of the hyperglycaemia effect on the tight junctions between retinal pigment epithelium (RPE) constituting the blood-retinal barrier which, under homeostasis, prevents the abnormal effusion from the choroid to the retina. Hyperglycaemia leads to increased glycolysis resulting in elevated levels of methylglyoxal, which in turn activates matrix metalloproteinases. They induce proteolytic degradation of tight junction proteins such as occludin, thereby facilitating an increase in vascular permeability. As a result, fluid leakage increases in the surrounding retinal tissue, leading to macular oedema and visual loss. (15) Ischaemic maculopathy, on the other hand, is characterised by capillary closure and presence of avascular zones. It may result in damage to ganglion cell complex (GCC), which consists of nerve fibre layer, ganglion cell layer and inner plexiform layer and is supplied by the superficial capillary plexus. GCC thickness is reduced in non-perfused areas. The capillary closure appears as widening of the foveal avascular zone (FAZ) on fundus fluorescent angiography (FFA) or OCT Angiography (OCTA). Increased FAZ area correlates with reduction of ganglion cells and is an indicator of macular ischaemia. (16)

Furthermore, the oxidative stress appears to play a crucial role in the pathogenesis of DR. The retina is susceptible to oxidative stress due to its hypermetabolic state. (13) Abnormal metabolism caused by hyperglycaemia can lead to overproduction of free radicals such as hydroxyl and superoxide radicals, which are known as reactive oxygen species (ROS). (17) The accumulation of ROS induces oxidative stress, which damages the tissue inside and adjacent to retinal vessels, ultimately resulting in DR. The levels of oxidative stress markers correspond to the severity of DR. (18) The damage caused by oxidative stress persists for a considerable time, despite the blood glucose concentration returning to a normal level. (14)

Many angiogenic stimulators and inhibitors have also been implicated in the disease process, including the vascular endothelial growth factor (VEGF). The main function VEGF-A is regulation of vascular permeability. However, it is also involved in angiogenesis, vasculogenesis and endothelial

cell growth under normal and pathological conditions. (19) Pharmacological inhibition of VEGF-A has been shown to prevent angiogenesis and vascular leakage (20) and is currently widely used as treatment for diabetic macular oedema.

The effect of the described processes can be visualised clinically on slit lamp biomicroscopy (**Figure 1**) or using imaging modalities such as FFA and OCTA:

- Microvascular occlusion occurs due to loss of pericytes, thickening of the basement membrane, damage to and proliferation of endothelial cells, deformation of red blood cells and augmented platelet aggregation. The resulting non-perfusion and hypoxia lead to formation of arteriovenous shunts and neovascularisation which can be identified on clinical examination. Similarly, intraretinal microvascular abnormalities (IRMAs) are shunt vessels growing from the venous side of the capillary bed within an area of arteriolar non-perfusion.
- Retinal ischaemia leads to microinfarcts in the nerve fibre layer, which appear clinically as cotton wool spots.
- Microvascular leakage occurring as a result of inner blood-retinal barrier leads to formation of several clinical diabetic retinopathy hallmarks such as microaneurisms, haemorrhages, exudates and oedema:
    - Microaneurisms, clinically appearing as red dots, are out-pouchings of the capillary wall formed by weakening of the capillary walls due to necrosis of the pericytes.
    - Hard exudates, clinically seen as yellow well-circumscribed deposits, are histologically eosinophilic masses containing macrophages with lipid in the cytoplasm. They are formed as under-perfusion of the vascular bed and damage to the endothelium of the deep capillaries lead to plasma leakage into the outer plexiform layer of the retina.
    - Haemorrhages are the result of breakdown of vessel walls leading to leakage of red blood cells. They can take the form of flame haemorrhages in the nerve fibre layer, dot haemorrhages in the outer plexiform layer and blot haemorrhages representing bleeding from capillaries with tracking between the photoreceptors and the retinal pigment epithelium. (16,21)

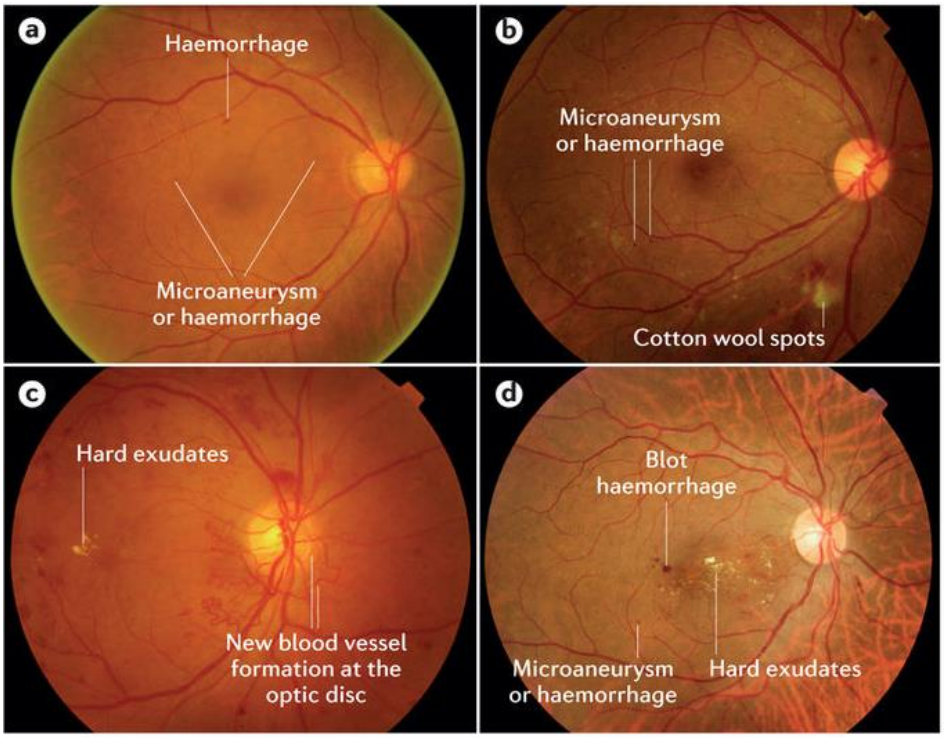

Figure 1. *Clinical signs of diabetic retinopathy found on slitlamp biomicroscopy. Adapted from Wong et al (2016). (22)*

1.2.3. Classification

Diabetic retinopathy can be classified into non-proliferative and proliferative stages, with sub-categories depending on the severity. The two main classifications are the American Academy of Ophthalmology (23) and Early Treatment Diabetic Retinopathy Study (ETDRS – the modified Airlie House classification), (3) widely used internationally (**Tables 1&2**).

Table 1. *Diabetic retinopathy classification as per American Academy of Ophthalmology (AAO) (23)*

Disease Severity Level		**Signs**
No Diabetic Retinopathy		-
Nonproliferative Diabetic Retinopathy (NPDR)	Mild	Microaneurisms
	Moderate	More changes than only microaneurisms, but less than in severe NPDR
	Severe	Any of the following: extensive (>20) intraretinal haemorrhages in each of 4 quadrants, definite venous beading in 2+ quadrants, prominent IRMA in 1+ quadrant, and no signs of proliferative DR.
Proliferative Diabetic Retinopathy (PDR)		At least one of the following: neovascularisation, vitreous or preretinal haemorrhage

Table 2. *Diabetic retinopathy classification as per Early Treatment Diabetic Retinopathy Study (ETDRS). (3)*

Category		**Signs**	**Management and Prognosis**
No DR		-	Review in 12 months.
Non-proliferative DR	Very mild NPDR	Microaneurisms only	Review most patients in 12 months.
	Mild NPDR	Any or all of: microaneurisms, retinal haemorrhages, exudates, cotton wool spots, up to the level of moderate NPDR. No significant beading or IRMAs.	Review range 6-12 months, depending on severity of signs, stability, systemic factors, and patient's personal circumstances.
	Moderate NPDR	Severe retinal haemorrhages (approximately 20 medium-large per quadrant) in 1-3 quadrant or mild IRMA, significant venous beading in no more than 1 quadrant, cotton wool spots commonly present	Review in approximately 6 months. PDR in up to 26%, high-risk PDR in up to 8% within a year.
	Severe NPDR	The 4-2-1 rule; one or more of: severe haemorrhages in all 4 quadrants, significant venous beading in 2 or more quadrants, moderate IRMA in 1 or more quadrants	Review in 4 months. PDR in up to 50%, high-risk PDR in up to 15% within a year.
Proliferative DR	Mild-moderate PDR	New vessels on the disc (NVD) or elsewhere (NVE), but extent insufficient to meet the high-risk criteria	Strongly consider treatment taking into account the severity of signs, systemic factors, stability and patient's personal circumstances. If not treated review in up to 2 months.
	High-risk PDR	NVD of at least ⅓ disc area, any NVD with vitreous haemorrhage, NVE greater than ½ disc area with vitreous haemorrhage	Treatment advised – should be performed immediately when possible, and certainly same day if symptomatic presentation with good retinal view.
Advanced diabetic eye disease		Complications of PDR including persistent vitreous haemorrhage, tractional retinal detachment and neovascular glaucoma	As per presentation.

The following descriptive categories are widely used in clinical practice:

- **Background diabetic retinopathy** (**BDR**), where the earliest changes identifiable on clinical examination are microaneurisms, followed by dot and blot retinal haemorrhages and exudates.
- **Preproliferative diabetic retionopathy** (**PPDR**) occurs due to capillary nonperfusion and carries a heightened risk of progression to proliferative DR. PPDR manifests with cotton wool spots, venous changes such as venous beading, deep retinal haemorrhages and IRMAs.
- **Proliferative diabetic retinopathy** (**PDR**) occurs when further retinal ischaemia leads to growth of new blood vessels on the surface of the optic disc - neovascularisation of the disc

(NVD) - and retina - neovascularisation elsewhere (NVE) as well as neovascularisation of the iris (NVI), also known as rubeosis iridis, which carries a high risk of progression to neovascular glaucoma.

- **Advanced diabetic eye disease** is characterised by the complications of proliferative diabetic retinopathy including significant persistent vitreous haemorrhage, retinal fibrosis, tractional retinal detachment and neovascular glaucoma.
- **Diabetic macular oedema** (**DMO**) can occur at any stage of the disease and results from increased vascular permeability in the macular area. DMO is currently the main cause of vision loss in diabetics. The fluid is initially located between the outer plexiform and inner nuclear layers of the retina. Subsequently, it can involve the inner plexiform and nerve fibre layers and eventually the entire thickness of the retina becomes oedematous. Chronic DMO increases the risk of vitroretinal complications, including formation of an epiretinal membrane and vitreo-macular traction. When the fovea assumes a cystoid appearance due to the fluid accumulation, it is termed **cystoid macular oedema** (**CMO**). CMO can be diagnosed by optical coherence tomography or fundus fluorescent angiography. (3,10,16) DMO can be classified into the following subcategories:
    - **Focal oedema -** characterised by well-circumscribed retinal leakage associated with a complete or incomplete ring of perifoveal hard exudates. FFA shows good macular perfusion and focal hyperfluorescence localising the leakage.
    - **Diffuse oedema** - widespread retinal thickening with severe oedema is present. FFA demonstrates diffuse spotty hyperfluorescence corresponding to microaneurisms and late widespread hyperfluorescence due to leakage.
    - **Ischaemic maculopathy** - typically decreased vision acuity is accompanied by a relatively normal clinical appearance of the macula. It is caused by capillary occlusion and is characterised by the presence of avascular zones on FFA or OCTA.
    - **Mixed maculopathy** - displays features of oedema and ischaemia.
    - **Clinically significant macular oedema** - macular oedema fulfilling any of the following criteria: retina thickening at or within 500 µm of the centre of the macula; hard exudates at or within 500 µm of the centre of the macula associated with thickening of the adjacent macular; one or more zones of retinal

thickening of at least one disc area diameter, any part of which is within one disc diameter of the centre of the macula. (16,21)

1.2.4. Risk factors

The strongest risk factor influencing the development of diabetic retinopathy is the duration of diabetes. (8) In patients diagnosed before the age of 30 years, the incidence of DR is 50% after 10 years and 90% after 30 years. (3) The modifiable risk factors include poor glycaemic control, hypertension and dyslipidaemia (8,10). Optimal glycaemic control has been shown to reduce the incidence and the progression rate of diabetic retinopathy, whereas raised glycated haemoglobin (HbA1c) is associated with an increased risk of proliferative diabetic retinopathy. According to the Diabetes Control and Complications Trial (DCCT) for Type 1 diabetes mellitus, each 1% decrease in HbA1c reduces the risk of retinopathy by 39%. (24) This effect was shown to persist long after the period of rigorous glycaemic control. (25) Similarly, in type 2 diabetes, the UK Prospective Diabetes Study (UKPDS) reported that each 10% decrease in HbA1c reduces the risk of microvascular events, including retinopathy, by 25%. (26)

With regards to blood pressure control, another UKPDS showed that in hypertensive diabetics each 10 mmHg decrease in systolic blood pressure reduces the risk of microvascular complications by 13%, independent of glycaemic control. (27) Tight blood pressure control appears to be particularly beneficial in Type 2 diabetics with maculopathy. (3)

The benefit of improving the lipid profile on the risk of developing diabetic retinopathy was demonstrated by the ACCORD Eye study which showed that a combination lipid therapy with fenofibrate and simvastatin reduced the progression of retinopathy by approximately one third, from 10.2% to 6.5% over 4 years, compared with simvastatin treatment alone. (28)

Other identified risk factors include renal impairment, pregnancy, genetic predisposition, smoking, cataract surgery, obesity an anaemia. (3,29)

1.2.5. Natural history and prognosis

According to natural history studies from the 1960s, at least half of people with proliferative diabetic retinopathy progress to visual acuity of less than 6/60 (20/200), as per Snellen chart, within 3 to 5 years. (30-32) After 4 years of follow-up, the rate of progression to visual acuity of less than 6/60 (20/200) in the better eye was reported as 1.5%, 2.7% and 3.2% in patients with type 1 diabetes, non-insulin-dependent type 2 diabetes and insulin-dependent type 2 diabetes, respectively. (9)

1.2.6. Diabetic retinopathy in children

The manifestations of diabetic retinopathy in children are consistent with those found in adults. Similarly, long duration of diabetes and poor glycaemic control are the most significant risk factors for developing DR. (33,34) However, differences have been reported regarding the prevalence, onset, and progression rate.

The risk of developing DR before puberty is very low. (16,21) De Abreu and colleagues (1994) found that the blood-retinal barrier of diabetic children remains stable until puberty, achieving maximal efficiency and protection, after which a progressive decline begins. (35) This is in agreement with the study by Scanlon and colleagues (2016) who examined the data for 2125 children with diabetes in United Kingdom screened for the first time at the age 12 or 13 years and found a low prevalence rate of referable DR. In those diagnosed with diabetes at 2 years of age or less, 20% and 11% were found to have retinopathy in one or both eyes, respectively. This decreased to 8% and 2% in patients diagnosed between 2 and 12 years. (36) Salardi's et al (2012) multicentre study found that if diabetes is diagnosed in infants or toddlers and the prepubertal duration of diabetes is very long, the patients appear to be protected against DR. This disappears if longterm metabolic control is suboptimal. Conversely, diabetes onset at puberty was associated with a higher risk of developing DR and appeared less dependent on metabolic control. (37) The Downie et al (2011) study found a gradual reduction in prevalence of diabetic retinopathy in adolescents with Type 1 diabetes from 1990s to 2009, associated with improved glycaemic control achieved by optimal insulin therapy in form of multiple daily injections or a continuous subcutaneous insulin infusion. (38) The beneficial effect of good glycaemic control was also highlighted by the White et al (2017) study, which showed that severe diabetic retinopathy was associated with higher paediatric HbA1c levels, independent of glycaemic control during adulthood. (39) In addition, Virk and colleagues (2016) showed that greater HbA1c variability predicted retinopathy and advocated that minimizing long term fluctuations in glycaemia may provide additional protection against the development of microvascular complications such as DR. (40)

1.2.7. Imaging in diabetic retinopathy

While the primary method for evaluating diabetic retinopathy involves clinical examination by direct and indirect ophthalmoscopy, various imaging modalities exist and are valuable tools for screening, diagnosis, follow-up and management. The principal imaging techniques used include colour fundus

photography, fundus fluorescein angiography (FFA), B-scan ultrasonography, and optical coherence tomography (OCT), including OCT- Angiography (OCTA).

1.2.7.1. Colour fundus photography

Colour fundus photographs are currently taken as digital images to enable easy and immediate review of the photographs, image magnification and enhancement. They are widely used for screening, documentation, monitoring of progression and counselling patients. There are different types of fundus photography including standard, wide field, and stereoscopic imaging.

Standard macular fundus photography captures 30° of the posterior pole of the eye, which includes the macula and the optic nerve. (41) This type of imaging is easily available and widely used for documentation. Hard exudates and haemorrhages are readily visible. However, fine detail is frequently not apparent and macular oedema cannot be appreciated. In addition, media opacity can significantly affect the quality of the images.

Widefield fundus photography allows a 75° field of view, enabling visualisation of the peripheral retina. Newer cameras can capture up to a 200° field of view, imaging 80% of the total retinal surface. (42) Their limitations include image distortion, eyelash artefacts, false colour representation and high costs.

Stereoscopic fundus photography allows fusion of two photographically created images, one for each eye, providing a three-dimensional examination. However, its utility in clinical practice is debatable as stereoscopic photographs can take more time to interpret and a comparative study of stereoscopic and monoscopic fundus photography found no difference in the ability of a trained ophthalmologist to evaluate the severity of DR using Early Treatment of Diabetic Retinopathy Study (ETDRS) criteria. (43) Hence, standard fundus photography remains the modality of choice. (44)

1.2.7.2. Ultrasonography

B-scan ultrasonography is a two-dimensional imaging technique which constructs images by using sound waves. They are transmitted from a transducer to the target tissue at a high frequency and return to the transducer at varying time intervals and amplitudes. Higher amplitudes correspond to higher tissue densities and appear hyperechoic, i.e. whiter, whereas lower amplitudes signify lower tissue density and appear hypoechoic, i.e. darker. (45) B-scan can be of use in proliferative diabetic retinopathy to demonstrate a retinal detachment, vitreous haemorrhage or posterior vitreous detachment when ocular media is not clear.

1.2.7.3. Fundus Fluorescein Angiography

The first fundus fluorescein angiography (FFA) was performed in 1960 by Novotny and Alvis and has since become the gold-standard imaging method for imaging the retinal vasculature network and for estimating foveal avascular zone (FAZ) in many retinovascular diseases. (46)

During the examination a contrast medium, sodium fluorescein, is injected intravenously. Most of the dye is protein-bound in the blood stream, but 20% remains unbound. The dye travels rapidly through the circulation and when it reaches the retinal and choroidal vasculature, black and white fundus photographs are taken. It is a fluorescent mineral-based dye which is excited by blue light (~480 nm) emits, or fluoresces, yellow-green light (~525 nm). FFA is performed using a fundus camera that is outfitted with excitation and barrier filters. White light passes through a blue excitation filter and subsequently it is absorbed by unbound fluorescein molecules in the eye circulation, which emit yellow-green light. The barrier filter in the camera blocks other wavelengths, and captures solely the light emitted by the fluorescein molecules. (47) The dye appears in the retinal arteries approximately 12 seconds after the injection. Over the next two to five seconds it travels through the capillaries and fills the retinal veins. Ten minutes after the injection, the dye has mostly evacuated from the eye, having stained the optic nerve head. Widefield FFA is also available, which allows improved imaging of the peripheral retina, including detection of peripheral neovascularization and evaluation of the extent of retinal nonperfusion. (48)

FFA is widely used for the diagnosis and follow-up of diabetic retinopathy. It enables to differentiate between dot haemorrhages and non-thrombosed microaneurisms. In the early frames microaneurisms show as small hyperfluorescent dots, typically more numerous than clinically visible. Late frames show diffuse hyperfluorescence due to leakage. Conversely, blot and dot haemorrhages are hypofluorescent. Areas of non-perfusion appear as homogeneous hypofluorescent or dark patches bordered by occluded blood vessels. Only large and dense exudates are visible on FFA as despite background choroidal fluorescence being masked, retinal capillary fluorescence is mostly preserved overlying the lesions. FFA can aid the diagnosis of ischaemic diabetic maculopathy, whereby the macula can look relatively normal on clinical examination. In those cases FFA shows capillary non-perfusion at the fovea, appearing as enlarged foveal avascular zone (FAZ), and frequently other areas of capillary nonperfusion at the posterior pole and periphery. Clinically significant macular oedema shows as focal hypofluorescence due to local ischaemia and blockage of background choroidal fluorescence. Intraretinal microvascular abnormalities can be visualised

by FFA and appear as focal hyperfluorescence with adjacent areas of capillary 'dropout' and no associated leakage. FFA highlights neovascularisation during the early phases of the angiogram and shows irregularly expanding hyperfluorescence in the later stages due to significant leakage of dye from neovascularisations. FFA can confirm the presence of neovascularisation, when clinically doubtful. It also delineates areas of retinal ischaemia which may be selectively targeted by laser treatment. (3,49)

FFA also allows 'in vivo' quantification of FAZ, a capillary-free zone surrounded by interconnected retinal capillary beds. (50) This allows detection and monitoring of vascular disease such as diabetic retinopathy, retinal vein occlusion and macular telangiectasia. The size of FAZ corresponds to the condition of the foveal microcapillary circulation and is strongly correlated with the severity of capillary nonperfusion (dropout) in several retinovascular diseases, including DR. (51) Depending on the vascular pattern, the physiological shape of the FAZ is round or oval and has an average diameter of 500 to 600 microns. (52) Mansour and colleagues (1993) found that FAZ measured by means of FFA in healthy subjects was significantly smaller (median value of 0.405 mm^2) that in eyes with background (median value of 0.737mm^2) and proliferative (0.866mm^2) diabetic retinopathy. (53) The enlargement of FAZ in diabetic retinopathy was also confirmed by other studies. (54-56). Other findings in diabetic retinopathy included capillary non-perfusion showed as increased perifoveal intercapillary areas (51,55 and reduction in capillary blood cell velocities. (55)

FFA has several limitation. Firstly, it has a number of potential side effects. These include nausea (2.9%) and vomiting (1.2%) (57) and allergic reactions of varying extent, from mild urticarial to life-threatening anaphylaxis. (58) No risks have been associated with pregnancy, however, most physicians refrain from using FFA in pregnant patients. (59) Secondly, visualisation of deep retinal and choroidal vessels is limited using FA. (44) Finally, FFA appearances do not form part of the ETDRS criteria for clinically significant macular oedema nor do they provide parameters for its treatment. (60)

1.2.7.4. Optical coherence tomography and angiography

Optical coherence tomography (OCT) and OCT angiography (OCTA) are new imaging techniques which are described in detail in the next chapters (see Optical coherence tomography and OCT angiography).

1.2.8. Treatment

The treatment for diabetic retinopathy varies depending on its severity. However, certain general measures are essential irrespective of it. These include patient education, optimising diabetic control, smoking cessation and eliminating modifiable risk factors including hypertension and hyperlipidaemia by pharmacological and lifestyle means. Anaemia and renal failure, if present, should also be addressed as necessary.

1.2.8.1. Treatment for proliferative diabetic retinopathy

Laser panretinal photocoagulation (PRP) remains the mainstay of PDR treatment. The Diabetic Retinopathy Study (DRS) demonstrated a clear benefit of PRP, e.g. severe NVD without haemorrhage carries a 26% risk of visual loss at 2 years without treatment, which is reduced to 9% with PRP. (61) The initial treatment consists of approximately 1500 burns. This can increased in cases of imminent sight loss due to vitreous haemorrhage. The number of burns required for regression of mild, moderate and severe PDR is approximately 2500-3000, 4000 and 7000 burns, respectively. (3)

Intravitreal anti-VEGF injections have an adjunctive role. Indications include attempted resolution of a persistent vitreous haemorrhage to avoid vitrectomy (provided that a retinal detachment has been excluded by means of B-scan ultrasound), the initial treatment of rubeosis iridis once a response to PRP is established and rapid control of very severe PDR in order to reduce the risk of haemorrhage.

Targeted retinal photocoagulation (TRP) also has a role. It allows selective treatment of peripheral capillary non-perfusion areas, which can be identified by wide-field fluorescein angiography. TRP can lead to regression of neovascularisation whilst minimising potential complications. (3,8)

1.2.8.2. Treatment for diabetic macular oedema

Until recently laser photocoagulation was the gold standard treatment for DMO. However, in the availability of new treatment modalities and increasing evidence of their efficacy have changed the treatment approach. The currently available therapies include:

- **Focal or grid laser photocoagulation**. In the focal approach diode or argon burns are applied to leaking aneurisms 500-3000µm from the foveola. In grid laser photocoagulation burns are applied to macular areas of diffuse thickening, not closer than 500µm from the folveola and optic disc.
- **Subthreshold micropulse diode laser** uses very short laser pulse duration with a longer interval. This minimises the collateral damage to retina and choroid by allowing energy

dissipation, whilst stimulating the RPE. The evidence indicates that results are comparable with those of conventional thermal laser.

- **Intravitreal anti-VEGF injections** have become an essential element of diabetic maculopathy treatment. The main pharmacological agents are ranibizumab, bevacizumab and alflibercept.
- **Intravitreal triamcinolone.** In pseudophakic eyes intravitreal triamcinolone steroid injections promptly followed by laser photocoagulation have been shown to be comparable to ranibizumab with regards to visual improvement and reduction of retinal oedema.
- **Pars plana vitrectomy** may be indicated when macular oedema is associated with vitreomacular traction syndrome. (3,8)

1.3. OPTICAL COHERENCE TOMOGRAPHY

1.3.1. History

The first reports regarding optical coherent tomography were by James Fuimotos from the Department of Electrical Engineering and Computer Science at Massachusetts Institute of Technology, where the first OCT images were obtained. In 1991 David Huang and colleagues described OCTs of post-mortem diseased coronary arteries and eyeball. (62) In 1993 Michael Hee et al visualised retina in vivo. (63) In 1994 Joseph Izatt and colleagues published the first reports on OCT applications in the anterior segment of the eye. (64) In 1996 the first commercial OCT - OCT1 was built. (65)

In 1997 the Ophthalmology Clinic of the Faculty of Medicine in Warsaw was the first in Poland to purchase an OCT1. In 1998 prof. Tadeusz Kęcik and colleagues were the first Polish researchers to publish a report on the application of OCT in eye examination. (66,67) In the subsequent years numerous reports on the use of OCT in macular and optic nerve pathologies were published. In 2002 time-domain OCT 3000 was introduced (Stratus OCT, Carl Zeiss Meditec) with a resolution of 10µm and a speed of 400 A-scans per second. Up from 2004 spectral-domain OCT became the gold standard with a resolution of 1-5µm and a speed of 26,000 - 70,000 A-scans/second. Adolf Fercher from Vienna University conducted intensive research into spectral-domain OCT. (65) The first Polish researchers who published a retina image obtained by means of SD-OCT were prof. Andrzej Kowalczyk and prof. Maciej Wojtkowski from the Mikołaj Kopernik University in Toruń. (68) The SD-OCT

technology enabled to obtain images with high resolution and a smaller number of artefacts. Currently, it is widely used in everyday ophthalmic clinical practice. (65)

In 2012 prof. James Fujimoto described the applications of split spectrum amplitude decorrelation angiography (SSADA) technology in OCT. (65) In December 2013 prof. Bruno Lumbroso organised the First International Congress on *en fac*' OCT in Rome, thereby introducing the technology into ophthalmic diagnostics. In September 2014 at the European Society of Cataract & Refractive Surgeons meeting in London the first non-contrast OCT Angiography system, AngioVue, was presented. The first commercially available AngioVue System appeared in December 2014. (65) Since then its applications have continued to expand along with intensive research employing the technology.

1.3.2. Principles and technology

Optical coherence tomography (OCT) is a non-contact imaging technique producing micrometre-resolution, cross-sectional images of the retina and vitreoretinal interface. It is based on the low-coherence optical inferometry principle. A light source emits low-coherence near-infrared light (800-850nm) with bandwith of 20-150nm. (69) The light beam is directed into the eye, where it gets partially reflected back and partially dispersed. Different tissues have different qualities that influence the back-reflectance and, hence, the light reflected by different layers of the retina contains signals of varying amplitudes and latencies. This then allows the OCT image to differentiate the individual retinal layers based on the relative differences in the back-reflectance of the tissue composites. Since the time delay difference from the light reflected from individual layers onto a detector cannot be quantified by a direct time-measurement delay, interferometry is employed. It involves use of a reference arm, which utilises a laser light beam split from light source with a beam splitter - a partially reflecting mirror. This allows to send a part of the light beam to the target tissue (target arm), and the remaining portion to the reference mirror (reference arm). Both beams are then reflected back to the beam splitter and directed to a detector together. The light from the two arms produces an interference pattern, allowing a comparative measurement. Detectable interference can only be created when the reflected light is within coherence of the laser light, i.e. when the distance to the reference mirror is equal to the distance to the reflecting tissue target. A series of axial depth scans (A-scans) is obtained and as the light source moves across the retina. By laterally combining these images a two-dimensional cross-sectional tomograph (B-scan)

is constructed and displayed in grey or colour scales. White and black correspond to areas of high and low reflectivity, respectively. (69-71)

1.3.2.1. Time-domain OCT

In the time-domain OCT (TD-OCT) the depth information is provided by the position of a movable reference mirror. A depth scan of the reflecting target tissues is obtained by moving the reference mirror closer and further from the beam splitter. The cross-sectional images obtained are superimposed to create a three-dimensional composite image. In TD-OCT the depth or axial scanning speed is limited by the speed at which the reference mirror can be moved and only 400 A-scans per second can be obtained. (69-71)

1.3.2.2. Spectral-domain OCT

In spectral-domain OCT, also known as Fourier-domain OCT (FD-OCT) the OCT interference is formed by a diffraction grating, based on the wavelength of light. The obtained spectrum is sent to a computer where it is analysed by Fourier transform (a frequency domain representation of the original signal) to give depth information. This eliminates the need for moving reference mirrors, and the entire axial depth scan is obtained for each tissue point 'simultaneously'. This results in high responsivity and speed. The FD-OCT can acquire over 20 000 A-scans per second. Due to the speed, the superimposition of the obtained images gives information on the three-dimensional structure of the examined tissues. (3)

1.3.2.3. Swept-source OCT

In swept source optical coherence tomography (SS-OCT) a short-cavity swept laser is used instead of the superluminescent diode laser typical of conventional spectral domain OCT. Although the wavelength is centred at approximately 1µm, the laser changes as it sweeps across a narrow band of wavelengths with each scan. Similarly to SD-OCT, SS-OCT has a fixed reference arm. However, the spectrometer is replaced by a complementary metal oxide semiconductor camera along with two fast parallel photodiode detectors. As a result. SS-OCT is able to achieve the highest commercially available imaging speed with 100 000 A-scans obtained per second. (70,72)

1.3.2.4. En face technology

En face OCT is a technique which combines the longitudinal cross-sectional SD-OCT with transverse confocal analysis, producing transverse images of the retinal and choroidal layers at a specified depth. It provides an *en face* of the retinal and choroidal layers. (70,73) This technology is available

in most modern OCTs. As per standard settings, the first layer of *en face* segmentation is at the level of superficial retina and shows the vitro-retinal surface. The second layer penetrates deeper and depicts plexiform and nuclear retinal layers, where the changes such as intraretinal fluid and hard exudates can be found. The third layer is parallel to the retinal pigment epithelium where RPE drusden and pigment epithelial detachment (PED) can be detected. The last *en face* segment is the level of Heller's layer of the choroid. (70)

1.3.2.5. Applications

OCT technology produces tissue cross-sections consistent with a histological examination. Therefore, it is frequently called a non-invasive optical biopsy. This technique is used in many areas of medicine - cardiology, gastroenterology, dermatology and oncology. However, its broadest range of applications is in ophthalmology, where it allows a detailed visualisation of the retina, choroid, optic nerve and anterior segment in real time. As far as retinal pathology is concerned, OCT is commonly used for evaluation of vitroretinal interface disorders, age-related macular degeneration (AMD) and diabetes, including diabetic macular oedema (DMO). (70)

1.4. OCT-ANGIOGRAPHY

1.4.1. Principles and technology

Conventional OCT technology allows a detailed assessment of the retinal and choroidal structures, however, it does not enable to examine the functioning of the microcirculation. Doppler OCT-angiography methods have been investigated, (74-79) however, their ability to examine the retina and choroid proved very limited as these structures are located perpendicularly to the OCT beam and Doppler OCT is only sensitive to motion in a plane parallel to the probe beam. (80) Speckle based OCT angiography has proved superior as it uses the variation of the spickle pattern in time to detect transverse and axial flow with comparable sensitivities. Several variants of the method have been described including amplitude-based, (81,82) phase-based (83) and combined amplitude-phase-based (84) technologies. (80)

OCT angiography (OCTA) (**Figure 2**), based on *en face* OCT, is the newest available imaging technique, which, in addition to depicting anatomical structures, enables assessment of the retinal and choroidal blood flow. The split spectrum amplitude decorrelation angiography (SSADA) technology forms

the basis of OCT Angiography. It identifies the blood vessels by means of detection and measurement of red blood cells' movement in the vasculature. The SSADA algorithm detects motion in blood vessel lumen by measuring the variation in reflected OCT signal amplitude between consecutive cross-sectional scans. This variation is quantified by the decorrelation function provided that the signal is strong enough to predominate over the optical and electronic noises. The SSADA influences how the OCT signal is processed to enhance flow detection and simultaneously reject axial bulk motion noise. This allows to obtain a high quality image of the microvasculature with less noise in the foveal avascular zone. (80)

To achieve this, the SSADA algorithm splits the OCT image into different spectral bands. This increases the number of usable image frames. Each new frame is characterised by a lower axial resolution and reduced susceptibility to axial eye motion secondary to retrobulbar pulsation. This also increases the speckle contrast as lower resolution creates a wider coherence gate over which the signal reflected from a moving blood cell can interfere with adjacent structures. Furthermore, each spectral band contains a different speckle pattern and different information on the flow. (80) The amplitude decorrelation images from multiple spectral bands are then combined, thereby increasing the flow signal. Due to this an SSADA using four-fold spectral splits improves the signal-to-noise ratio (SNR), by a factor of two, i.e. reduces the scanning time by a factor of four. (85) The newer OCTAs use more than a four-fold split in order to further enhance the SNR of flow detection. A linear relationship exists between the decorrelation and the flow velocity over a limited range dependant on the time scale of the SSADA measurement. Higher decorrelation values correspond to higher flow velocity. With a 70kHz spectral OCT and 200+ A-scans per cross-sectional B-scan, SSADA would be sensitive to the slowest capillary flow on the basis of the estimated flow velocity of 0.4 to 3mm/s. (86,87) In large vessels with higher velocities the signal saturates. (80)

***Figure 2**. OCT Angiography Imaging System – DRI OCT Triton Swept Source OCT. (88)*

1.4.2. OCTA Advantages

OCTA has several advantages over the FFA or indocyanine green (ICG) angiography, the gold-standard retinal imaging vascular techniques. Firstly, OCTA is a significantly shorter examination with the images acquired in a few seconds. Secondly, it does not require intravenous contrast, thus eliminating the risk of adverse effects. The speed and non-invasiveness allow for follow-up scans to be obtained more frequently, resulting in closer monitoring. Thirdly, as the leakage and staining of the dye do not occur in OCTA, the structures adjacent to the leak, including neovascularisations and areas of capillary dropout can be identified and measured. The visualisation of the intra- and subretinal fluid provides information analogous to fluid leakage. In addition, OCT allows to quantification of the retinal thicknesses and, hence, the determination of the location as well as the extent of oedema. Finally, due to the 3D nature of OCTA, the structures of the fundus can be visualised together, as a composite, or reviewed separately as individual layers, allowing a detailed assessment of abnormalities in the retinal and choroidal circulation. (44,80)

1.4.3. OCTA Limitations

OCTA has several limitations. Firstly, it cannot directly visualise vascular leakage. This can, however, be overcome by other ways of detecting vascular abnormality and fluid accumulation (see OCTA Advantages). As a result, it cannot distinguish between leaking and non-leaking microaneurisms.

Nonetheless, it is possible to superimpose the microvascular images, containing intrinsically co-registered volumetric structural data, with retinal thickness maps and thereby obtain indirect information on leakage. (89) Secondly, compared to FFA, it can detect most, but not all microaneurisms. However, it can also detect some microaneurisms not visible on FFA. Thirdly, shadow graphic flow projection artefacts make the interpretation of deeper vascular beds *en face* angiograms more challenging. These artefacts result from fluctuating shadows cast by flowing blood in the superficial vascular layer causing signal variation in deeper highly reflective layers. They can be removed by software processing. This is usually effective in deeper layers, with the exception of choriocapillaris, which is almost confluent and, therefore, casts projection and shadows that are difficult to remove from the deeper choroidal layers. Other artefacts can appear due to blinking and motion or vessel ghosting, vessel doubling or stretching of the image. Furthermore, in large vessels the OCT and flow signal fade due to an interferometric fringe washout effect associated with very fast blood flow, more prominent in the axial flow component. As a result, the central retinal vessels in the optic disc and large calibre vessels in the deep choroid cannot be visualised. Another disadvantage of OCTA is a relatively small scan area - from 3x3 to 9x9 mm, which does not allow to assess the periphery. (90) Lastly, the obtained images require post-processing software for accurate layer segmentation as well as removal of motion and projection artefacts. (80-91)

1.4.4. OCTA Applications in Ophthalmology

OCTA provides detailed information on the vascular status of the posterior segment of the eye including the structure, blood flow and dimensions of the foveal avascular area, presence and extent of capillary non-perfusion areas and detection of retinal and choroidal neovascularisation. Therefore, it is a valuable tool in the diagnosis and management of a variety of ophthalmic pathologies such as diabetic retinopathy, retinal artery occlusion, branch or central retinal vein occlusion, choroidal neovascularisation linked to age-related macular degeneration as well as other diseases, degenerative myopia, central serous chorioretinopathy, multiple choroiditis, polypodal choroidal vasculopathy, optic nerve assessment including glaucoma and corneal and anterior segment disorders. (89,92-94)

1.4.5. Interpretation of OCTA

The OCTA generates 3D images *en face* presentation of the flow between the internal limiting membrane and the choroid. The segmentation into different layer allows to optimally assess any

abnormalities. Computer segmentation provides the following reference planes, relative to which individual tissue layers are defined:

- **The inner limiting membrane** (**ILM**)
- **Outer boundary of the inner plexiform layer** (**IPL**)
- **Outer boundary of the outer plexiform layer** (**OPL**)
- **Bruch's membrane** (**BM**) (**Figure 3**).

Automated algorithms are very accurate at identifying these reference planes, however, their margins can be manually amended if required. (95)

In cross-sectional OCT angiograms the colour coded flow information (decorrelation) is superimposed on the grey scale structural image based on the reflectance signal. Due to this combined data display the depth of the identified abnormalities can be easily assessed (**Figure 3**). (95)

The *en face* angiograms are generated by combining the flow signals within the depth of individual anatomic structures. This projection compresses a 3D examination into several 2D images to facilitate the interpretation. Using the previously outlined reference planes the following structures can be identified:

- **Vitreous** - above ILM, avascular in healthy eyes
- **Superficial retinal plexus** - between ILM and the outer margin of the IPL
- **Deep retinal plexus** - between the outer boundary of the IPL and the outer boundary of the OPL
- **Inner retina** - comprises the superficial and deep retinal plexuses and is located between the ILM and the outer boundary of the OPL
- **Outer retina** - between the outer border of the OPL and RPE, normally avascular
- **Choriocapillaris** - below RPE, normally near confluent
- **Deeper choroid** - below choriocapillaris, consists of larger choroidal vessels

- **Choroid** - comprises choriocapillaris and deeper choroid (**Figure 3**). (95)

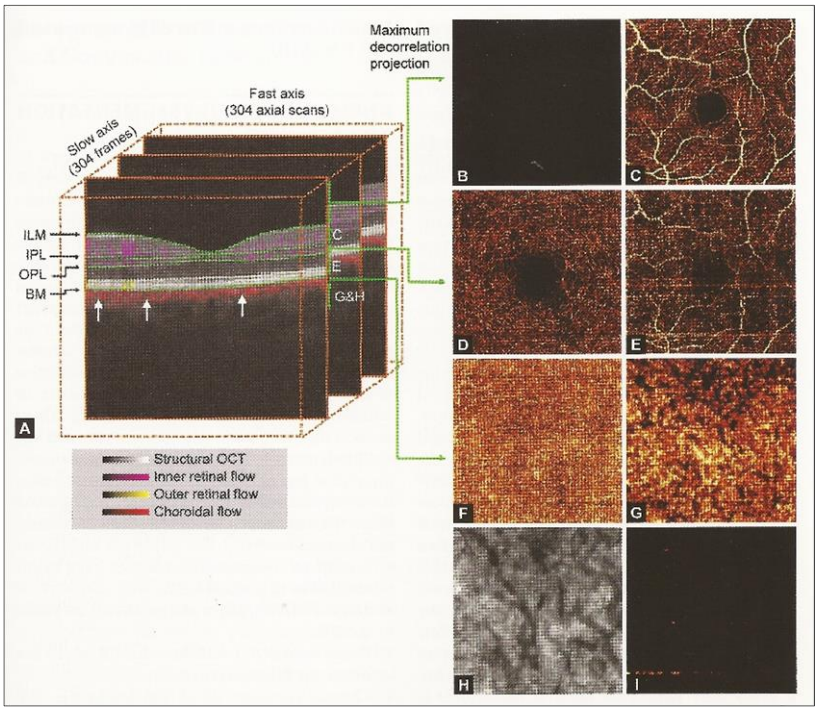

Figure 3. *OCT Angiography segmentation and processing of a normal macula. A) The cross sectional diagram shows that flow in the inner retinal vessels (purple) is projected onto photoreceptors and retinal pigment epithelium (white arrows). The image processing software separates vitreous, inner retina, outer retina and choroid along the flowing reference planes: ILM, IPL, OPL and BM. B) Vitreous. C) Superficial retinal plexus. D) Deep retinal plexus. E) Outer retina. F) Choriocapillaris. G) Deeper choroid angiogram. H) Deeper choroid en face structural OCT. I) The outer retina angiogram after removal of the projection artefact using a post-processing algorithm. Adopted from Lumbroso et al (2016). (96)*

For each examination OCTA provides the cross-sectional images for four default segmentation planes using an automated algorithm:

- **Superficial retinal capillary plexus** (**SCP**) - 3µm below the ILM to 15µm below IPL
- **Deep retinal capillary plexus** (**DCP**) - 15-70µm below the IPL
- **Outer retina** - 70µm below the IPL to 30µm below the RPE
- **Choroid** - 30-60µm below the RPE (**Figure 2**). (95)

The above planes are also depicted together in a composite image where individual layers are colour-coded (**Figure 4**).

As with the reference planes, the boundaries of the above segments can be manually corrected if required. Artefacts in each segment can be removed using the 'remove artefacts' check box.

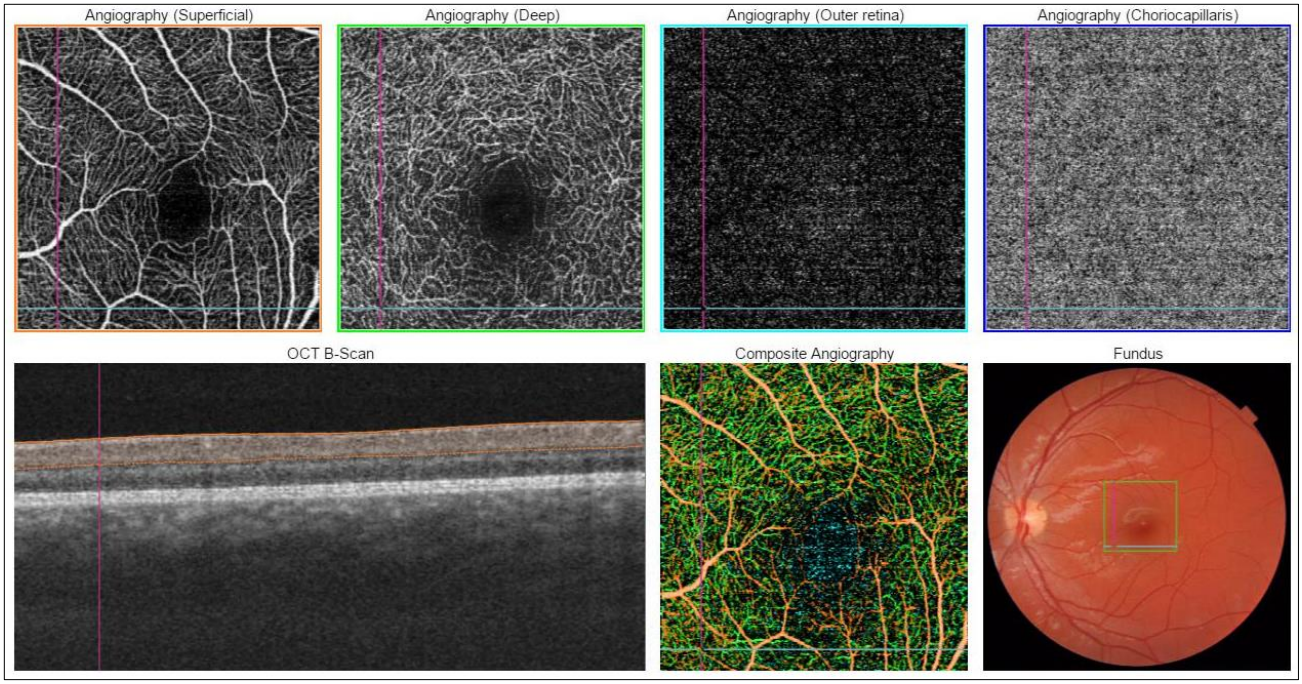

Figure 4. *OCTA cross-sectional images for four default segmentation planes using an automated algorithm as they appear on Topcon OCT Angiography report viewed by the IMAGE net software. Top left to right is angiography of the superficial capillary plexus (orange frame), deep capillary plexus (green frame), outer retina (light blue frame) and choriocapillaries (navy blue frame). Bottom left to right: Cross-sectional view of the retinal layers, composite angiography with the 4 individual planes represented in their corresponding colours (as per frames in the top photographs) and a fundus photograph.*

1.4.6. OCTA in diabetic retinopathy

OCTA can demonstrate several pathological findings in diabetic retinopathy. Firstly, it allows a detailed assessment of the foveal avascular zone. FAZ dimensions can be measured to quantify any enlargement. Segmentation enables to examine FAZ separately in the superficial and deep capillary plexuses. (97)

Secondly, the phenomenon of capillary dropout can be appreciated. This is more readily visible in the deep capillary plexus and is characterised by the disappearance to the ramification of small capillaries in the ischaemic areas. Depending on the OCTA machine and software used, flow area and flow density can be calculated.

Microaneurisms can be visualised particularly well in the deep capillary plexus layer in the presence of intravessel flow. Thrombosed microaneurisms are silent and undetected by OCTA. Similarly, microaneurisms with very slow flow may not be detected. (97)

OCTA can help distinguish between intraretinal vascular abnormalities, found in the same plane as retinal blood vessels, and early retinal neovascularisations, which develop anterior to the ILM. (92) It also facilitates the detection of microvascular changes such as telangiectatic vessels and capillary loops which are difficult to appreciate using other imaging modalities. Retinal capillary tortuosity and capillary dilation are clearly depicted. It also allows for accurate detection of neovascularisations (NVD and NVEs) and choriocapillaris abnormalities. (89)

The presence of cystoid macular oedema can be best diagnosed and monitored looking at the deep inner retinal plexus, where the majority of the fluid collects. It is recorded as absence of flow due to the 'sliding' of retinal tissue linked to intraretinal cystic spaces. (97,98)

1.4.7. Up to date studies of diabetic retinopathy using OCTA

Following its introduction, OCTA has been used by researchers to investigate changes occurring in diabetic retinopathy previously shown by FFA studies, including increased size of FAZ and perifoveal intercapillary areas and reduction in capillary blood cell velocities (See Fundus Fluorescent Angiography). (51,53,55,56)

Takase and colleagues (2015) reported that on OCTA examination diabetic eyes showed statistically significant FAZ enlargement in the superficial and deep plexus layers compared with healthy eyes, regardless of the presence of retinopathy, thereby highlighting that changes in the microcirculation can be detected before the development of DR. (99) This was confirmed by Dimitrova et al (2017) who noted that FAZ in the superficial retina of diabetic patients without clinical features of diabetic retinopathy was greater than in the control group. (100) Similarly, Gozlan et al (2017) study reported a statistically significant increase in FAZ area and perimeter in association with progession of non-proliferative diabetic retinopathy, noting a clear relationship between the extent of OCTA changes and the severity of NPDR. (101) Nonetheless, contradictory findings have been reported by Carnevali et al (2017) who found no significant difference in FAZ area of the superficial and deep capillary plexuses comparing diabetic and control groups. (102)

Further studies additionally showed reduced parafoveal and perifoveal vessel density in patients with diabetic retinopathy by OCTA. (100,102-105) Agemy and colleagues (2015) found significantly lower capillary perfusion density values in diabetics compared with controls and a significant decrease in capillary perfusion density values corresponding to retinopathy progression. (106) This was in agreement with Sambhav et al (2017) study which showed an inverse correlation between

the vessel density of the perifoveal zone and the level of NPDR severity (107) and with Gozlan et al (2017) study which reported a statistically significant increase in the superficial plexus nonperfusion index in association with progression of non-proliferative diabetic retinopathy. (101) Ishibazawa and colleagues (2016) used OCTA to characterise the morphology of neovascularisations in patients with PDR and concluded that exuberant vascular proliferation on OCT angiograms should be considered as an active sign of neovascularisation and that the imaging technique may be useful for estimating the activity of new vessels in eyes with PDR. (108) Krawitz and colleagues found significant differences in the acircularity index and axis ratio of FAZ in diabetic retinopathy compared with healthy eyes and proposed that OCTA can be used to help noninvasively stage DR and, therefore, is promising as a method for monitoring disease progression and response to treatment. (109)

OCTA was successfully used in children by Yilmaz and colleagues (2017) who investigated vascular changes in amblyopia and found the vessel density of SCP and DCP of eyes with amblyopia to be lower than that of the companion eye and the age-matched controls. (110) Nonetheless, to date no studies using OCTA have been conducted in children with diabetes.

Saying and colleagues (2014) used structural OCT to determine subfoveal choroidal thickness (SFCT) in children with type 1 diabetes without diabetic retinopathy and found no significant differences with the healthy control group or correlation with fasting glucose level, HbA1c, age, or duration of diabetes. (111) Similarly, Elhabashy et al (2015) used structural OCT to examine retinal volume, nerve fibre layer volume (temporal and nasal quadrants) and ganglion cell layer area in the eyes of diabetic children without clinical diabetic retinopathy and found no differences with the control group. (112) These findings raise doubts as abnormalities of the choroidal circulation, which receives approximately 95% of all ocular blood flow, have been implicated in the development and progression of DR. (16) Histologically, diabetic choroidopathy is characterised by arteriosclerosis, choriocapillaris degeneration, vessel tortuosity, localised dilation or closure of capillaries, areas of ischaemia and neovascularisations, (16) which suggests that choroidal thickness could be altered in the course of diabetes. In type 2 adult diabetics choroidal thickness has been shown to be reduced in comparison with healthy subjects and to be associated with microalbuminuria. (113) In view of the disparities the choroidal parameters in diabetes merit further investigation, which OCT technology is well suited for.

2. AIMS

OCTA has proved to be an effective tool for the assessment of the microcirculation in adult diabetic patients. It has been shown that abnormal changes in the retinal microcirculation can be detected in the absence of clinical diabetic retinopathy. However, no analogical studies have been conducted in children with diabetes.

In view of the differences between child and adult physiology as well as the different rate of onset and progression of diabetic retinopathy described in children, the results of studies of adult diabetics cannot be extrapolated to the paediatric patients. Furthermore, young children with early onset type 1 diabetes will inevitably have a very long duration of diabetes by late adulthood, which is the main risk factor for the development of diabetic retinopathy. Hence, in this group primary prevention is essential and identifying abnormal features before the appearance of clinical DR could be valuable for informing the management. The non-invasive nature of OCTA examination makes it suitable for paediatric patients.

Therefore, the aims of the present study are:

- Analysis of the possibility of using OCT Angiography to evaluate microvascular retinal changes in children with type 1 diabetes;
- Determination of the prerequisites and indications for OCTA in this patient group;
- Evaluation of whether a correlation exists between retinal changes identified by OCTA and the duration of diabetes, biochemical diabetic parameters and anthropometric factors;
- Assessment of the implications of the results for clinical management.

3. ETHICAL CONSIDERATIONS

The study was approved by the Ethics Committee of the University of Medical Sciences im. Karola Marcinkowskiego in Poznań on 3rd March 2016, Act Number 303/16 (See **Appendix)**.

4. METHODOLOGY

4.1. Patient recruitment

Children, defined as up to and inclusive of the age of 18 years, with Type 1 diabetes under the care of Diabetes Clinics in the region of Wielkopolska were recruited. Children and their parents were offered to participate in the study during routine follow-up appointments and the volunteers were included in the study.

The control group consisted of age-matched healthy siblings of diabetic patients included in the study as well as healthy volunteers under the care of General Practitioner and Psychological-Pedagogical Counselling Centres in the region of Wielkopolska referred for a routine eye examination.

Parents of all participants and all children above the age of 16 years signed a consent for the examination.

4.2. Inclusion and exclusion criteria

Diabetic children were included in the study regardless of the type of insulin therapy, diet, anthropometric factors and refractive error. Patients with other concurrent chorioretinal diseases, previous photocoagulation treatment, previous ocular surgery, myopia or hypermetropia greater than 6 diopters (D) or poor quality of OCT images were excluded from the study.

4.3. Data collection

The following information was collection on patient interview: date of birth, age, weight, height, date of diagnosis and duration of diabetes, type of insulin therapy, duration of therapy with insulin pump and its brand where relevant, presence of other diseases, including other autoimmune disorders, family history of type 1 diabetes, diet regimes, frequency of exercise, previous examinations of the eye fundus and their outcome and glycaemic control measures including the last HbA1c and its date, the lowest and highest BG in the last week and month and the BG on examination.

The data on the date of diagnosis, details of insulin therapy, the last HbA1c and its date and weight and height were verified using patient documentation from their Diabetes Clinics to ensure accuracy. The information on the minimum and maximum BGs was collected at the time of examination from patient's BG diaries, glucometers, data from contactless BG measurement devices such as Libre Flash

Glucose Monitoring System, and in few cases based on patient's recollection in no other data was available. The BG on examination was measured before the OCT and OCTA examination using patients' own glucometers.

The clinical examination of each patient involved visual acuity (VA) recorded in decimal scale from 0-1.0, 1 being full vision, for far and near (for patients wearing glasses the VAs were tested with their current spectacles), auto-refraction (Topcon RM-800 Autorefractometer), ocular movement assessment, confrontational visual field assessment, slit lamp anterior segment and dilated fundus examination using Topcon IS-600 slitlamp. All abnormalities were noted, including diabetes related and other changes.

All patients underwent Radial macular OCT examination (Topcon DRI OCT Triton, Tokyo, Japan; software: Topcon DRI OCT Triton v. 10.11.003.01) and 3x3mm OCT Angiography (Topcon DRI OCT Triton with Angio-OCT module, Tokyo, Japan; Software: IMAGEnet 6 v. 1.19.11030). Pupils of all patients were dilated with Cyclopentolate 1% prior to scanning. All examination were performed in darkness by the same technician trained in the use of the equipment. For each patient one eye was selected for each examination based on image quality.

4.4. FAZ area measurement in the superficial and deep capillary plexuses by OCT Angiography

A 3×3mm OCTA acquisition centred on the fovea was performed. The *en face* image was then automatically segmented to obtain images of the superficial capillary plexus, deep capillary plexus, outer retina and choroid, as well as a colour-coded composite angiogram (**Figure 4**).

4.4.1. Superficial capillary plexus FAZ

The FAZ contour in the superficial capillary plexus was manually traced and the surface area within the drawn-in contour was automatically computed by Topcon software (**Figure 5&6**).

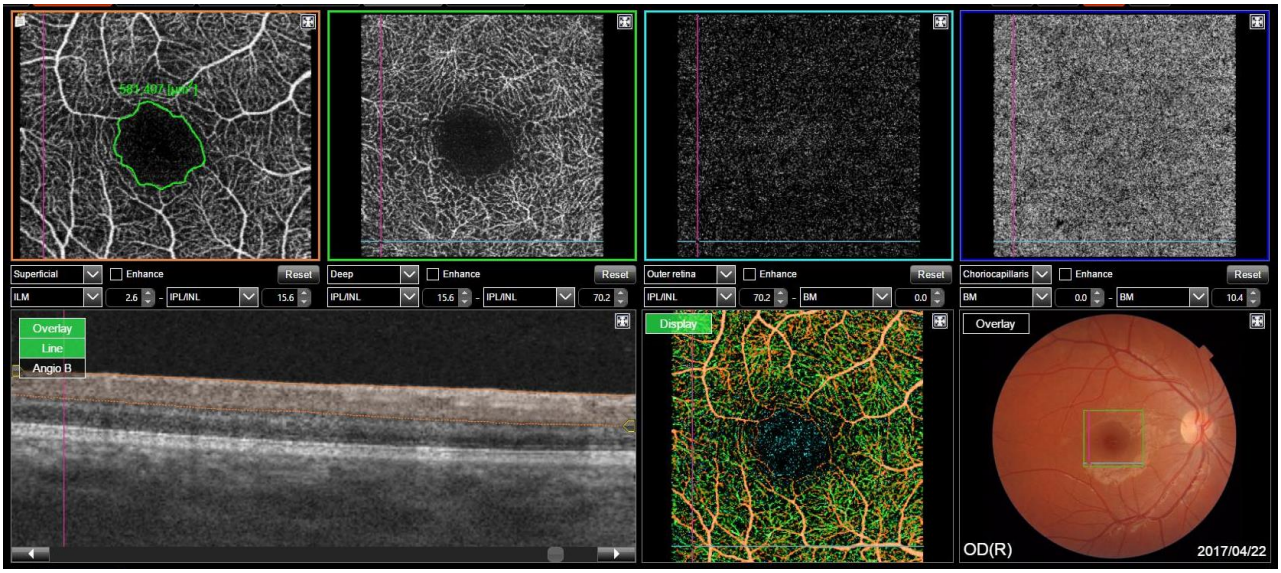

Figure 5. *FAZ area measurement in the superficial capillary plexus. Top left to right: manually contoured FAZ in the SCP with automatically computed surface area, deep capillary plexus, outer retina and choriocapillaris. Bottom left to right: cross-section of retina and choroid, composite angiography and fundus photo.*

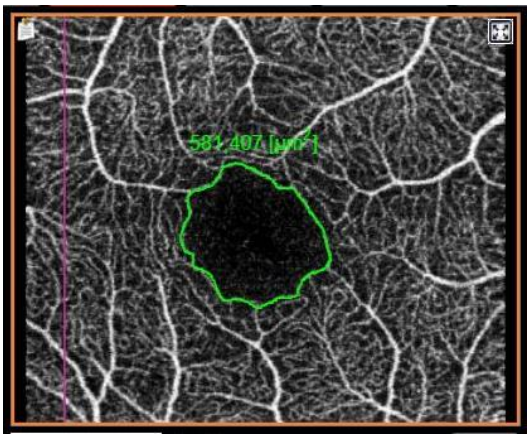

Figure 6. *Enlarged SCP angiogram with manually contoured FAZ and automatically computed surface area.*

4.4.2. Deep capillary plexus FAZ

To obtain the FAZ surface area in the deep capillary plexus, the DCP angiogram was enhanced by ticking the 'enhance' box below the DCP angiogram (**Figure 7**&**8**). This enhanced algorithm allows to increase the sensitivity of the detection of vessels in the DCP. Subsequently, the FAZ contour in the DCP was manually traced on the composite angiogram following the green-coloured DCP vessels (**Figure 8**). Using the colour-coded composite allowed to differentiate between the DCP

and SPC vessels which can appear superimposed on the DPC angiogram alone. In addition, the Angio-B function was used (**Figure 9**) to visualise the presence of red blood cells in the individual retinal layers. This allowed to verify the colour-coded flow representation in the composite angiogram. The surface area within the drawn-in FAZ margins was automatically computed by Topcon software (**Figure 8**). The use of the Enhance algorithm and Angio-B function allowed drawing in an accurate FAZ contour in the DCP, where FAZ is not as clearly demarcated as in the SCP. These tools helped increase the detection sensitivity of the DCP vessels and to avoid mistaking SCP for DCP.

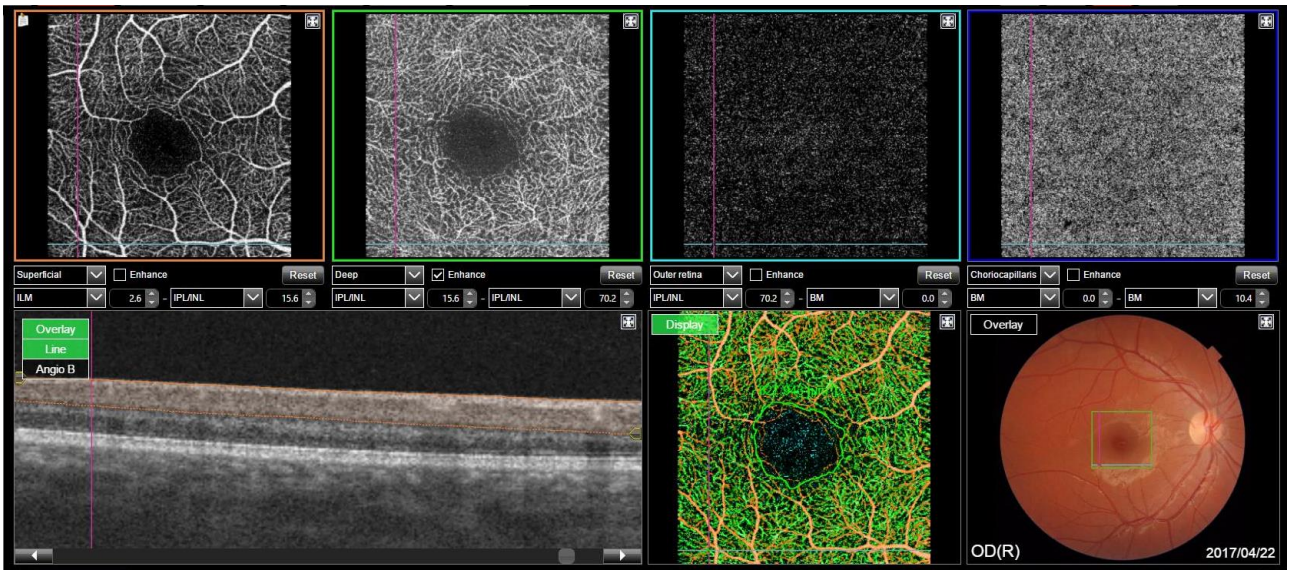

Figure 7. *Enhancement of the deep capillary plexus vessels by ticking the 'enhance' box underneath the DCP angiogram (green frame).*

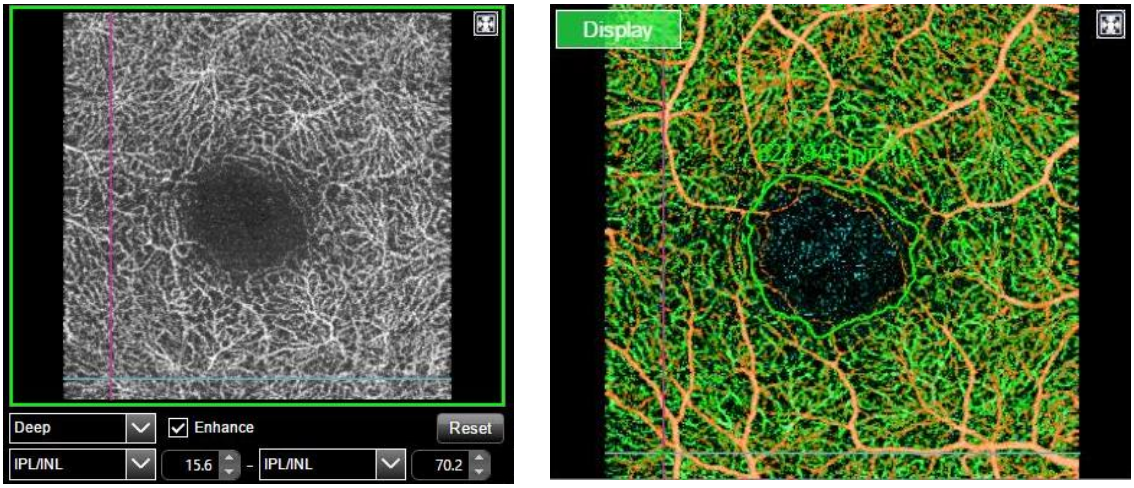

Figure 8. *Left: Enlarged DCP angiogram with ticked 'enhance' box underneath. Right: enlarged composite angiogram showing the DCP in green. The manually contoured FAZ is shown with an automatically computed surface area.*

A

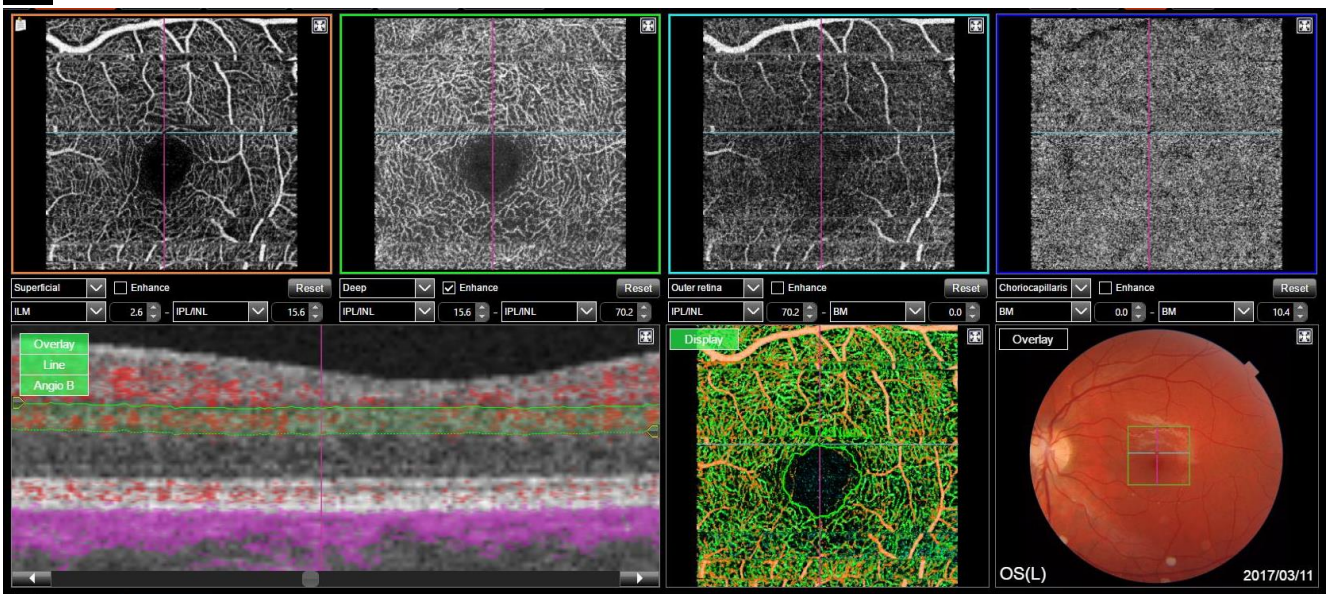

B

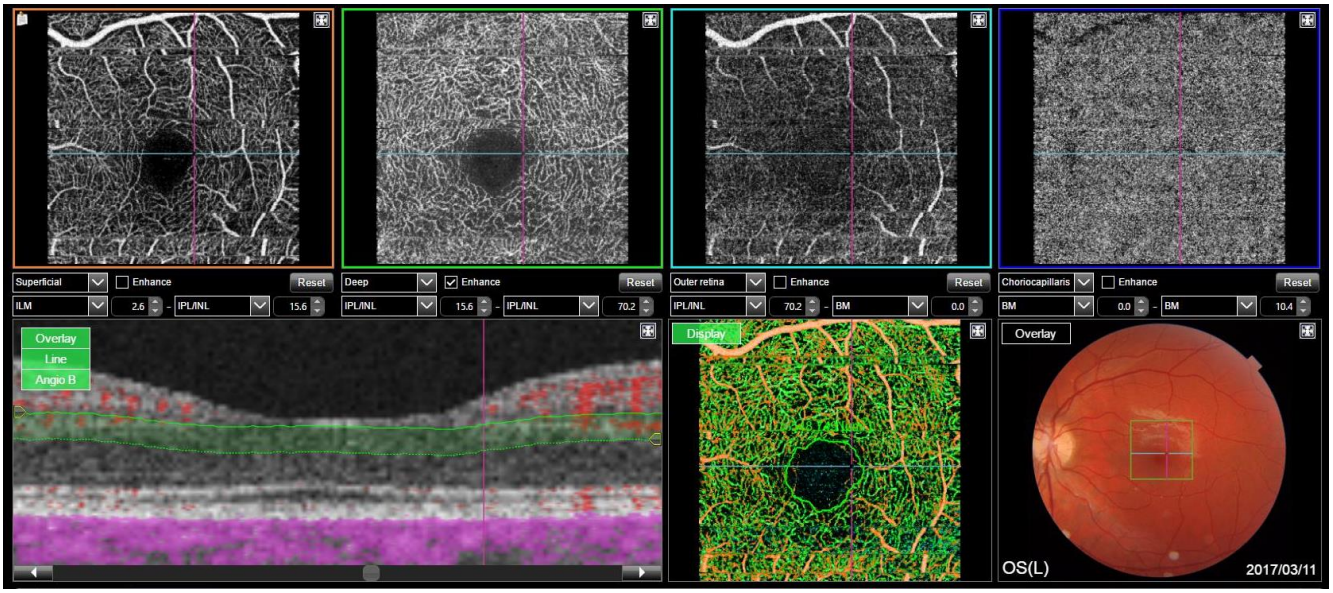

Figure 9. *Angio-B function. The pointer formed by the intersection of the blue horizontal pink vertical lines is directed to the point of interest. The indicated area is visualised in Angio-B setting, which shows the red blood cells, i.e. flow in each layer at the given location.* ***A)*** *Blood cells present in DCP at the indicated location.* ***B)*** *Blood cells absent in DCP at the indicated location.*

4.5. Central retina and choroid measurements

In the Radial OCT macula examination the central retinal (**Figure 10**) and choroidal (**Figure 11**) thickness was measured in 9 areas of the macula using the automated Topcon software (Radial scan module). The retinal layers were determined automatically by the software (**Figure 10).** This accuracy of this division was ascertained by the researcher and was found to be correct in all cases.

The average retina thickness was automatically computed by the Topcon software and displayed in the automatically generated report from the examination (**Figure 12**). The average choroid thickness was calculated as an arithmetic mean from the measurements obtained for the 9 macular areas. All examinations were performed in the late afternoon, at the same time of the day due to the known diurnal variability of choroidal thickness.

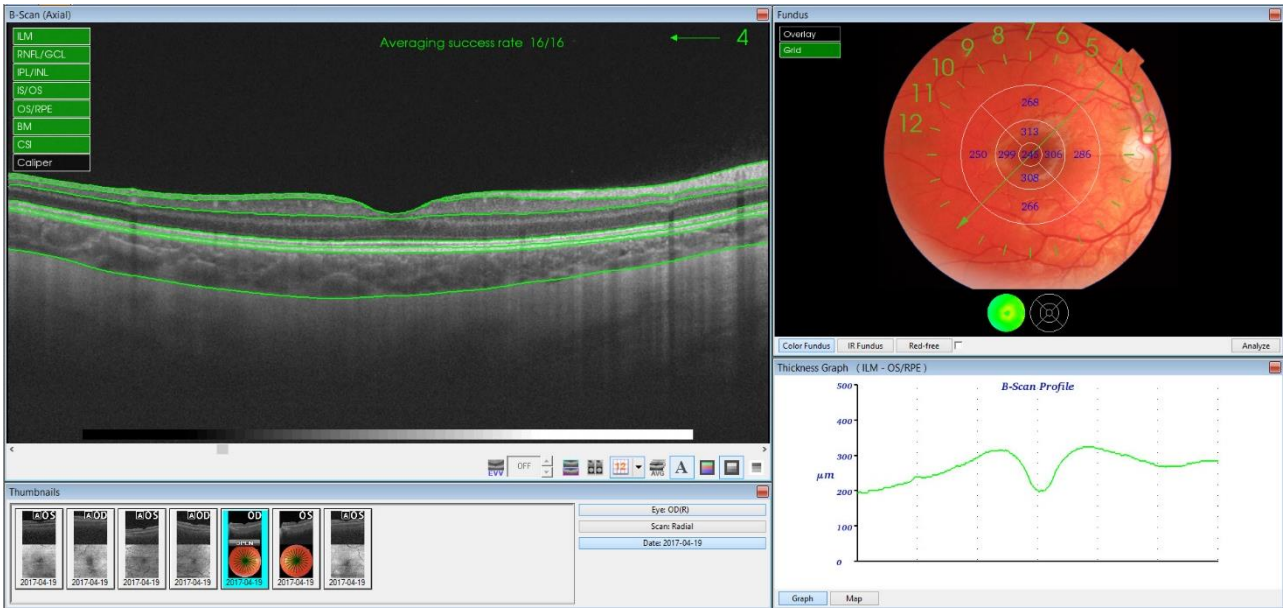

Figure 10. *Retina thickness measurement using Radial macular OCT. Top left: Cross-section with highlighted retinal layers and choroid. Top right: fundus photograph with retinal thickness measurements in 9 areas of the macula. Bottom right: Retinal thickness B-scan profile.*

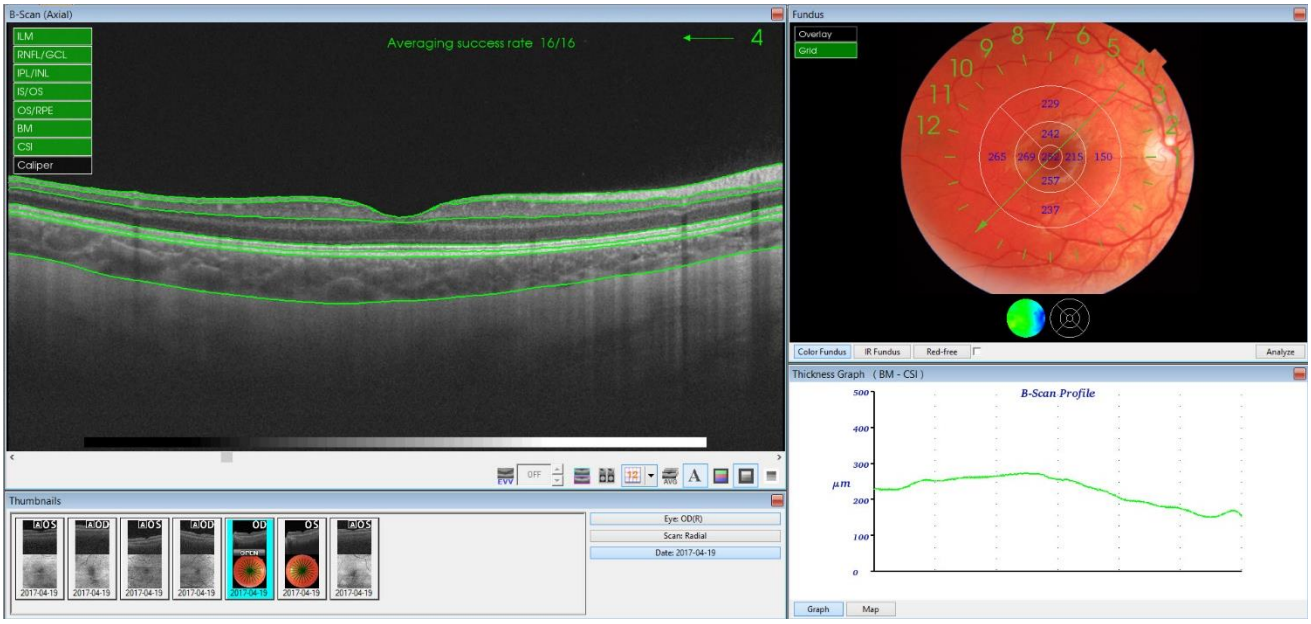

Figure 11. *Choroid thickness measurement using Radial macular OCT. Top left: Cross-section with highlighted retinal layers and choroid. Top right: fundus photograph with choroid thickness measurements in 9 areas of the macula. Bottom right: Choroid thickness B-scan profile.*

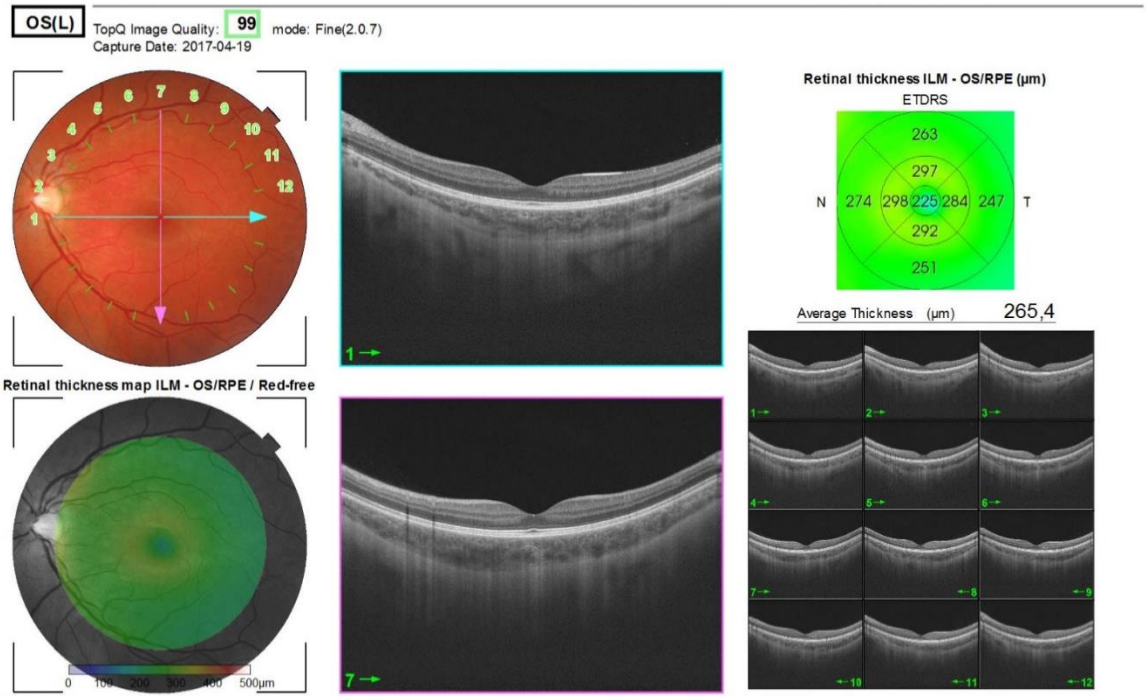

Figure 12. *Radial report showing an automatically computed average retinal thickness.*

4.6. Data and statistical analysis

Patients were divided into 3 groups depending on the duration of diabetes: Group 1: less than 5 years, Group 2: 5-10 years and Group 3: more than 10 years.

For the retinal and choroid thickness analysis, two parameters were considered for each layers: central and average retina and choroid thickness. The central choroid and retina thickness was defined as the measurement in the innermost circular area in the centre of the 9 areas measured by radial macular OCT. The choroid to retina thickness ratio was calculated by dividing the average choroid thickness by the average retina thickness for each patient. In OCT angiography the DCP/SCP FAZ surface area ratio was computed for each patient.

For the interpretation of anthropometric data, the Cole's Index (114) was calculated for each diabetic child on the basis of their weight and height as well as the standard 50th centile weight and height for their age. (115) The children were then divided into subgroups corresponding to their nutritional status as per Cole's index interpretation:

- >120%: Obese
- 110-120%: Overweight
- 90-110%: Normal

- 85-90%: Mildly malnourished
- 75-85%: Moderately malnourished
- <75%: Severely malnourished. (114)

The presence of correlation was analysed between the choroid and retina thickness status and the FAZ surface area parameters and DM duration, the last HbA1c and BG on examination in the study and control group as well as the subgroups of the study group. Subgroup analysis was also performed based on the type of insulin therapy, the presence of family history of T1DM, the nutritional status and gender.

Descriptive statistics was computed for the demographic data, FAZ parameters and choroid and retina parameters for the entire study group and the control group, as well as subgroups of the study group (Groups 1-3). This involved calculating the means, standard deviations (SD), 95% confidence intervals (95%CI), medians, the 25th and 75th quartiles (Q25 and Q75) and the minimum and maximum values. Descriptive statistics analysis was also performed as part of the subgroup analysis based on the type of insulin therapy, the presence of family history of T1DM, the nutritional status and gender. The Shapiro-Wilk test was used to verify the normal distribution of data. As the data was consistent with the Gaussian distribution, parametric statistical tests were used for the comparison of the means between the groups and for the correlation analyses. The comparisons of two unpaired groups were performed using the Student's t-test whereas the comparison of several unpaired groups by means of one way ANOVA variance analysis with post-hoc Least Significant Difference test.

The correlation between two features was analysed using the Pearson's linear correlation coefficient. The positive value of the correlation coefficient signifies the same direction of movement of the two variable, i.e. e.g. when one value increases, so does the other, whereas a negative coefficient value shows that the two variables move in the opposite direction. Correlation coefficient values between 0 and 0.5 depict a weak correlation, whereas between 0.5 and 1 show a strong correlation. The significance of the correlation coefficient was verified with the Student's t-test. The interpretation of the correlation coefficient was aided by the determination coefficient, which is the proportion of the variance in the dependent variable that is predictable from the independent variable. It is calculated as the correlation coefficient to the power of 2, multiplied by 100%.

The statistical significance threshold employed was $p<0.05$. The statistical analysis was completed using the Statistica v. 12.0 (Statsoft Inc.) software.

5. RESULTS

Some children could not tolerate one part of the OCT examination, either OCT Angiography or Structural OCT Macula. In those cases, a child was not excluded and instead, only the part of examination that could be performed was included in the analysis. As a result, the number of children with OCT macula examination results differs from the number of children with OCT Angiography data. Therefore, to account for this difference, the demographics analysis was performed separately for these two examinations.

5.1. FAZ parameters

5.1.1. Demographics

5.1.1.1. Study size and image quality

In total, 129 diabetic children were examined with OCT angiography. Due to poor image quality, 17 children were excluded. The analysis was performed for 112 diabetic children and included 62 right and 50 left eye examinations.

For the purpose of some analyses, the study group was divided into 3 subgroups depending on the duration of diabetes:

- Group 1: less than 5 years;
- Group 2: 5-10 years;
- Group 3: more than 10 years.

Groups 1, 2 and 3 consisted of 40, 42 and 30 children, respectively.

In terms of the control group, 37 healthy children were examined and 7 were excluded due to inadequate image quality. The analysis was completed for 30 controls and included 12 right and 18 left eye examinations.

The quality of all Angio-OCT images included in the analysis ranged from 65 to 78 and was within Topcon's recommended range. The mean image quality was 71.79 (SD 2.61; 95% CI: 0.49).

5.1.1.2. Age and gender

The study group consisted of 59 (52.68%) boys and 53 (47.32%) girls (**Figure 13**). In the control group, the proportion of boys was larger, with 22 (73.33%) males compared with 8 (26.67%) females. In the subgroups of the study group, the proportion of boys to girls was similar in each group (**Figure 14**). The age of children in the study and control group was comparable, with the mean age of 13.87 and 11.81 years in the study and control group, respectively (**Table 3**).

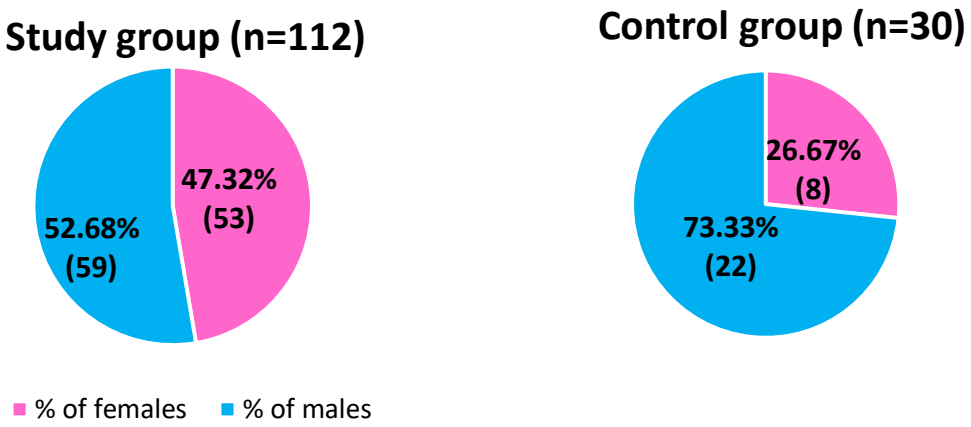

Figure 13. *Sex distribution in study and control group. Absolute numbers are given in brackets.*

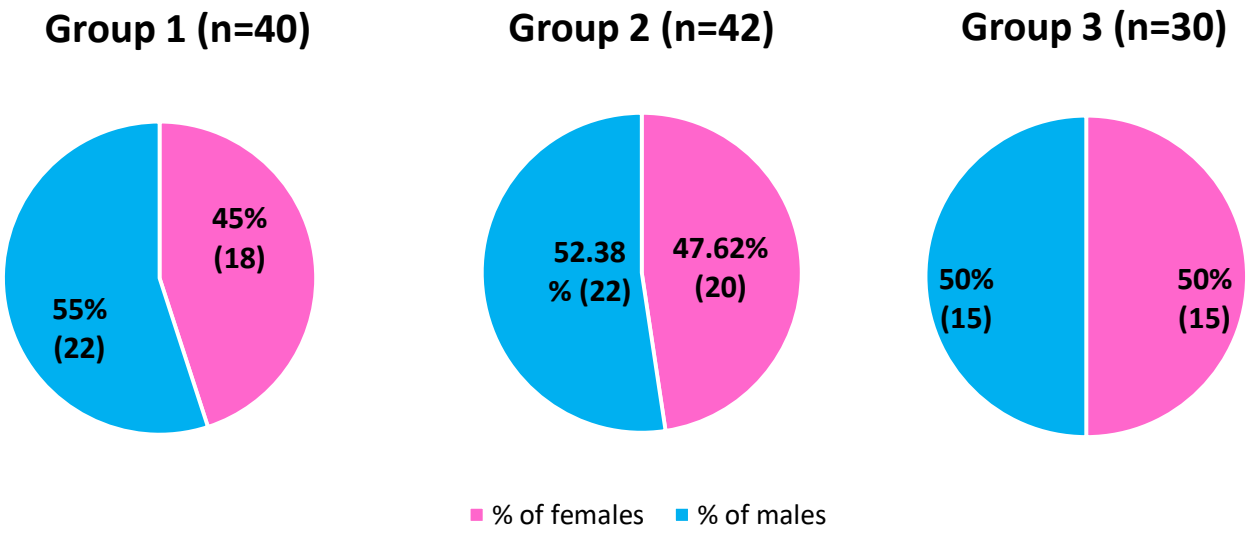

Figure 14. *Sex distribution in subgroups of the study group. Absolute numbers are given in brackets.*

Table 3. *Age distribution in the control and study group.*

	Mean	Median	Min	Max	SD
Study group (n=112)	13.78	14.23	6.07	18.00	3.00
Control group (n=30)	11.81	11.63	7.60	16.20	2.40

5.1.1.3. Diabetes duration

The duration of diabetes in the study group ranged from the minimum of 0.14 (less than 2 months) to the maximum of 15.61 years. The mean duration of diabetes was 7.01 years (SD 4.18; 95%CI: 6.23-7.80) and the median DM duration was 6.92 years.

5.1.1.4. HbA1c

The HbA1c ranged from the minimum of 4.80 to the maximum of 11.60%. The median glycated haemoglobin was 7.35% and the mean HbA1c was 7.64% (SD 1.31; 95%CI: 7.40-7.89%).

5.1.1.5. Treatment

In the study group, 94 children (83.93%) used an insulin pump and 18 children (16.07%) received injection insulin therapy (**Figure 15**). **Figure 15** also shows the breakdown for individual subgroups.

Out of the children using insulin pumps, 83 i.e. 88.30% used Medtronic and 11, i.e. 11.70% used Roche brand. The duration of insulin pump therapy ranged from 0.08 (1 month) to 13.2 years, with the mean of 5.73 years and the median of 5.16 years (95%CI: 0.73, SD: 3.55).

Among the children using injection insulin therapy, the treatment regimens included: Lantus (Glargine) with Apidra (Glulisine) (10 children, i.e. 55.56%), Lantus (Glargine) with NovoRapid (Aspart) (5 children, i.e. 27.78%), Abasaglar (Glargine) with Humalog (Lispro) (3 children, i.e. 16.66%).

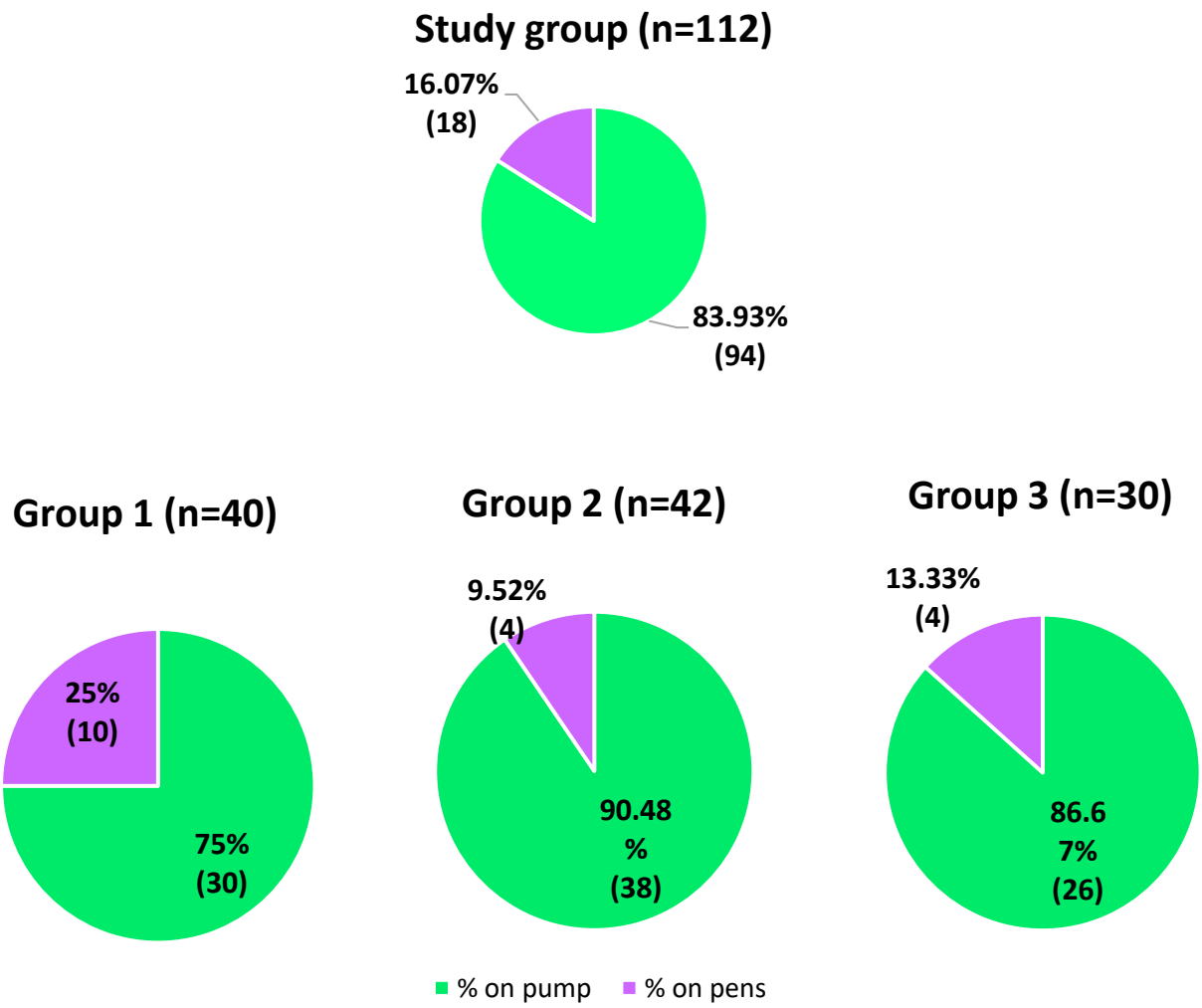

Figure 15. *Number and percentage of children on insulin pump and injection therapy in the study group cumulatively and in each subgroup. Absolute numbers are given in brackets.*

5.1.1.6. Family history of DM

Among the diabetic children, 28, i.e. 25% had family history of T1DM. This included mother or father (3 children), sibling (14 children, 2 of which were twins), grandparents (3 children), aunt or uncle (6 children) and cousins (7 children). Six children had more than one affected family member.

5.1.1.7. Comorbidities

Other co-existing autoimmune disease were present in 29 children, i.e. 25.89%. These included 8 children with coeliac disease (7 confirmed, 1 suspicion) and 23 children with autoimmune thyroid disease. Two children were suffering from both.

Other concurrent disorders included allergies (10 children), asthma (4 children), eczema (1 child), nephrotic syndrome (1 child) and congenital adrenal hypertrophy (1 child).

5.1.1.8. Diet and exercise

Out of all the diabetic children, 24 (21.43%) were adherent to a special diet. This included gluten free diet (3 children) and reduction of sugars and/or fats (21 children).

Almost all, 106 children (94.64%), reported undertaking regular exercise, with the frequency ranging from 1 to 7 times a week.

Due to large variability of the diets and types and frequencies of physical exercise described, as well as potential bias in the information obtained (this data was collected from children and their parents during an interview), adherence to a diet and physical exercise were not considered in the subsequent analysis.

5.1.1.9. BG amplitude

Data was collected on the lowest and highest BG in the last week and month. However, due to the unreliable nature of the data a decision was made not to use it in the analysis to avoid bias.

5.1.1.10. Diabetic screening

Out of all the diabetics, 50 (44.64%) children attended regular diabetic retinopathy screening 6-monthly, yearly or 2 yearly.

5.1.1.11. Visual acuity and ophthalmic examination

In the study group the visual acuity ranged from 0.6 to 1, with the mean of 0.95 (SD 0.09). In 22 children no spherical refractive error was detected, whereas 41 children were myopic ranging from -0.25D to -5D and 49 children were hypermetropic ranging from +0.25D to +5D. A degree of astigmatism was found in 31 children ranging from -2.25D to +0.25D. Glasses were worn by 26 children.

None of the children had any evidence of diabetic retinopathy. On examination vessel tortuosity was noted in 14 children and dilated vessels in 17 children. Mild cataract was noted in 5 cases.

Others coincidental examination findings included: a crowded optic disc (6 children), nasal shifting of optic disc vessels (2 children), diluted fundus (2 children), mild lid retraction (1 child), peripapillary atrophy (1 child), pigmented disc margin (27 children), choroidal naevus (1 child) and conjunctival papillae (6 children).

In the control group, the visual acuity ranged from 0.7 to 1, with the mean of 0.9 (SD 0.1). In 3 children no spherical refractive error was noted, whereas 7 children were myopic ranging from -0.25D to -3D

and 20 children were hypermetropic ranging from +0.25D to +1.25D. A degree of astigmatism was found in 24 children ranging from -1D to +0.5D. Glasses were worn by 18 children.

The coincidental examination findings in the control group included: vein tortuosity (3 children), dilated veins (1 child), choroidal naevus (1 child), crowded optic disc (2 children), dilated fundus (1 child), conjunctival papillae (4 children) and a pigmented disc margin (4 children).

5.1.2. FAZ measurements

Large differences in the FAZ parameters were noted between the study (n=112) and control group (n=30). The mean DCP FAZ surface area in the study group, 520.36µm^2 (SD 160.02µm^2), was significantly larger than in the control group, 408.56µm^2 (SD 114.97µm^2) (p=0.0005) (**Figure 16**). Analogically, the mean DCP to SCP FAZ surface area ratio in the study group, 1.88 (SD 0.68), was significantly greater than in the control group, 1.58 (SD 0.48) (p=0.0232) (**Figure 17**).

The mean SCP FAZ area in the study group, 302.74µm^2 (SD 119.15µm^2), was also larger than in the control group, 284.37µm^2 (SD 123.20µm^2), however, the difference was not statistically significant (p=0.46).

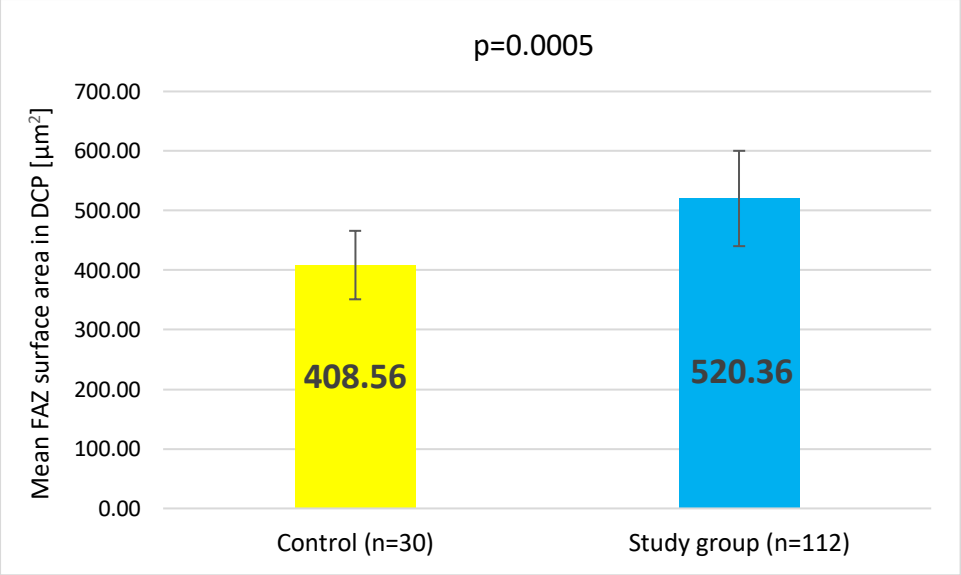

Figure 16. *Deep capillary plexus FAZ surface area in the study and control group.*

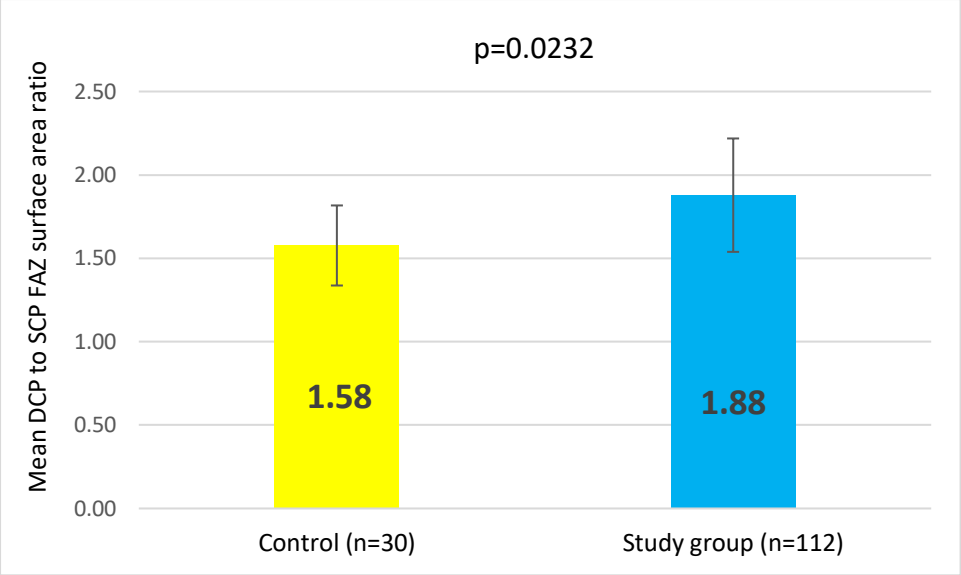

Figure 17. *DCP to SCP FAZ surface area ratio in the study and control group.*

Another comparison was made between the control group and the 3 subgroups of the study group, depending on the duration of diabetes.

The mean FAZ surface area in the deep capillary plexus was smallest in the control group (408.6µm^2) (**Table 4, Figure 18**). It gradually increased to 502.2µm^2 in Group 1 and 523.9µm^2 in Group 2 and was largest, 539.7µm^2, in Group 3. (**Table 4, Figure 18**). Significant differences were found between the DCP FAZ surface area in the control group and Group 1 (p=0.0120), Group 2 (p=0.0019) and Group 3 (p=0.0011). The differences between the subgroups of the study group were not statistically significant.

Similarly, the mean DCP to SCP FAZ surface area ratio was lowest in the control group (1.58) and gradually increased in the study group from 1.75 in Group 1, through 1.93 in Group 2 to 1.98 in Group 3 (**Table 5, Figure 19**). Significant differences were found between this ratio in the control group and Group 2 (p=0.0210) and Group 3 (p=0.0169).

The mean FAZ surface area in the superficial capillary plexus was smallest in the control group (284.4µm^2) and largest in Group 1 (314.1µm^2). However, no trend or significant difference was noted between the subgroups of the study group and the control group (**Table 6**).

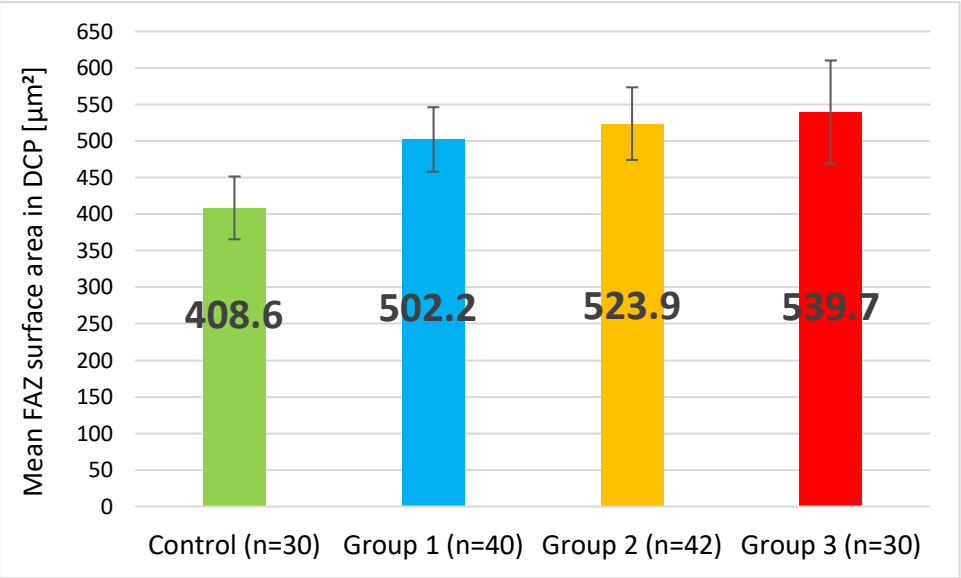

Figure 18. *Mean FAZ surface area in DCP in the control group and subgroups of the study group. Significant differences were found between the DCP FAZ surface area in the control group and Group 1 (p=0.0120), Group 2 (p=0.0019) and Group 3 (p=0.0011). The differences between the subgroups of the study group were not statistically significant.*

Table 4. *FAZ surface area in DCP in the control group and subgroups of the study group – descriptive statistics.*

Group	Mean [µm²]	95% CI [µm²]	SD [µm²]	Min [µm²]	Max [µm²]	Q25 [µm²]	Median [µm²]	Q75 [µm²]
Control (n=30)	408.6	365.6 – 451.5	115.0	176.8	733.0	338.7	386.0	456.9
1 (n=40)	502.2	458.1 – 546.3	137.8	265.3	833.7	412.5	487.0	598.2
2 (n=42)	523.9	474.2 – 573.5	159.2	220.9	958.6	428.7	526.2	624.8
3 (n=30)	539.7	469.1 – 610.3	189.1	187.1	851.3	411.0	530.0	703.7

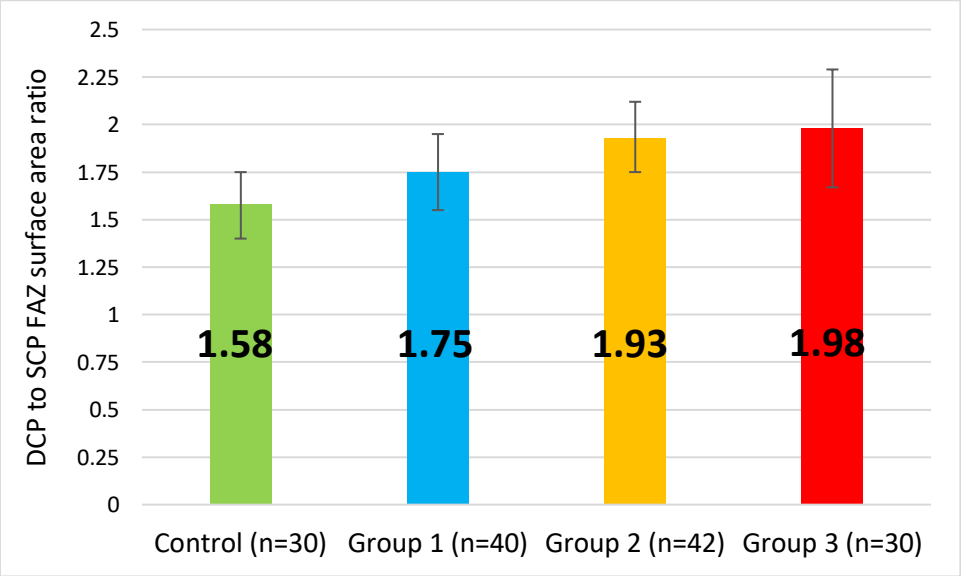

Figure 19. *Mean DCP to SCP FAZ surface area ratio in the control group and subgroups of the study group. Significant differences were found between the ratio in the control group and Group 2 (p=0.0210) and Group 3 (p=0.0169).*

Table 5. *DCP to SCP FAZ surface area ratio in the control group and subgroups of the study group – descriptive statistics.*

	Mean	95.00% CI	SD	Q25	Median	Q75
Control (n=30)	1.58	1.40 – 1.75	0.48	1.20	1.52	1.77
1 (n=40)	1.75	1.55 – 1.95	0.62	1.30	1.63	1.95
2 (n=42)	1.93	1.75 – 2.12	0.60	1.56	1.83	2.06
3 (n=30)	1.98	1.67 – 2.29	0.83	1.59	1.74	2.07

Table 6. *FAZ surface area in SCP in the control group and subgroups of the study group – descriptive statistics.*

Group	Mean [μm^2]	95.00% CI [μm^2]	SD [μm^2]	Min [μm^2]	Max [μm^2]	Q25 [μm^2]	Median [μm^2]	Q75 [μm^2]
Control (n=30)	284.4	238.4 – 330.4	123.2	90.3	545.6	198.4	248.9	372.3
1 (n=40)	314.1	279.0 – 349.1	109.6	73	515	250.4	312.3	397.0
2 (n=42)	289.7	253.9 – 325.5	115.0	105.5	616.0	198.4	269.4	369.7
3 (n=30)	305.9	254.4 – 357.5	138.1	92.2	522.3	193.9	278.4	449.8

The difference between the DCP and SCP FAZ surface area was calculated for the study and control group as well as all subgroups of the study group. The DCP and SCP FAZ surface area difference in the study group was significantly larger than in the control group ($p<0.0001$) (**Table 7**). The difference between FAZ areas in the control group was significantly smaller than in Group 1 ($p<0.006$), Group 2 ($p<0.0001$) and Group 3 ($p<0.0001$) (**Table 7, Figure 20**).

Significant differences were also noted between the subgroups. Group 1 differed significantly from Group 2 ($p<0.03$), Group 3 ($p<0.05$).

Table 7. *Difference between DCP and SCP FAZ surface area in the study group, control group and all subgroups of the control group.*

Group	Δ DCP and SCP FAZ surface area [μm^2]	
	Mean	SD
Control (n=30)	124.2	72.8
Group 1 (n=40)	188.1	95.5
Group 2 (n=42)	234.2	98.6
Group 3 (n=30)	233.8	104.9
Entire study group (n=121)	217.6	100.8

The DCP and SCP FAZ surface area difference in the study group was significantly larger than in the control group ($p<0.0001$). The difference between FAZ areas in the control group was significantly smaller than in Group 1 ($p<0.006$), Group 2 ($p<0.0001$) and Group 3 ($p<0.0001$). Significant differences were also noted between the subgroups. Group 1 differed significantly from Group 2 ($p<0.03$), Group 3 ($p<0.05$).

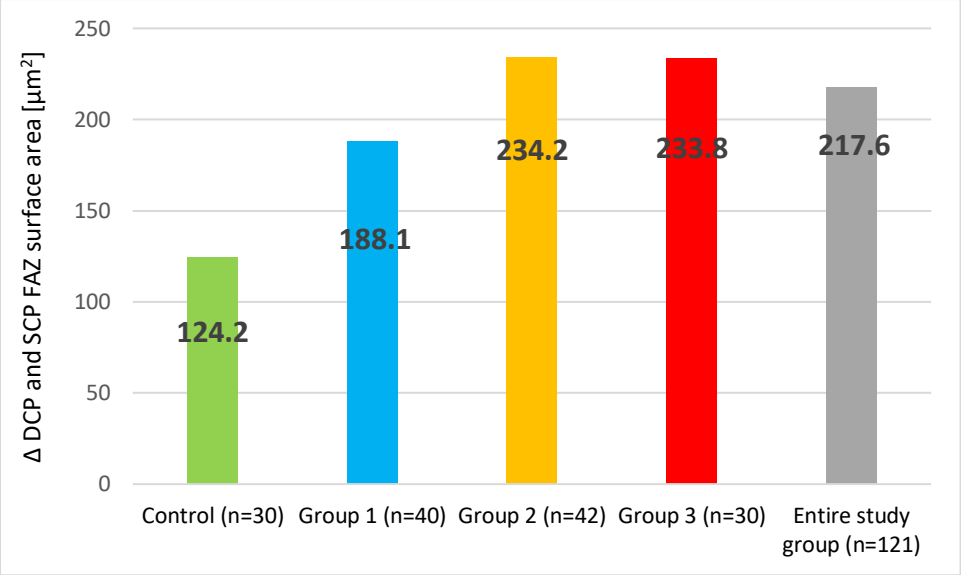

Figure 20. *Difference between DCP and SCP FAZ surface area in the study group, control group and all subgroups of the control group. The DCP and SCP FAZ surface area difference in the study group was significantly larger than in the control group (p<0.0001). The difference between FAZ areas in the control group was significantly smaller than in Group 1 (p<0.006), Group 2 (p<0.0001) and Group 3 (p<0.0001). Significant differences were also noted between the subgroups. Group 1 differed significantly from Group 2 (p<0.03), Group 3 (p<0.05).*

5.1.3. Correlation analysis

5.1.3.1. SCP and DCP FAZ surface area

A very strong positive correlation was found between the SCP and DCP FAZ surface areas in the study and control group, with r=0.7774 (p<0.05) and r=0.815357 (p<0.05), respectively (**Figure 21**).

This strong correlation was also noted in each subgroup of the study group, with r=0.7244, r=0.7878 and r=0.8391 for Group 1, 2 and 3, respectively (p<0.05).

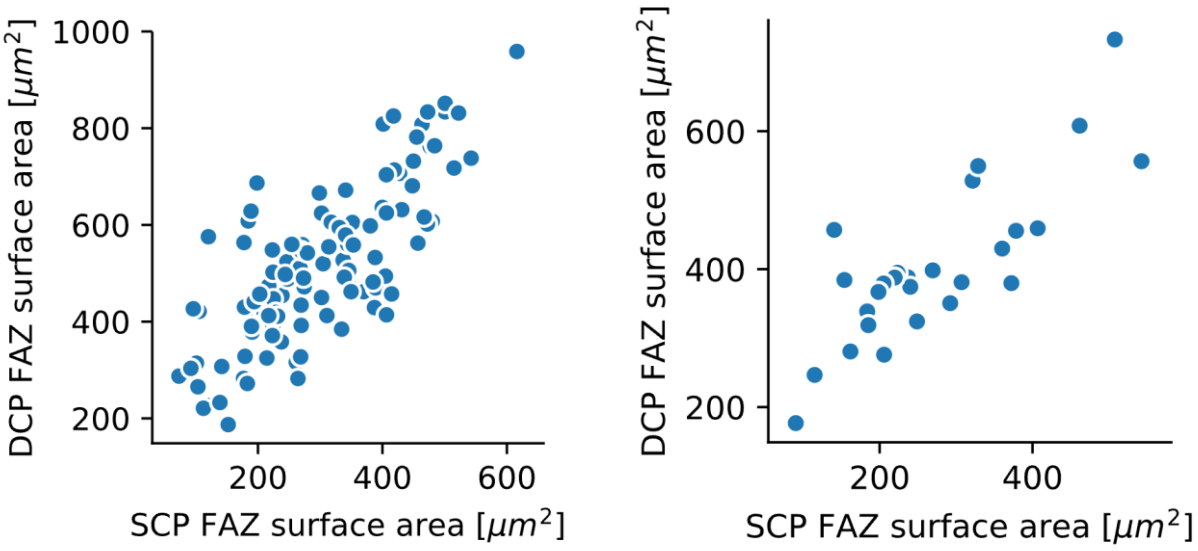

Figure 21. *Correlation between DCP and SCP surface area. Left: the study group (r=0.7774), p<0.05. Right: control group r=0.815357, p<0.05.*

5.1.3.2. HbA1C, DM duration and BG on examination and age and FAZ parameters

In the study group a very weak correlation was found between the SCP FAZ surface area and BG on examination, r=-0.2052 (p<0.05) (**Table 8**). The determination coefficient was very low, 4.20%, showing that the variability of the SPC FAZ parameters is dependent on the BG on examination in only 4.20% of cases and in approximately 96% of cases it is affected by other factors. The correlation between the BG on examination and the DCP to SCP FAZ surface area ratio was even weaker with a Pearson's correlation coefficient of r=0.1887 (p<0.05) (**Table 8**) and a determination coefficient of 3.56%, showing that the ratio variability is dependent on the BG on examination in only 3.6% of cases. No correlation was found between the FAZ parameters and the DM duration or HbA1c (**Table 8**).

No correlation was found between the FAZ parameters and age in the study group. The correlation coefficients were r=0.0423, r=0.0540 and r=0.0185 for the SCP FAZ surface area, DCP FAZ surface area and DCP to SCP FAZ surface area ratio, respectively.

Similarly, in the control group no correlation was found between age and FAZ parameters, with correlation coefficients of r=-0.2250, r=-0.1312 and r=0.2228 for the SCP FAZ surface area, DCP FAZ surface area and DCP to SCP FAZ surface area ratio, respectively.

Table 8. *Pearson's correlation coefficient for the correlation between the FAZ parameters and the last HbA1C, DM duration and BG on examination in the study group.*

	SCP FAZ surface area	DCP FAZ surface area	DCP to SCP FAZ surface ratio
last HbA1c [%]	-0.1449	-0.1222	0.0331
BG On Exam	**-0.2052 (p<0.05)**	-0.0705	**0.1887 (p<0.05)**
DM duration [years]	-0.0317	0.1089	0.1421

Significant correlations are highlighted in bold and their p-values given in brackets.

On a subgroup level, in Group 1 a weak negative correlation was found between the last HbA1c and the SPC and DCP FAZ surface area with r=-0.3480 (p<0.05) and r=-0.4496 (p<0.05), respectively. This suggests a decrease of the SCP and DCP surface areas with increasing HbA1c in children with a short duration of diabetes (**Table 9**). However, the determination coefficients were only 12.11% and 20.21% for the correlation of HbA1c with the SPC and DCP FAZ surface area, respectively. This shows that the variability of the SPC and DCP FAZ area depends on HbA1c in only 12.11% and 20.11% of cases, respectively. No significant correlation was found between the SPC and DCP FAZ surface area and the DM duration or BG on examination in Group 1 (**Table 9**).

In Groups 2 and 3 no significant correlation was found between the FAZ parameters and the last HbA1c, DM duration or BG on examination (**Tables 10&11**).

Table 9. *Pearson's correlation coefficient for the correlation between the FAZ parameters and the last HbA1C, DM duration and BG on examination in Group 1 of the study group.*

Group 1	SCP FAZ surface area	DCP FAZ surface area	DCP to SCP FAZ surface ratio
last HbA1c [%]	**-0.3480 (p<0.05)**	**-0.4496 (p<0.05)**	0.0643
BG On Exam	-0.2034	-0.2366	0.1462
DM duration [years]	-0.1147	-0.0220	0.1722

Notable correlation coefficients are shown in bold and their p-values given in brackets.

Table 10. *Pearson's correlation coefficient for the correlation between the FAZ parameters and the last HbA1C, DM duration and BG on examination in Group 2 of the study group.*

Group 2	SCP FAZ surface area	DCP FAZ surface area	DCP to SCP FAZ surface ratio
last HbA1c [%]	0.1903	0.1782	-0.1119
BG On Exam	-0.1846	-0.1284	0.1350
DM duration [years]	0.0616	0.1934	0.1502

Table 11. *Pearson's correlation coefficient for the correlation between the FAZ parameters and the last HbA1C, DM duration and BG on examination in Group 3 of the study group.*

Group 3	SCP FAZ surface area	DCP FAZ surface area	DCP to SCP FAZ surface ratio
last HbA1c [%]	-0.3014	-0.2705	0.0178
BG On Exam	-0.1968	0.0829	0.2309
DM duration [years]	0.0364	0.0132	-0.1778

5.1.4. FAZ parameters in relation to HbA1c

The study group was divided into 3 subgroups depending on the last HbA1c. The subcategories comprised:

- children with HbA1c ≤ 7.0% (n=40), i.e. optimal diabetic control;
- children with HbA1c > 7.0% < 8.5% (n=51), i.e. suboptimal diabetic control;
- children with HbA1C ≥ 8.5% (n=51), i.e. poor diabetic control

The mean DCP FAZ was smallest in children with HbA1c equal to or greater than 8.5% (**Table 12**) and this group differed significantly from the others ($p<0.006$).

The mean SCP FAZ was also smallest in children with HbA1c equal to or greater than 8.5%, however, that difference was not statistically significant.

Table 12. *FAZ parameters in relation to HbA1c.*

	SCP FAZ surface area [μm^2]	DCP FAZ surface area [μm^2]	DCP to SCP FAZ surface ratio
HbA1c ≤ 7.0% (n=40)	318.12 (SD 120.11)	524.94 (SD 145.15)	1.82 (SD 0.71)
HbA1c > 7.0% < 8.5% (n=51)	304.17 (SD 122.78)	537.21 (SD 169.12)	1.91 (SD 0.60)
HbA1C ≥ 8.5% (n=51)	278.44 (SD 115.76)	**434.15** (SD 138.16)	1.71 (SD 0.64)

Significant results are shown in bold. The DCP of children with HbA1c equal to or greater than 8.5% differed significantly from the other groups (p<0.006).

5.1.5. The effect of anthropometric factors on FAZ parameters

No trends were noted between the FAZ parameters and the nutritional status of diabetic children (**Tables 13-15**). No significant differences were found in the FAZ dimensions between children in different nutritional status categories, as per Cole's index.

However, a comparison between diabetic (n=65) and healthy children (n=20) with a 'Normal' Cole's ratio, showed large difference in the FAZ parameters between these groups. The mean DCP FAZ

in the diabetic children was significantly larger than in the control group (p=0.0019) (**Table 16**). The same trend was observed for the difference between the DCP and SCP FAZ surface area which was also significantly greater in diabetic children (p=0.0002) (**Table 16**).

Table 13. *Mean SCP FAZ surface area in relation to the nutritional status of children the study group, as Cole's index, including descriptive statistics.*

Interpretation of Cole's Index	Mean [µm^2]	95.00% CI [µm^2]	SD [µm^2]	Q25 [µm^2]	Median [µm^2]	Q75 [µm^2]
Normal (n=65)	301.2	272.3 – 330.0	116.3	223.2	279.4	399.7
Obese (n=14)	315.0	228.2 – 401.7	150.2	190.6	266.8	401.3
Moderately malnourished (n=12)	281.6	194.8 – 368.3	136.6	157.1	338.8	387.1
Mildly malnourished (n=7)	313.1	247.6 – 378.6	70.9	268.6	271.3	388.2
Overweight (n=14)	310.8	244.5 – 377.2	114.9	217.3	320.4	414.7

Table 14. *Mean DCP FAZ surface area in relation to the nutritional status of children the study group, as Cole's index, including descriptive statistics.*

Interpretation of Cole's Index	Mean [µm^2]	95.00% CI [µm^2]	SD [µm^2]	Q25 [µm^2]	Median [µm^2]	Q75 [µm^2]
Normal (n=65)	524.8	486.5 – 563.2	154.6	422.9	523.8	624.3
Obese (n=14)	519.0	387.5 – 650.5	227.8	324.8	432.1	763.7
Moderately malnourished (n=12)	473.7	395.1 – 552.4	123.8	398.9	475.9	567.1
Mildly malnourished (n=7)	507.6	356.9 – 658.4	163.0	392.2	505.9	559.2
Overweight (n=14)	547.3	464.0 – 630.6	144.3	449.9	532.9	631.5

Table 15. *Mean DCP to SCP FAZ surface area ratio in relation to the nutritional status of children the study group, as Cole's index, including descriptive statistics.*

Interpretation of Cole's Index	Mean	95.00% CI	SD	Q25	Median	Q75
Normal (n=65)	1.88	1.73 – 2.03	0.62	1.57	1.74	2.03
Obese (n=14)	1.76	1.45 – 2.08	0.55	1.52	1.60	2.02
Moderately malnourished (n=12)	2.11	1.38 – 2.85	1.16	1.26	1.77	2.42
Mildly malnourished (n=7)	1.62	1.32 – 1.92	0.32	1.37	1.46	1.98
Overweight (n=14)	1.91	1.55 – 2.28	0.63	1.49	1.72	2.17

Table 16. *FAZ parameters in diabetic and healthy children with a ''normal' Cole's index.*

	Diabetics with a 'normal' Cole's index		Healthy children with a 'normal' Cole's index		P-value
	Mean	SD	Mean	SD	
SCP FAZ surface area [µm^2]	301.2	116.3	271.4	120.0	0.3241
DCP FAZ surface area [µm^2]	524.8	154.6	404.4	114.9	0.0019
Δ DCP and SCP FAZ surface area [µm^2]	223.7	92.6	133.0	79.0	0.0002
DCP/SCP FAZ surface area ratio	1.9	0.622	1.6	0.526	0.1197

The mean DCP FAZ in the diabetic children was significantly larger than in the control group (p=0.0019). Similarly, the difference between the DCP and SCP FAZ surface area was also significantly greater in diabetic children (p=0.0002).

5.1.6. The effect of family history of T1DM on FAZ parameters

No significant differences were found in the FAZ parameters between children with and without a family history of T1DM (**Tables 17-19**).

Table 17. *SCP FAZ area in diabetic children with and without family history of T1DM, including descriptive statistics. P=0.3939.*

T1DM Family History	Mean [µm^2]	95.00% CI [µm^2]	SD [µm^2]	Q25 [µm^2]	Median [µm^2]	Q75 [µm^2]
Yes (n=28)	286.0	238.9 – 333.1	121.5	189.7	242.6	393.4
No (n=84)	308.3	282.6 – 334.0	118.6	224.4	300.4	403.0

Table 18. *DCP FAZ area in diabetic children with and without family history of T1DM, including descriptive statistics. P=0.8892.*

T1DM Family History	Mean [µm^2]	95.00% CI [µm^2]	SD [µm^2]	Q25 [µm^2]	Median [µm^2]	Q75 [µm^2]
Yes (n=28)	516.7	455.0 – 578.4	159.0	416.9	478.0	633.9
No (n=84)	521.6	486.6 – 556.6	161.3	413.3	508.2	603.7

Table 19. *SCP to DCP FAZ surface area ratio in diabetic children with and without family history of T1DM, including descriptive statistics. P=0.2546*

T1DM Family History	Mean	95.00% CI	SD	Q25	Median	Q75
Yes (n=28)	2.00	1.71 – 2.30	0.77	1.56	1.70	2.20
No (n=84)	1.84	1.70 – 1.98	0.64	1.48	1.72	1.98

5.1.7. The effect of insulin therapy delivery mode on FAZ parameters

The FAZ surface area in the SCP and DCP was smaller in children on insulin pumps compared with children on multiple daily injections (**Tables 20&21**) and the DCP to SCP FAZ surface area ratio was slightly larger (**Table 22**), however, the differences were not statistically significant. The diabetic

control was slightly worse in children treated with injections compared with children on insulin pumps, with the mean HbA1c of 8.17% (SD 1.68%) and 7.54% (SD 1.21%), respectively.

Table 20. *SCP FAZ area in diabetic children treated with insulin pump and injections including descriptive statistics. P=0.5015*

Treatment	Mean [µm^2]	95.00% CI [µm^2]	SD [µm^2]	Q25 [µm^2]	Median [µm^2]	Q75 [µm^2]
Pump (n=94)	299.4	275.3 – 323.5	117.7	204.2	272.2	404.8
Injections (n=18)	320.1	256.2 – 384.1	128.7	224.1	350.7	389.1

Table 21. *DCP FAZ area in diabetic children treated with insulin pump and injections including descriptive statistics. P=0.5599.*

Treatment	Mean [µm^2]	95.00% CI [µm^2]	SD [µm^2]	Q25 [µm^2]	Median [µm^2]	Q75 [µm^2]
Pump (n=94)	516.5	484.6 – 548.4	155.8	412.6	515.2	616.4
Injections (n=18)	540.6	449.1 – 632.2	184.1	449.9	489.8	605.1

Table 22. *DCP to SCP FAZ area ratio in diabetic children treated with insulin pump and injections including descriptive statistics. P=0.8798.*

Treatment	Mean	95.00% CI	SD	Q25	Median	Q75
Pump (n=94)	1.88	1.74 – 2.02	0.69	1.51	1.71	2.06
Injections (n=18)	1.86	1.54 – 2.17	0.64	1.49	1.74	2.02

5.1.8. Gender differences in FAZ parameters

In the study group the SCP FAZ surface area was significantly smaller in boys (266.7µm^2) than in girls (342.9µm^2) (p=0.0006) (**Table 23, Figure 22**). The DCP FAZ surface area was also significantly smaller in males (474.0µm^2) compared with females (572.0µm^2) (p=0.0010) (**Table 23, Figure 22**). The mean DCP to SCP FAZ surface area ratio was larger in boys (2.0) than in girls (1.8), however, the difference was not statistically significant (**Table 23**).

Analogical differences between genders were noted on a subgroup level, where diabetics were divided according to the duration of the disease. In each subgroup, the mean SCP and DCP FAZ areas in boys were smaller than in girls (**Tables 24-26**).

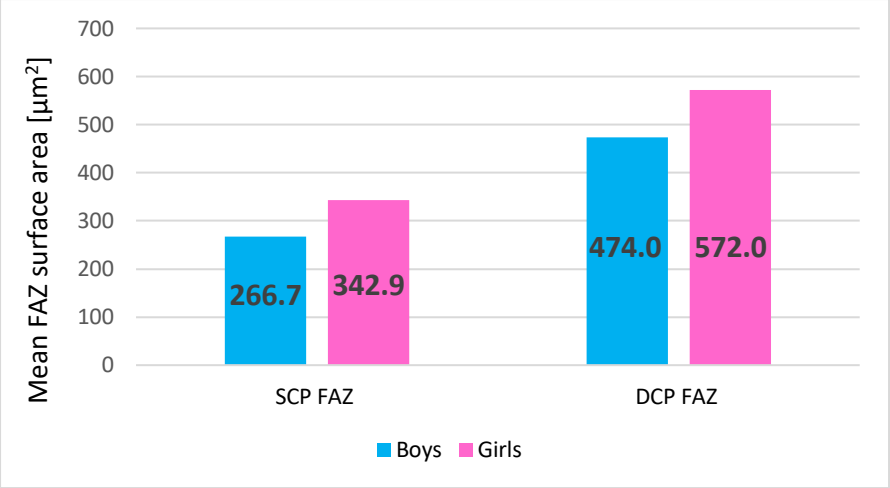

Figure 22. *Differences in FAZ parameters between genders in the study group. The difference between genders in SCP FAZ area (p=0.0006) and DCP FAZ area (p=0.0010) was statistically significant.*

Table 23. *Differences in FAZ parameters between genders.*

Study group	Boys (n=59)		Girls (n=53)		P-value
	Mean	SD	Mean	SD	
Mean SCP FAZ [µm²]	**266.7**	108.6	**342.9**	118.5	**0.0006**
Mean DCP FAZ [µm²]	**474.0**	138.6	**572.0**	167.6	**0.0010**
Mean DCP/SCP FAZ ratio	2.0	0.7	1.8	0.6	0.1746

Significant differences are shown in bold.

Table 24. *Differences in FAZ parameters between genders in group 1 of the study group.*

Group 1	Boys (n=22)		Girls (n=18)		P-value
	Mean	SD	Mean	SD	
Mean SCP FAZ [µm²]	285.8	109.9	348.5	101.7	0.0713
Mean DCP FAZ [µm²]	**457.6**	130.4	**556.6**	129.8	**0.0217**
Mean DCP/SCP FAZ ratio	1.8	0.7	1.7	0.5	0.5759

Significant differences are shown in bold.

Table 25. *Differences in FAZ parameters between genders in group 2 of the study group.*

Group 2	Boys (n=22)		Girls (n=20)		P-value
	Mean	SD	Mean	SD	
Mean SCP FAZ [µm²]	**247.8**	99.3	**335.8**	115.6	**0.0114**
Mean DCP FAZ [µm²]	486.7	130.9	564.7	180.0	0.1141
Mean DCP/SCP FAZ ratio	**2.1**	0.7	**1.7**	0.5	**0.0456**

Significant differences are shown in bold.

Table 26. *Differences in FAZ parameters between genders in group 3 of the study group.*

Group 3	Boys (n=15)		Girls (n=15)		P-value
	Mean	SD	Mean	SD	
Mean SCP FAZ [µm²]	266.2	121.6	345.7	146.1	0.1165
Mean DCP FAZ [µm²]	479.3	166.3	600.0	196.6	0.0802
Mean DCP/SCP FAZ ratio	2.0	0.8	2.0	0.9	0.9585

Like in the study group, in the control group the mean DCP FAZ surface area was significantly smaller in boys (381.6µm^2) than in girls (482.8µm^2) (p=0.0302). The SCP FAZ surface area was also smaller in males, however, the difference was not statistically significant (**Table 27**). Unlike in the study group, the DCP to SCP FAZ surface area ratio in the control was smaller in boys than in girls (**Table 27**).

Table 27. *Control group FAZ parameter differences between genders.*

Control group	Boys (n=22)		Girls (n=8)		P-value
	Mean	SD	Mean	SD	
Mean SCP FAZ [µm^2]	261.2	100.6	348.2	161.8	0.0870
Mean DCP FAZ [µm^2]	**381.6**	111.3	**482.8**	95.0	**0.0302**
Mean DCP/SCP FAZ ratio	1.5	0.3	1.7	0.8	0.5312

The differences in DCP FAZ area between genders was statistically significant (p=0.0302) – shown in bold.

In order to account for the gender differences, a comparison was made between the FAZ parameters in diabetic vs healthy girls and diabetic vs healthy boys. Previously identified trends were confirmed in both gender groups, with larger mean SCP and SCP FAZ surface areas and mean DCP to SCP FAZ surface area ratios in diabetic children compared with the controls (**Tables 28-29**).

Table 28. *FAZ parameters in diabetic and healthy boys.*

Boys	Diabetic boys (n=59)		Healthy boys (n=22)		P-value
	Mean	SD	Mean	SD	
SCP FAZ [µm^2]	266.65	108.55	261.15	100.61	p=0.84
DCP FAZ [µm^2]	474.01	138.58	381.56	111.25	**p=0.006**
DCP/SCP FAZ ratio	1.96	0.70	1.54	0.30	**p=0.009**

Significant differences are show in bold.

Table 29. *FAZ parameters in diabetic and healthy girls.*

Girls	Diabetic girls (n=53)		Healthy girls (n=8)		P-value
	Mean	SD	Mean	SD	
SCP FAZ [µm^2]	342.91	118.48	348.21	348.21	p=0.91
DCP FAZ [µm^2]	571.96	167.59	482.81	482.81	p=0.15
DCP/SCP FAZ ratio	1.79	0.64	1.67	1.67	p=0.64

5.2. Central retinal and choroid thickness

5.2.1. Demographics

5.2.1.1. Study size and image quality

In total, 129 diabetic children were examined by radial macular OCT. Eight children were excluded due to unsatisfactory quality or of the images obtained. The analysis was performed for 121 diabetic children and included 70 right and 51 left eye examinations.

For the purpose of some analyses, the study group was divided into 3 subgroups depending on the duration of diabetes:

- Group 1: less than 5 years;
- Group 2: 5-10 years;
- Group 3: more than 10 years.

Groups 1, 2 and 3 consisted of 52, 39 and 30 children, respectively.

In terms of the control group, 37 healthy children were examined and 5 were excluded due to inadequate images. The analysis was completed for 32 controls and included 19 right and 13 left eye examinations.

The quality of the radial macula OCT images ranged from 97 to 100 with the mean of 98.52 (SD 0.69; 95% CI: 0.13).

5.2.1.2. Age and gender

The gender distribution in the study and control group was very similar with a slightly larger proportion of males in both groups (**Figure 23**). The number of boys and girls was also similar in each subgroup of the study group (**Figure 24**). The age of children in the study and control group was comparable with the mean age of 13.35 and 11.24 years, respectively (**Table 30**) The range of ages was slightly broader in the study group where children were aged 6 to 18 years old, compared with the control group which comprised children between 7 and 16 years of age (**Table 30**).

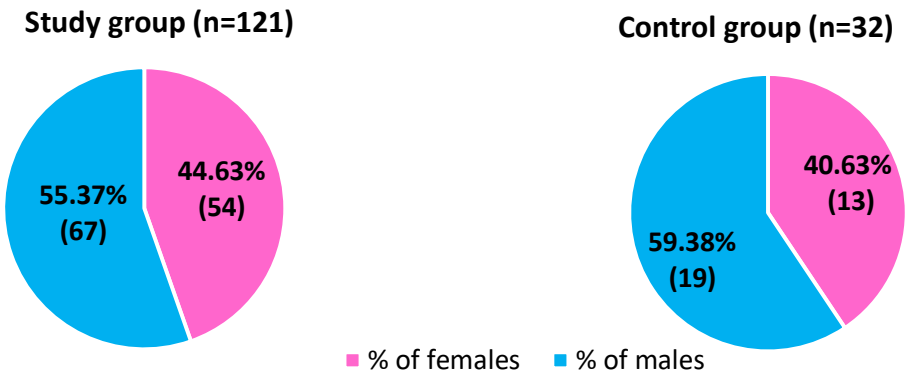

Figure 23. *Sex distribution in the study and control group. Absolute numbers are given in brackets.*

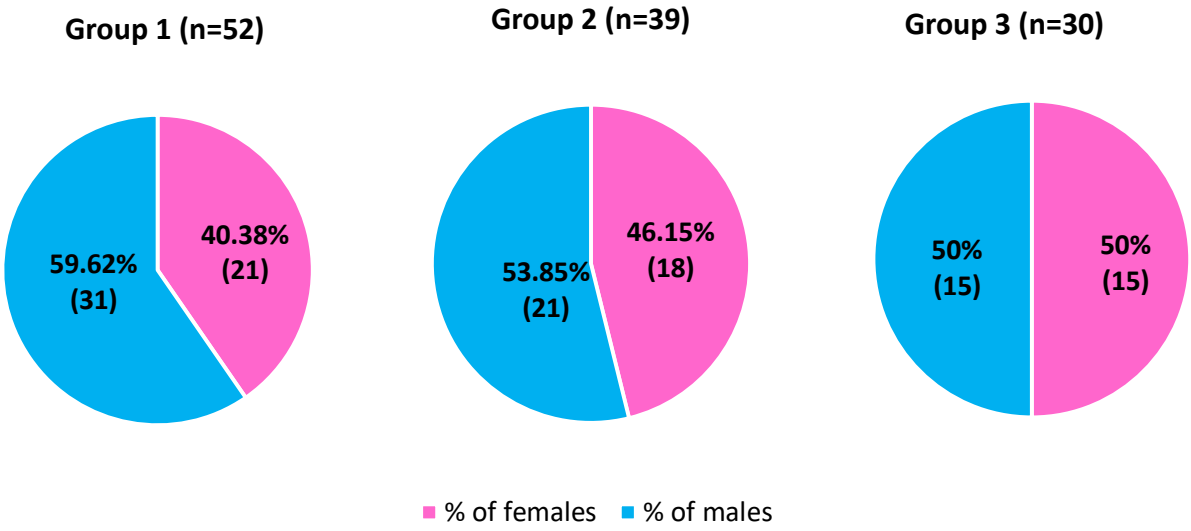

Figure 24. Sex distribution in the 3 subgroups of the study group. Absolute numbers are given in brackets.

Table 30. *Age characteristics of the study and control group.*

	Mean age	Median	Minimum	Maximum	SD
Study group (n=121)	13.34	13.8	6.01	18.00	3.23
Control group (n=32)	11.24	11.25	7.3	16.2	2.63

5.2.1.3. Diabetes duration

For the entire study group, the duration of diabetes ranged from the minimum of 0.14 (less than 2 months) to the maximum of 15.61 years. The median DM duration was 5.85 and the mean DM duration was 6.53 years (SD 4.32; 95%CI: 2.69-11.48).

5.2.1.4. HbA1c

The HbA1c in the study group ranged from the minimum of 4.80% to the maximum of 12.40%. The median glycated haemoglobin was 7.3% and the mean was 7.67% (SD 1.4; 95%CI: 6.43-9.27%).

5.2.1.5. Treatment

Among the diabetic children, 95 (78.51%) used an insulin pump and 26 (21.49%) received injection insulin therapy (**Figure 25**). The breakdown for individual subgroups can be found in **Figure 25**. Out of the children using insulin pumps, 85 i.e. 89.47% used Medtronic and 10 children, i.e. 10.53% used Roche brand. The duration of insulin pump therapy ranged from 0.08 (1 month) to 13.2 years, with the mean of 5.62 years (95%CI: 0.73, SD: 3.61) and the median of 4.74 years. Among the children using injection insulin therapy, the treatment regimens included: Lantus (Glargine) with Apidra (Glulisine) (11 children, i.e. 42.31%), Lantus (Glargine) with NovoRapid (Aspart) (8 children, i.e. 30.77%), Abasaglar (Glargine) with Humalog (Lispro) (7 children, i.e. 26.92%).

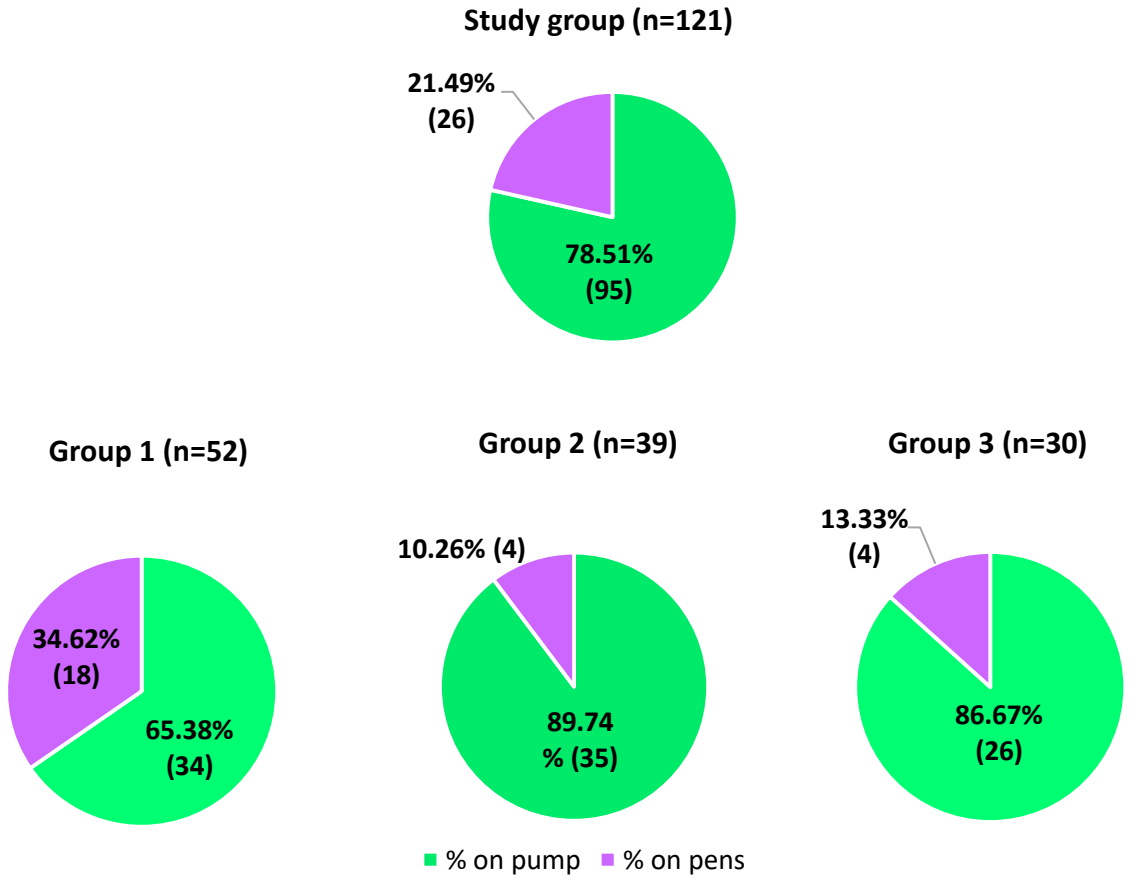

ge of children on insulin pump and injection therapy in the study group cumulatively and in each subgroup. Absolute numbers are given in brackets.

5.2.1.6. Family History of DM

Among the diabetic children, 29, i.e. 23.97% had family history of T1DM. This included mother or father (3 children), a sibling (13 children, 2 of which were twins), grandparents (3 children), aunt or uncle (6 children), cousins (9 children). Seven children had more than one affected family member.

5.2.1.7. Comorbidities

Other autoimmune diseases were present in 28 children, i.e. 23.14%. These included 8 children with coeliac disease (7 confirmed, one suspicion) and 22 children with autoimmune thyroid disease. Two children were suffering from both.

Other concurrent disorders included allergies (11 children), asthma (5 children), eczema (1 child), nephrotic syndrome (1 child) and congenital adrenal hypertrophy (1 child).

5.2.1.8. Diet and exercise

Out of all the diabetic children, 25 (20.66%) were adherent to a special diet. This included a gluten free diet (3 children) and reduction of sugars and/or fats (22 children).

Almost all, 115 children (95.04%), reported engaging in regular physical exercise with the frequency ranging from 1 to 7 times a week.

Due to large variability of the diets and types and frequencies of physical exercise described, as well as potential bias in the information obtained (this data was collected from children and their parents during an interview), adherence to a diet and physical exercise were not considered in the subsequent analysis.

5.2.1.9. BG amplitude

Data was collected on the lowest and highest BG in the last week and month. However, due to the unreliable nature of the data a decision was made not to use it in the analysis to avoid bias.

5.2.1.10. Diabetic screening

Out of all the diabetics, 45 (37.19%) children attended regular diabetic retinopathy screening 6-monthly, yearly or 2 yearly. Sixty nine children did not attend regular DR screening.

5.2.1.11. Vision acuity and ophthalmic examination

The visual acuity in the diabetic children ranged from 0.5 to 1, with the mean of 0.9 (SD 0.1). All children with the visual acuity less than 1 had a corresponding refractive error.

No spherical correction was required in 24 children, 41 children were myopic ranging from -0.25D to -5D and 56 children were hypermetropic ranging from +0.25D to +5D. A degree of astigmatism was found in 77 children ranging from -2.25D to +0.25D. Twenty-nine children were wearing glasses.

None of the children had any evidence of diabetic retinopathy. On slit lamp examination the following retinal vessel changes were noted: vessel tortuosity in 14 children, dilated vessels in 15 children. Six children had a small degree of cataract.

Other coincidental findings included a crowded optic disc (4 children), nasal shifting of central vessels at the optic disc (3 children), mild eyelid retraction (1 child), conjunctival papillae (5 children), pigmented disc margin (29 children), peripapillary atrophy (1 child), choroidal naevus 2 children) and a diluted fundus (2 children).

In the control group the visual acuity ranged from 0.7 to 1, with the mean of 0.9 (SD 0.1). All children with the visual acuity less than 1 had a corresponding refractive error. Three children required no spherical correction, 8 were myopic ranging from -0.25D to -3D and 21 children were hypermetropic ranging from +0.25D to +1D. A degree of astigmatism was found in 23 children ranging from -2.75D to +0.25D. Ten children were wearing glasses.

The examination findings in the control group included: retinal vessel tortuosity (3 children), choroidal naevus (1 child), crowded discs (2 children), dilated fundus (2 children), conjunctival papillae (4 children), and pigmented disc margin (4 children).

5.2.2. Choroid and retina parameters

Comparing the entire study group (n=121) with the control group (n=32), the central and average choroid thickness was noticeably greater in the study group, however, the differences were not statistically significant (**Table 31**). The differences in the retina thickness between the groups were very small, of the magnitude of up to 2µm, and were not statistically significant (**Table 31**).

Table 31. *Choroid and retina parameters in the study and control group.*

	Study group		Control group		P-value
	Mean	SD	Mean	SD	
Central choroid thickness [µm]	325.58	71.00	305.53	61.65	p=0.15
Average choroid thickness [µm]	306.24	63.86	285.85	51.14	p=0.10
Central retina thickness [µm]	247.91	19.91	248.03	18.26	p=0.98
Average retina thickness [µm]	284.14	12.53	282.91	12.91	p=0.63
Choroid/retina thickness ratio	1.08	0.22	1.01	0.17	p=0.11

Subsequently, a comparison was made between the control group and the three subgroups of the study group, depending on the duration of diabetes. The smallest mean central choroid thickness was observed in the control group (305.5μm). It was thicker in diabetic patients in Group 1 (309.2μm), further increased in Group 2 (315.2μm) and the thickest in Group 3, in children with the longest duration of DM, (367.4μm) (**Figure 26**, **Table 32**). Statistically, the mean central choroid thickness in diabetic children from Group 3 was significantly thicker that in Group 1 (p=0.0002), Group 2 (p=0.0014) and in the control group (p=0.0003). This is further evidenced by the 95% confidence interval of the measurement - the higher, +95.00%, confidence interval margin for Group 3 was very large (392.1μm), whereas the lower, -95.00%, margin (342.7μm) was larger than the upper +95.00% CI margin for Group 2 (336.0μm) (**Table 32**).

Analogically, the same tendency was noted for the average choroid thickness, with 285.9μm, 291.0μm, 294.4μm and 348.0μm for the control group, Group 1, Group 2 and Group 3, respectively (**Figure 27**, **Table 33**). The average choroid thickness in patients from Group 3 was also, significantly greater than in Group 1 (p=0.0001), Group 2 (p=0.0003) the control group (p<0.00001). In addition, the large difference in the average choroid thickness in Group 3 was well depicted by the 95% confidence interval with a very large +95.00% CI margin, 369.8μm, and a large -95.00% CI lower margin (326.3μm), which was higher than the upper +95.00% CI margin for Group 2 (312.7μm) (**Table 33**).

The mean choroid to retina thickness ratio was smallest in the control group (1.01). It was slightly larger in Groups 1 and 2 (1.03) and the largest in Group 3 (1.21) (**Figure 28**, **Table 34**). The choroid to retina thickness ratio in Group 3 was significantly different from all the remaining groups, with the statistical significance level of p=0.0002, p=0.0014 and p=0.0001 for Group 1, Group 2 and the control group, respectively. Similarly, the upper +95.00% CI margin was high (1.29), and the lower -95.00%CI margin (1.14) was higher than the upper +95.00% CI margin for Group 2 (1.09) (**Table 34**).

No trend was observed with regards to the central retinal thickness (**Table 35**) and the differences between the groups were not statistically significant.

With regards to the average retinal thickness, it was thinnest in Group 1 (282.0μm) and thickest in Group 3 (287.1μm) (**Table 36**). However, the differences between the study subgroups or control group were not statistically significant.

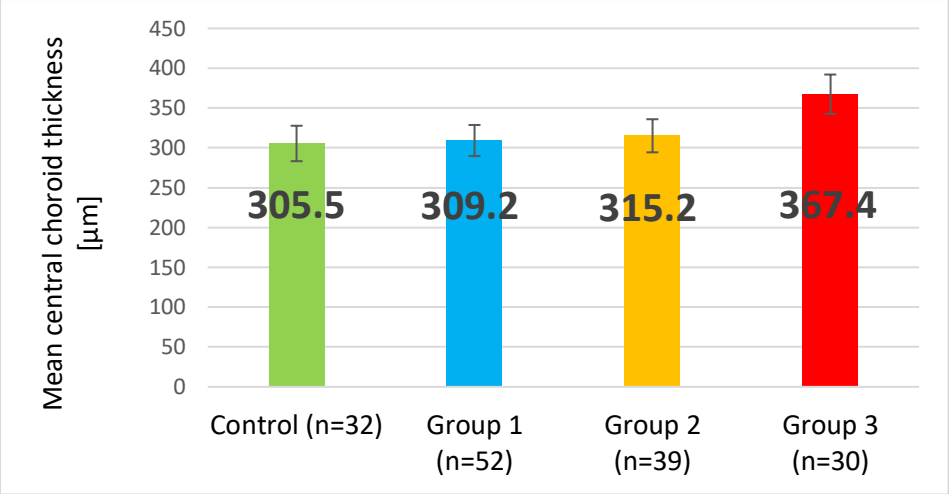

Figure 26. *Mean central choroid thickness in the control group and 3 subgroups of the study group. Statistically, the mean central choroid thickness in diabetic children from Group 3 was significantly thicker that in Group 1 (p=0.0002), Group 2 (p=0.0014) and in the control group (p=0.0003).*

Table 32. *Central choroid thickness in the control group and 3 subgroups of the study group – descriptive statistics.*

	Mean central choroid thickness [µm]	95% CI [µm]	SD [µm]	Min [µm]	Max [µm]	Q25 [µm]	Median [µm]	Q75 [µm]
Control (n=32)	**305.5**	283.3 – 327.8	61.7	212	453	250	308.5	347
Group 1 (n=52)	**309.2**	289.7 – 328.8	70.1	186	475	259.5	292.5	351
Group 2 (n=39)	**315.2**	294.4 – 336.0	64.3	175	443	264	316	359
Group 3 (n=30)	**367.4**	342.7 – 392.1	66.0	239	487	330	364.5	405

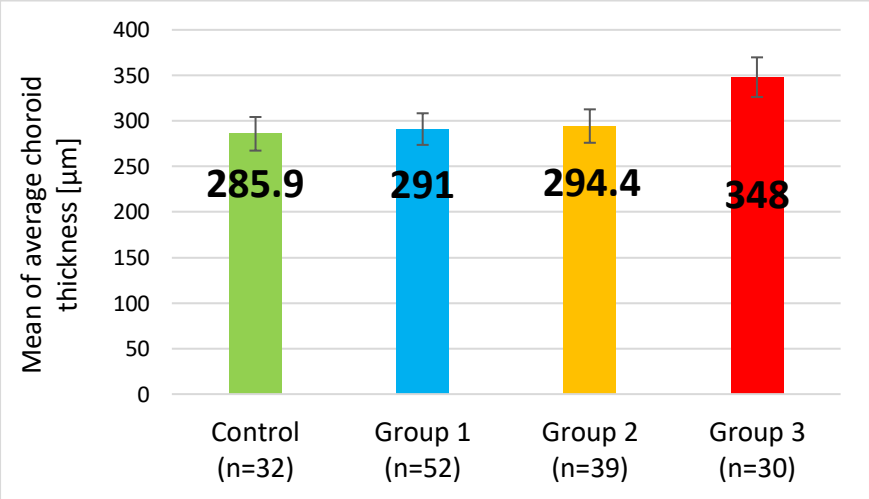

Figure 27. *Average choroid thickness in the control group and 3 subgroups of the study group. The average choroid thickness in patients from Group 3 was also, significantly greater than in Group 1 (p=0.0001), Group 2 (p=0.0003) the control group (p<0.00001).*

Table 33. *Average choroid thickness in the control group and 3 subgroups of the study group – descriptive statistics.*

	Mean of average choroid thickness [µm]	95% CI [µm]	SD [µm]	Min [µm]	Max [µm]	Q25 [µm]	Median [µm]	Q75 [µm]
Control (n=32)	**285.9**	267.4 – 304.3	51.1	202.4	409.8	242.5	286.8	311.4
Group 1 (n=52)	**291.0**	273.7 – 308.4	62.5	171.1	447.6	253.9	279.8	325.8
Group 2 (n=39)	**294.4**	276.0 – 312.7	56.7	175.3	414.9	266.2	289.1	342.6
Group 3 (n=30)	**348.0**	326.3 – 369.8	58.3	239.4	445.7	315.0	347.1	380.1

Table 34. *Choroid to retina thickness ratio in the control group and 3 subgroups of the study group – descriptive statistics.*

	Mean choroid to retina thickness ratio	95% CI	SD	Min	Max	Q25	Median	Q75
Control (n=32)	**1.01**	0.95 – 1.07	0.17	0.71	1.42	0.87	1.03	1.12
Group 1 (n=52)	**1.03**	0.97 – 1.10	0.23	0.66	1.71	0.89	0.98	1.15
Group 2 (n=39)	**1.03**	0.97 – 1.09	0.18	0.59	1.41	0.91	1.03	1.15
Group 3 (n=30)	**1.21**	1.14 – 1.29	0.2	0.86	1.64	1.05	1.2	1.34

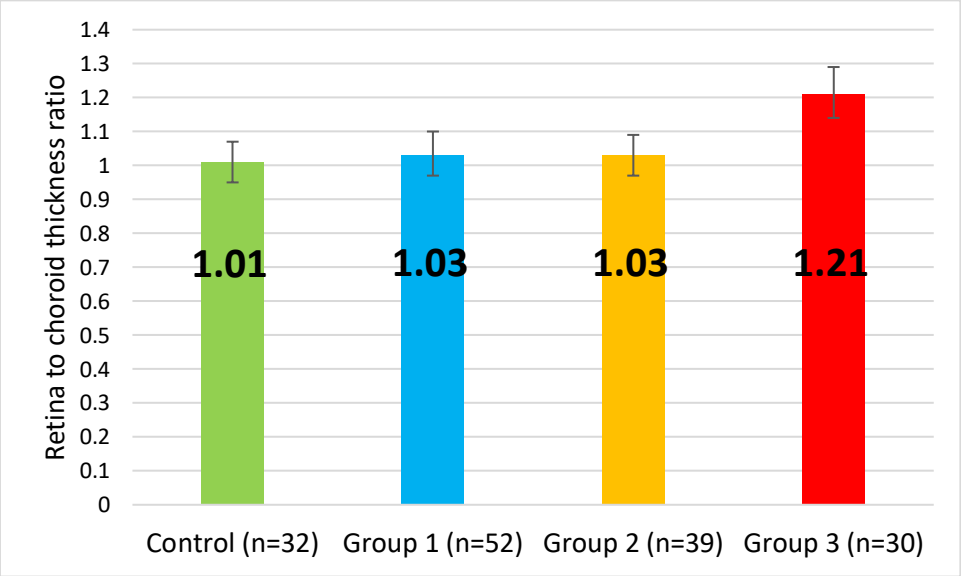

Figure 28. *Retina to choroid thickness ratio in the control group and 3 subgroups of the study group. The choroid to retina thickness ratio in Group 3 was significantly different from all the remaining groups, with the statistical significance level of p=0.0002, p=0.0014 and p=0.0001 for Group 1, Group 2 and the control group, respectively.*

Table 35. *Central retina thickness in the control group and 3 subgroups of the study group – descriptive statistics. The differences between groups were not statistically significant – please refer to main text.*

	Mean central retina thickness [µm]	95% CI [µm]	SD [µm]	Min [µm]	Max [µm]	Q25 [µm]	Median [µm]	Q75 [µm]
Control (n=32)	**248.0**	241.4 – 254.6	18.3	206	281	236.5	247.5	263.5
Group 1 (n=52)	**249.4**	244.0 – 254.8	19.3	205	294	237	251.5	261
Group 2 (n=39)	**245.7**	239.0 – 252.4	20.6	197	288	233	248	260
Group 3 (n=30)	**248.3**	240.7 – 255.9	20.4	211	286	233	246.5	264

Table 36. *Average retina thickness in the control group and 3 subgroups of the study group – descriptive statistics. The differences between groups were not statistically significant – please refer to main text.*

	Mean of average retina thickness [µm]	95% CI [µm]	SD [µm]	Min [µm]	Max [µm]	Q25 [µm]	Median [µm]	Q75 [µm]
Control (n=32)	**282.9**	278.3 – 287.6	12.9	260.9	307.8	273.6	279.45	296
Group 1 (n=52)	**282.0**	279.0 – 285.0	10.7	256.8	306.1	274.6	281.1	289.6
Group 2 (n=39)	**284.7**	280.2 – 289.1	13.8	254.2	329	275.8	283.8	292.1
Group 3 (n=30)	**287.1**	282.1 – 292.2	13.5	259.3	310.5	277.5	284.65	298.4

5.2.3. Correlation analysis

5.2.3.1. Choroid and retina parameters correlation

In the study group a weak positive correlation was noted between the retina average thickness and choroid average and central thickness, with r=0.3126 (p<0.05) and r=0.2625 (p<0.05), respectively (**Table 37**). In the individual analysis of the subgroups a weak correlation (r=0.4003, p<0.05) between the retina average thickness and choroid average thickness was only found in Group 2. No correlation was found between the choroid and retina thickness parameters in the control group (**Table 38**).

Table 37. *Pearson's correlation coefficients for the correlation between the choroid and retina parameters in the study group.*

Study group	Mean central retina thickness	Mean of average retina thickness
Mean central choroid thickness	-0.0866	**0.2625 (p<0.05)**
Mean of average choroid thickness	-0.0663	**0.3126 (p<0.05)**

Notable correlation coefficients are shown in bold with their p-values given in brackets.

Table 38. *Pearson's correlation coefficients for the correlation between the choroid and retina parameters in the study group.*

Control group	Mean central retina thickness	Mean of average retina thickness
Mean central choroid thickness	0.0322	0.2766
Mean of average choroid thickness	-0.0043	0.2572

5.2.3.2. Correlation analysis between the choroid and retina parameters and age, HbA1c, DM duration and BG on examination

In the study group a weak correlation was noted between the age and all choroid and retina thickness parameters except for central retinal thickness (**Table 39**). The determination coefficients were low with 6.11%, 5.78%, 3.82% and 4.14% for the central choroid thickness, average choroid thickness, retina average thickness and the choroid to retina thickness ratio, respectively. This means that these parameters depend on the age in only less than 7% of cases and in the remaining 93% of cases, on different factors. No correlation between the above parameters and age was noted in the control group (**Table 40**).

Furthermore, a weak positive correlation was found between the DM duration and the central choroid thickness ($r=0.2721$, $p<0.05$), the average choroid thickness ($r=0.2938$, $p<0.05$) and the choroid to retina thickness ratio ($r=0.2666$, $p<0.05$) (**Table 41**). However, the coefficients of determination for these correlations were low with 7.40%, 8.63% and 7.12% for the central choroid thickness, average choroid thickness and the choroid to retina thickness ratio, respectively. This means that the choroid parameters depend on the DM duration in only less than 9% of cases and in over 91% cases they are affected by other factors.

For Groups 1-3 no significant correlation was found between the central choroid and retina thickness, average choroid and retina thickness or choroid to retina thickness ratio and the last HbA1c, DM duration or BG on examination (**Tables 42-44**).

Table 39. *Pearson's correlation coefficient for the correlation between the age and choroid and retina thickness parameters in the study group.*

Study group (n=121)	Mean central choroid thickness	Mean of average choroid thickness	Mean central retina central thickness	Mean of average retina thickness	Mean choroid to retina thickness ratio
Age	**0.2471 (p<0.05)**	**0.2404 (p<0.05)**	0.0062	**0.1954 (p<0.05)**	**0.2034 (p<0.05)**

Notable correlation coefficients are marked in bold with their p-values given in brackets.

Table 40. *Pearson's correlation coefficient for the correlation between the age and choroid and retina thickness parameters in the control group (n=32).*

Control group (n=32)	Mean central choroid thickness	Mean of average choroid thickness	Mean central retina central thickness	Mean of average retina thickness	Mean choroid to retina thickness ratio
Age	0.1724	0.1090	0.3251	0.1427	0.0770

Table 41. *Pearson's correlation coefficient for the correlation between the choroid and retina thickness parameters and the last HbA1C, DM duration and BG on examination in the study group (n=121).*

Study group (n=121)	Mean central choroid thickness	Mean of average choroid thickness	Mean central retina central thickness	Mean of average retina thickness	Mean choroid to retina thickness ratio
last HbA1c [%]	-0.0033	-0.0113	0.0238	0.0868	-0.0311
DM duration [years]	**0.2721 (p<0.05)**	**0.2938 (p<0.05)**	-0.0343	0.1402	**0.2666 (p<0.05)**
BG on exam	-0.0676	-0.0599	-0.0573	0.1694	-0.1040

Notable correlation coefficients are marked in bold and their p-values given in brackets.

Table 42. *Pearson's correlation coefficient for the correlation between the choroid and retina thickness parameters and the last HbA1C, DM duration and BG on examination in Group 1 (n=52) of the study group.*

Group 1 (n=52)	Mean central choroid thickness	Mean of average choroid thickness	Mean central retina central thickness	Mean of average retina thickness	Mean choroid to retina thickness ratio
last HbA1c [%]	-0.2148	-0.2056	0.2536	0.2491	-0.2510
DM duration [years]	-0.0615	-0.0669	-0.0119	-0.0614	-0.0558
BG on exam	-0.2525	-0.2579	-0.1684	0.0496	-0.2642

Table 43. *Pearson's correlation coefficient for the correlation between the choroid and retina thickness parameters and the last HbA1C, DM duration and BG on examination in Group 2 (n=39) of the study group.*

Group 2 (n=39)	Mean central choroid thickness	Mean of average choroid thickness	Mean central retina central thickness	Mean of average retina thickness	Mean choroid to retina thickness ratio
last HbA1c [%]	0.2110	0.2133	-0.2986	0.0012	0.2330
DM duration [years]	-0.0784	-0.0923	0.1146	0.1090	-0.1269
BG on exam	0.0133	0.0504	0.0439	0.1346	0.0137

Table 44. *Pearson's correlation coefficient for the correlation between the choroid and retina thickness parameters and the last HbA1C, DM duration and BG on examination in Group 3 (n=30) of the study group.*

Group 3 (n=30)	Mean central choroid thickness	Mean of average choroid thickness	Mean central retina central thickness	Mean of average retina thickness	Mean choroid to retina thickness ratio
last HbA1c [%]	-0.2230	-0.3187	0.0239	-0.1778	-0.2690
DM duration [years]	-0.0365	-0.0391	-0.1704	-0.2136	0.0061
BG on exam	0.0813	0.0820	0.0160	0.3301	-0.0138

5.2.4. Choroid and retina parameters in relation to HbA1c

The study group was divided into 3 subgroups depending on the last HbA1c. The subcategories comprised:

- children with HbA1c ≤ 7.0% (n=45), i.e. optimal diabetic control;
- children with HbA1c > 7.0% < 8.5% (n=52), .i.e. suboptimal diabetic control;
- children with HbA1C ≥ 8.5% (n=56), i.e. poor diabetic control.

The mean central and average choroid was thinnest in children with HbA1c equal to or greater than 8.5% (**Table 45**). However, the differences were not statistically significant. No trend was found with regards to the retina thickness parameters (**Table 45**).

Table 45. *Choroid and retia parameters in relation to HbA1c. No statistically significant differences were found between the groups.*

	Mean central choroid thickness [µm]	Mean of average choroid thickness [µm]	Mean central retina central thickness [µm]	Mean of average retina thickness [µm]	Mean choroid to retina thickness ratio
HbA1c ≤ 7.0% (n=45)	320.0 (SD 73.2)	300.8 (SD 69.0)	249.0 (SD 19.8)	283.0 (SD 12.9)	1.06 (SD 0.24)
HbA1c > 7.0% < 8.5% (n=52)	332.2 (SD 71.6)	313.5 (SD 63.9)	246.7 (SD 20.7)	284.9 (SD 13.2)	1.10 (SD 0.22)
HbA1C ≥ 8.5% (n=56)	312.4 (SD 64.0)	292.2 (SD 52.5)	248.3 (SD 18.4)	283.7 (SD 11.9)	1.03 (SD 0.18)

5.2.5. The effect of anthropometric factors on the retinal and choroid parameters

As per the Cole's index interpretation, the study group comprised 71 normal, 16 overweight, 15 obese, 7 mildly malnourished and 12 moderately malnourished children. A statistically significant difference was noted in the central choroid thickness between the mildly and moderately malnourished subgroups (p=0.0346), with a thicker central choroid thickness in the moderately malnourished group (354.8µm) (**Table 46**). Analogically, a significant difference was noted between these group with regards to the average choroid thickness (p=0.0417) (**Table 47**). No statistically significant differences or trends were noted with regards to the retina thickness parameters (**Tables 48-49**). Finally, a significant differences was found between the mildly and moderately malnourished subgroups with regards to the choroid to retina thickness ratio (p=0.0476) (**Tables 50**). This analysis was not performed for the control group as the size of individual subcategories based on the Cole's index would be insufficient.

Subsequently, diabetic (n=71) and healthy children (n=22) in the ''Normal' Cole's index were compared. The central and average choroid thickness in the children from the study group was noticeably greater than in the control group, however, the differences were not statistically significant (**Table 51**). The differences in the retina parameters were negligible (**Table 51**).

Table 46. *Central choroidal thickness in diabetic children in different body habitus subcategories as per Cole's index.*

Interpretation of Cole's Index	Mean [µm]	95% CI [µm]	SD [µm]	Min [µm]	Max [µm]	Q25 [µm]	Median [µm]	Q75 [µm]
Normal (n=71)	324.5	308.4 - 340.5	67.8	175	466	284	322	366
Obese (n=15)	336.5	288.6 -384.4	86.5	200	487	266	318	386
Moderately malnourished (n=12)	354.8	312.0 -397.7	67.4	251	469	308.5	338	397.5
Mildly malnourished (n=7)	283.0	240.0 - 326.0	46.5	238	348	240	268	331
Overweight (n=16)	317.1	275.9 - 358.3	77.3	199	470	260	303.5	364.5

A statistically significant difference was noted in the central choroid thickness between the mildly and moderately malnourished subgroups (p=0.0346), with a thicker central choroid thickness in the moderately malnourished group (354.8µm).

Table 47. *Average choroid thickness in diabetic children in different body habitus subcategories as per Cole's index.*

Interpretation of Cole's Index	Mean [µm]	95% CI [µm]	SD [µm]	Min [µm]	Max [µm]	Q25 [µm]	Median [µm]	Q75 [µm]
Normal (n=71)	304.6	290.0 - 319.3	61.9	171.1	445.7	268.1	301.0	348.4
Obese (n=15)	313.1	274.0 - 352.2	70.6	220.7	447.6	255.2	284.6	364.3
Moderately malnourished (n=12)	330.2	288.9 - 371.4	64.9	240.3	439.0	281.9	319.0	370.1
Mildly malnourished (n=7)	267.8	235.1 - 300.4	35.3	232.2	319.1	235.4	256.1	311.0
Overweight (n=16)	305.8	267.1 - 344.6	72.7	195.7	439.8	251.2	295.8	349.9

A significant difference was noted in the average choroid thickness between the mildly and moderately malnourished children (p=0.0417).

Table 48. *Central retina thickness in diabetic children in different body habitus subcategories as per Cole's index.*

Interpretation of Cole's Index	Mean [µm]	95.00% CI [µm]	SD [µm]	Min [µm]	Max [µm]	Q25 [µm]	Median [µm]	Q75 [µm]
Normal (n=71)	248.2	243.8 - 252.6	18.6	205	294	237	247	261
Obese (n=15)	249.6	237.3 - 261.9	22.1	201	285	238	256	264
Moderately malnourished (n=12)	251.0	236.0 - 266.0	23.6	221	285	231	243.5	273.5
Mildly malnourished (n=7)	237.0	226.0 - 248.0	11.9	222	253	227	234	248
Overweight (n=16)	247.6	235.0 - 260.2	23.6	197	282	232.5	253.5	260.5

Table 49. *Average retina thickness in diabetic children in different body habitus subcategories as per Cole's index.*

Interpretation of Cole's Index	Mean [µm]	95% CI [µm]	SD [µm]	Min [µm]	Max [µm]	Q25 [µm]	Median [µm]	Q75 [µm]
Normal (n=71)	284.7	281.6 - 287.9	13.4	254.2	329	275.6	282.2	293.1
Obese (n=15)	283.5	279.3 - 287.7	7.5	269.4	298.4	278.8	283.8	289.6
Moderately malnourished (n=12)	284.4	274.5 - 294.3	15.6	259.3	310.5	273	284.2	294.05
Mildly malnourished (n=7)	281.3	269.5 - 293.1	12.7	267.1	304.2	270.7	282.5	287.1
Overweight (n=16)	283.1	277.3 - 288.9	10.9	256.8	306.1	276	284.75	288.85

Table 50. *Choroid to retina thickness ratio in diabetic children in different body habitus subcategories as per Cole's index.*

Interpretation of Cole's Index	Mean	95% CI	SD	Min	Max	Q25	Median	Q75
Normal (n=71)	1.07	1.02 - 1.12	0.21	0.59	1.64	0.95	1.05	1.18
Obese (n=15)	1.10	0.97 - 1.24	0.24	0.79	1.61	0.88	1.03	1.28
Moderately malnourished (n=12)	1.16	1.02 - 1.30	0.22	0.85	1.58	0.99	1.13	1.34
Mildly malnourished (n=7)	0.95	0.84 - 1.06	0.12	0.81	1.18	0.86	0.92	1.02
Overweight (n=16)	1.09	0.93 - 1.24	0.28	0.69	1.71	0.89	1.06	1.24

A significant difference was noted in the choroid to retina thickness ratio between the mildly and moderately malnourished children (p=0.0476).

Table 51. *Choroid and retina parameters in diabetic and healthy children with a 'normal' Cole's index.*

	Diabetics with 'normal' Cole's index (n=71)		Healthy children with 'normal' Cole's index (n=22)		P-value
	Mean	SD	Mean	SD	
Central choroid thickness [µm]	324.5	67.8	299.4	64.6	0.1293
Average choroid thickness [µm]	304.6	61.9	280.2	52.5	0.0973
Central retina thickness [µm]	248.2	18.6	251.9	12.8	0.3829
Average retina thickness [µm]	284.7	13.4	284.1	13.1	0.8538
Choroid to retina thickness ratio	1.1	0.205	1.0	0.173	0.0898

5.2.6. The effect of presence or absence of T1DM family history on the retinal and choroid thickness

No significant differences were found between patients with and without a family history of T1DM with regards to the choroid and retia thickness parameters (**Tables 52-56**).

Table 52. *Central choroid thickness in diabetic children with and without family history of T1DM.*

Family History	Mean [µm]	95% CI [µm]	SD [µm]	Min [µm]	Max [µm]	Q25 [µm]	Median [µm]	Q75 [µm]
Yes (n=29)	310.9	289.6 – 332.3	56.1	186	405	272	312	350
No (n=92)	330.2	314.7 – 345.7	74.8	175	487	273	325.5	375.5

No significant differences were found between groups.

Table 53. *Average choroid thickness in diabetic children with and without family history of T1DM.*

Family History	Mean [µm]	95% CI [µm]	SD [µm]	Min [µm]	Max [µm]	Q25 [µm]	Median [µm]	Q75 [µm]
Yes (n=29)	292.6	274.9 – 310.4	46.7	171.1	386.1	272.7	284.0	324.6
No (n=92)	310.5	296.4 – 324.6	68.0	175.3	447.6	258.8	304.5	350.6

No significant differences were found between groups.

Table 54. *Central retina thickness in diabetic children with and without family history of T1DM.*

Family History	Mean [µm]	95% CI [µm]	SD [µm]	Min [µm]	Max [µm]	Q25 [µm]	Median [µm]	Q75 [µm]
Yes (n=29)	250.1	242.1 – 258.1	21.0	205	285	237	252	264
No (n=92)	247.2	243.2 – 251.3	19.6	197	294	233.5	246	260

No significant differences were found between groups.

Table 55. *Average retina thickness in diabetic children with and without family history of T1DM.*

Family History	Mean [µm]	95% CI [µm]	SD [µm]	Min [µm]	Max [µm]	Q25 [µm]	Median [µm]	Q75 [µm]
Yes (n=29)	283.8	279.0 – 288.6	12.6	259.8	307.4	274.2	282.5	292.6
No (n=92)	284.2	281.6 – 286.9	12.6	254.2	329	276.7	283.25	291.2

No significant differences were found between groups.

Table 56. *Choroid to retina thickness ratio in diabetic children with and without family history of T1DM.*

Family History	Mean [µm]	95% CI [µm]	SD [µm]	Min [µm]	Max [µm]	Q25 [µm]	Median [µm]	Q75 [µm]
Yes (n=29)	1.03	0.97 – 1.09	0.15	0.66	1.35	0.95	1.01	1.13
No (n=92)	1.09	1.04 – 1.14	0.24	0.59	1.71	0.93	1.08	1.21

No significant differences were found between groups.

5.2.7. The effect of insulin therapy delivery mode on the retina and choroid thickness

No significant differences were shown with regards to the choroid and retina parameters between the patients treated with insulin pump and insulin pens (**Tables 57-61**). In children using insulin pump the mean HbA1c was 7.5% (SD 1.2%) compared with 8.2% (SD 1.8%) in children on injection therapy.

Table 57. *Central choroid thickness in diabetic children treated with insulin pump and insulin pens.*

Insulin therapy	Mean [µm]	95% CI [µm]	SD [µm]	Min [µm]	Max [µm]	Q25 [µm]	Median [µm]	Q75 [µm]
Pump (n=95)	328.2	314.2 – 342.3	69.1	175.0	487.0	272.0	323.0	366.0
Injections (n=26)	315.9	284.3 – 347.5	78.2	186.0	469.0	256.0	309.5	375.0

No significant differences were found between groups.

Table 58. *Average choroid thickness in diabetic children treated with insulin pump and insulin pens.*

Insulin therapy	Mean [µm]	95% CI [µm]	SD [µm]	Min [µm]	Max [µm]	Q25 [µm]	Median [µm]	Q75 [µm]
Pump (n=95)	309.0	296.4 – 321.7	62.2	175.3	447.6	268.8	301.0	349.3
Injections (n=26)	296.0	267.7 – 324.3	70.1	171.1	439.8	252.7	285.3	341.0

No significant differences were found between groups.

Table 59. *Central retina thickness in diabetic children treated with insulin pump and insulin pens.*

Insulin therapy	Mean [µm]	95% CI [µm]	SD [µm]	Min [µm]	Max [µm]	Q25 [µm]	Median [µm]	Q75 [µm]
Pump (n=95)	247.5	243.6 – 251.5	19.4	197.0	288.0	233.0	249.0	261.0
Injections (n=26)	249.4	240.5 – 258.3	22.0	201.0	294.0	237.0	246.5	261.0

No significant differences were found between groups.

Table 60. *Average retina thickness in diabetic children treated with insulin pump and insulin pens.*

Insulin therapy	Mean [µm]	95% CI [µm]	SD [µm]	Min [µm]	Max [µm]	Q25 [µm]	Median [µm]	Q75 [µm]
Pump (n=95)	284.5	281.9 – 287.1	12.7	254.2	329.0	275.6	283.4	292.4
Injections (n=26)	283.0	278.2 – 287.8	11.9	256.8	306.1	278.3	282.3	289.6

No significant differences were found between groups.

Table 61. *Choroid to retina thickness ratio in diabetic children treated with insulin pump and insulin pens.*

Insulin therapy	Mean [µm]	95% CI [µm]	SD [µm]	Min [µm]	Max [µm]	Q25 [µm]	Median [µm]	Q75 [µm]
Pump (n=95)	1.09	1.04 – 1.13	0.21	0.59	1.64	0.96	1.05	1.20
Injections (n=26)	1.05	0.94 – 1.15	0.26	0.66	1.71	0.87	0.99	1.21

No significant differences were found between groups.

5.2.8. Gender differences in retinal and choroid thickness

In the study group notable differences were found between genders in the choroid and retina thickness parameters. The central retina thickness was significantly greater in boys compared with girls with 254.1µm and 240.2µm, respectively (p=0.0001) (**Table 62**). The average retina thickness was also greater in boys with 285.8µm, compared with 282.0µm in girls (**Table 62**).

Conversely, the central and average choroid was thinner in boys than in girls, however, the differences were not statistically significant (**Table 62**). The choroid to retina thickness ratio

in boys was also smaller, with 1.0 and 1.1 for boys and girls, respectively, and the difference was statically significant (p=0.4441) (**Table 62**).

The same differences between genders were noted in the control group, however, they were not statistically significant (**Table 63**).

Table 62. *Gender differences in choroid and retina parameters in the study group.*

Study group	Boys (n=67)		Girls (n=54)		P-value
	Mean [µm]	SD [µm]	Mean [µm]	SD [µm]	
Central choroid thickness	316.4	69.2	336.9	72.2	0.1155
Average choroid thickness	297.4	63.6	317.2	63.1	0.0895
Central retina thickness	**254.1**	17.0	**240.2**	20.7	**0.0001**
Average retina thickness	285.8	11.7	282.0	13.3	0.0964
Choroid to retina thickness ratio	**1.0**	0.2	**1.1**	0.2	**0.0441**

The central retina thickness was significantly greater in boys compared with girls with 254.1µm and 240.2µm, respectively (p=0.0001). The difference in the choroid to retina thickness ratio was statically significant (p=0.4441). Statistically significant differences are shown in bold.

Table 63. *Gender differences in choroid and retina parameters in the control group.*

Control	Boys (n=19)		Girls (n=13)		P-value
	Mean [µm]	SD [µm]	Mean [µm]	SD [µm]	
Central choroid thickness	291.6	44.9	325.9	77.7	0.1235
Average choroid thickness	276.4	39.9	299.6	63.5	0.2134
Central retina thickness	252.4	13.4	241.6	22.7	0.1008
Average retina thickness	283.4	13.0	282.2	13.3	0.8115
Choroid to retina thickness ratio	0.98	0.14	1.06	0.21	0.1850

The differences between genders in the control group were not statistically significant.

The above trends were also found in each subgroup of the study group, where diabetic children were divided into groups depending on the duration of diabetes.

In Group 2 the central retina thickness was significantly larger in boys (252.8µm; SD 15.9µm) than in girls (237.4µm; SD 22.8µm) (p=0.0181) (**Table 64**). In group 3 significant differences were shown between the genders in central retinal thickness (p=0.0004) and average retinal thickness (p=0.0009),

which were thicker in boys (**Table 64**). In that group the central retinal thickness in boys was 260.3µm (SD 16.1µm) compared with 236.2µm (SD 17.0µm) in girls and the average retinal thickness was 294.7µm (SD 12.6µm) and 279.5µm (SD 9.7µm) in boys and girls, respectively (**Table 64**).

Table 64. *Gender differences in choroid and retina parameters in subgroups of the control group.*

Group	Central choroid thickness [µm]		Average choroid thickness [µm]		Central retina thickness [µm]		Average retina thickness [µm]		Choroid to retina thickness ratio [µm]	
	Boys	Girls	Boys	Girls	Boys	Girls	Boys	Girls	Boys	Girls
1 (n=31)	306.5 (72.1)	313.2 (68.6)	288.3 (65.0)	295.0 (59.9)	252.0 (18.0)	245.5 (21.0)	282.6 (9.3)	281.2 (12.8)	1.02 (0.25)	1.05 (0.19)
2 (n=21)	301.2 (70.2)	331.6 (53.9)	280.3 (63.1)	310.8 (44.3)	252.8 (15.9)	237.4 (22.8)	284.3 (11.5)	285.1 (16.3)	0.99 (0.21)	1.09 (0.13)
3 (n=15)	358.3 (44.2)	376.5 (83.1)	340.1 (42.0)	356.0 (71.7)	260.3 (16.1)	236.2 (17.0)	294.7 (12.6)	279.5 (9.7)	1.15 (0.14)	1.27 (0.24)

Standard deviations are given in brackets. In Group 2 the central retina thickness was significantly larger in boys (252.8µm; SD 15.9µm) than in girls (237.4µm; SD 22.8µm) (p=0.0181). In group 3 significant differences were shown between the genders in central retinal thickness (p=0.0004) and average retinal thickness (p=0.0009), which were thicker in boys.

In view of the above gender differences, two separate comparisons were made, for boys and girls, of the choroid and retina parameters in diabetic and healthy children. The trends were consistent with those previously described, with notably thicker choroids in diabetic children, compared with sex-matched healthy children (**Tables 65-66**).

Table 65. *Choroid and retina parameters in diabetic and healthy girls.*

Girls	Diabetic girls (n=54)		Healthy girls (n=13)		P-value
	Mean [µm]	SD [µm]	Mean [µm]	SD [µm]	
Central choroid thickness	336.9	72.2	325.9	77.7	p=0.63
Average choroid thickness	317.2	63.1	299.6	63.5	p=0.37
Central retina thickness	240.2	20.7	241.6	22.7	p=0.83
Average retina thickness	282.0	13.3	282.2	13.3	p=0.96
Choroid to retina thickness ratio	1.1	0.2	1.1	0.2	p=0.33

Table 66. *Choroid and retina parameters in diabetic and healthy boys.*

Boys	Diabetic boys (n=67)		Healthy boys (n=19)		P-value
	Mean [µm]	SD [µm]	Mean [µm]	SD [µm]	
Central choroid thickness	316.4	69.2	291.6	44.9	p=0.14
Average choroid thickness	297.4	63.6	276.4	39.9	p=0.18
Central retina thickness	254.1	17.0	252.4	13.4	p=0.69
Average retina thickness	285.8	11.7	283.4	13.0	p=0.43
Choroid to retina thickness ratio	1.0	0.2	1.0	0.1	p=0.24

5.3. Relationship between FAZ dimensions and choroid and retina parameters

A very strong positive correlation was found between central choroid thickness and SCP FAZ in the study as well as control group, with r=0.9458 and r=0.9315, respectively (p<0.01) (**Figure 29**).

Analogically, a very strong positive correlation was found between average choroid thickness and SCP FAZ in both groups, with r=0.9726 and r=0.9671, for the study and control group, respectively (p<0.01) (**Figure 30**).

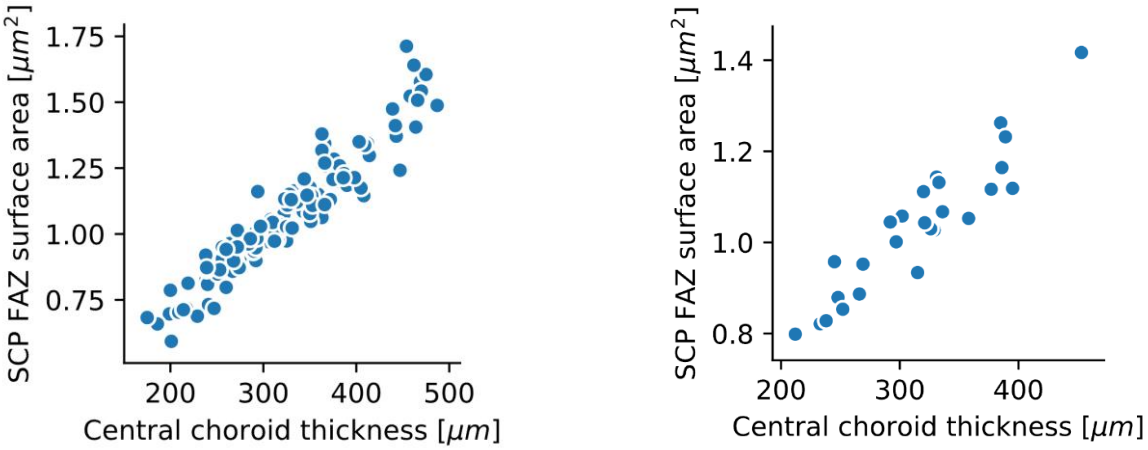

Figure 29. *Correlation between central choroid thickness and SCP FAZ area. Left: study group: r=0.9458 (p<0.01). Right: Control group: r=0.9315 (p<0.01).*

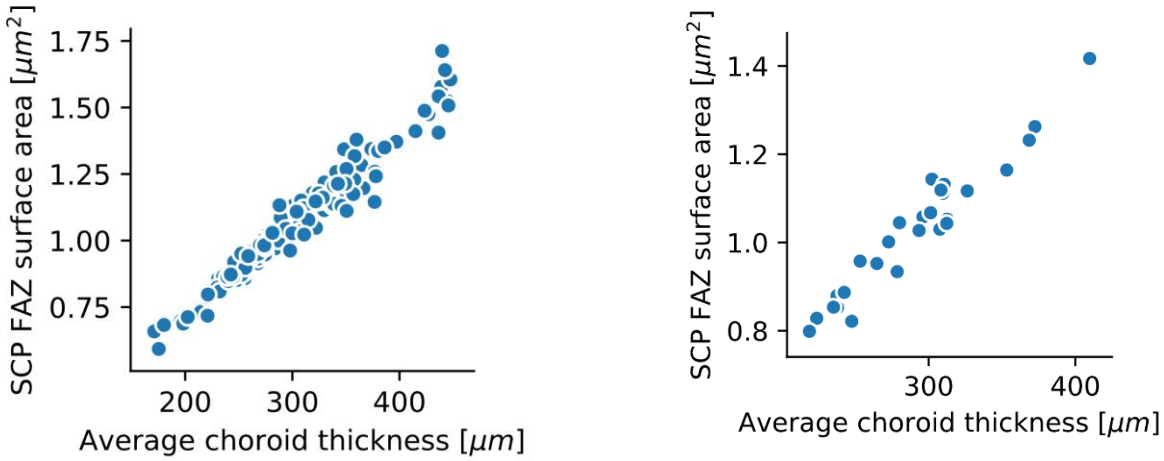

Figure 30. *Correlation between average choroid thickness and SCP FAZ area. Right: study group: r=0.9726 (p<0.01). Left: control group: r=0.9671 (p<0.01).*

On the other hand, a moderate negative correlation was found between the central retinal thickness and the DCP FAZ in the study group with r=-0.562054 (p<0.01) (**Figure 31**). This association was not found in the control group. No correlation was found between the average retina thickness and DCP FAZ (r=-0.0609).

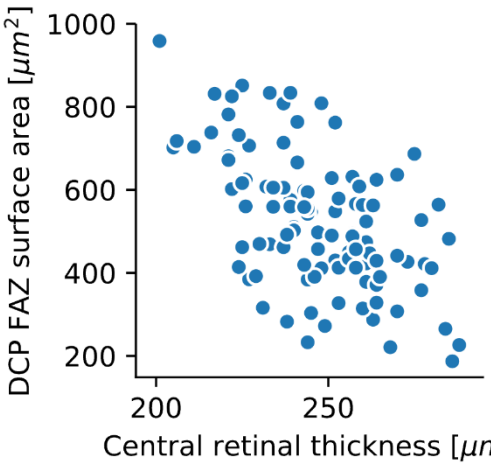

Figure 31. *Negative correlation between central retina thickness and DCP FAZ area in the study group: r=-0.562054 (p<0.01).*

6. DISCUSSION

6.1. Possibilities of using OCT and OCT Angiography in children

Diabetic retinopathy is a major cause of loss of vision in the industrialised world. (116) Currently the standard screening tests for DR are fundus photography, which only provides a two-dimensional image and can lack fine detail and a dilated biomicroscopic fundus examination, which is subjective and can vary depending on the examiner. OCT Angiography is a rapid, non-invasive technique which allows to image the retinal and choroidal vasculature in exquisite detail and to identify early retinal changes otherwise undetectable on clinical examination or with photographic telemedicine techniques.

This study compared the vasculature in the eyes of diabetic children determined to have no clinical evidence of diabetic retinopathy with a healthy control group using structural OCT and OCTA.

Both, OCT-Angiography and radial macular OCT examinations were successful conducted in children aged from 6 to 18 years. The obtained images were of high quality with the mean of 71.79 and 98.52 for the OCT-Angiography and macula OCT, respectively. Yilmaz and colleagues (2017) also described successfully examining children up from the age of 6 years with OCT-Angiography. (110) This shows that both examinations can be performed in children, including those of young age, yielding satisfactory images. In addition, the non-invasiveness of these examination methods makes them well suited for paediatric patients.

6.2. FAZ parameters in the study and control

Following the studies using fluorescent angiography, which demonstrated FAZ enlargement in diabetic retinopathy and a correlation between FAZ dimensions and the extent of capillary non-perfusion, FAZ enlargement has been considered an indicator of DR progression and a marker of its extent. (54,55)

The present study showed pronounced differences in the FAZ surface in the superficial and deep capillary plexuses area between the control group and diabetic children using OCT Angiography despite the absence of diabetic retinopathy in the study group.

To the best of my knowledge, this is the first study to find enlargement of the FAZ and increase in the difference between the DCP and SCP FAZ surface area in the eyes of diabetic children by means of OCTA.

The DCP FAZ surface area in the study group (520.36μm^2) was significantly larger than in the control group (408.56μm^2) (p=0.0005) (**Figure 16**). Analogically, the DCP to SCP ratio in the study group (1.88) was significantly greater than in the control group (1.58) (p=0.0232) (**Figure 17**). Considerably larger SCP was also noted in the study group (302.74μm^2) compared with the control group (284.37μm^2), although the difference was not statistically significant (p=0.46) (**Table 6**). Furthermore, the difference between DCP and SCP FAZ surface area in the study group (217.6μm^2) was significantly larger than in the control group (124.2μm^2) (p<0.0001) (**Table 7**), reflecting a significant enlargement of the DCP FAZ surface area in relation to the SCP FAZ surface area in the study group.

On a subgroup level, in children in all three subgroups of the study group, regardless of the duration of diabetes, the superficial capillary plexus FAZ surface area was larger than in the control group (**Table 6**). The difference was more pronounced in the deep capillary plexus FAZ surface area which was significantly larger in each group of diabetic children, regardless of the duration of the disease, compared with the control group (p=0.0011 - 0.0120) (**Figure 18**). Similarly, in comparison with the control group, the DCP to SCP FAZ surface area ratio was significantly larger in children with longer DM duration – Group 2 (p=0.0210) and Group 3 (p=0.0169) (**Figure 19**).

In addition, in the control group the difference between the DCP and SCP FAZ surface area in the control group was significantly smaller than in Group 1 (p<0.006), Group 2 (p<0.0001) and Group 3 (p<0.0001) (**Table 7**), further suggesting a greater responsiveness of the deep capillary plexus to changes secondary to diabetes.

This is in agreement with Takase and colleagues (2015) who reported statistically significant FAZ enlargement in adult diabetics in the superficial and deep plexus layers compared with healthy eyes, regardless of the presence of retinopathy (99) as well as with Dimitrova et al (2017), Gong et al (2016) and de Carlo et al (2015) who also noted that FAZ surface area in SCP of adult diabetic patients without clinical features of diabetic retinopathy was greater than in the control group. (100,117,118) The lack of significance in the differences in the SCP in this study may reflect greater susceptibility and earlier involvement of the DCP to changes secondary to diabetes. The duration of DM in patients examined in the studies by Dimitrova et al (2017) and Takase et al (2015) was not reported (6,7) and, therefore, it is not possible to speculate whether this could have been a factor. The lack of a significant difference in the SCP FAZ surface area between the control and study group in the present study may also be related to the methodology – this includes the manual contouring of FAZ, which is prone to subjectivity and error despite being carried out with the help of AngioB

function to minimise the error, and potential unavoidable inaccuracies in the determined duration of diabetes, as there could have been a delay between the onset and diagnosis, which was used as a start point of the disease.

The enlargement of FAZ surface area in diabetic children without DR evidence a compromise in retinal circulation before manifested DR. The fact that the changes were more significant in the deep capillary plexus is in line with the previous reports and studies that had found microaneurisms to be more pronounced in the deep vascular plexus, compared with the superficial plexus. (119-121) The findings of the present study suggest that the deep capillary plexus may be the first part of the retina to be effect by the ischaemia secondary to diabetes. A similar finding was reported by Norihiro et al (2016) who found significant enlargement of FAZ area in the deep capillary plexus in retinal vein occlusion without enlargement of FAZ area in the superficial capillary plexus (122) further pointing to primary involvement of deep capillary plexus in ischaemia secondary to vascular pathology.

The present study highlights that that by means of OCT Angiography changes can be identified in the microcirculation of diabetic children before the development of diabetic retinopathy, as it has been suggested in adults. (99) OCT Angiography may therefore be a potential tool for evaluating the risk of developing DR in patients without any retinal changes on clinical examination. Such detection of early pathology before the sequelae of DR informs the treatment, such as optimisation of diabetic control before any sight-threatening complications develop. This can result in preventing the onset of DR or prolonging the period before its development, which is beneficial for long-term prognosis. Miyamoto and colleagues (1999) showed that the closure obstructed capillary blood vessels in diabetes were temporally associated with leukocyte aggregation and the early retinal capillary closure was transient. (123) Furthermore, Gill et al (2017) showed a decrease in the FAZ surface area with time and anti-VEGF intravitreal injections in patients with diabetic macular oedema. (124) The decrease in FAZ area was most pronounced in the deep capillary plexus. This suggests that the FAZ enlargement shown in the present study may be reversible, in which case the FAZ dimensions could be a very sensitive marker of the fluctuations of diabetic control. However, further studies are required to confirm the reversibility of FAZ changes in DM as well

as on the predictive value of OCTA changes for the development of DR. The non-invasive nature of OCTA allows frequent re-examination leading to tighter and more detailed monitoring. As duration

of diabetes is the main risk factor for the development of DR, this is of particular importance in diabetic children as they will have a long DM duration of adulthood. Therefore, delaying the onset of DR by detecting earlier changes can significantly improve their long-term visual outcome.

6.3. FAZ parameters: differences in subgroups

Previous studies shown a correlation between the extent of changes found on OCT-Angiography and the DR severity. This included a statistically significant increase in FAZ area and perimeter in association with the progression of non-proliferative diabetic retinopathy (101), further increase in FAZ area in proliferative diabetic retinopathy (55) and a significant decrease in capillary perfusion density values corresponding to retinopathy progression (101,106,107)

Since the duration of diabetes is the major risk factor for development of DR, it was hypothesised that the duration of the disease may affect the severity of microvasculature changes even in the absence of DR. This suspicion was confirmed as notable differences were noted in the FAZ parameters between the subgroups of the study group, depending on the duration of diabetes. The deep capillary plexus FAZ surface area, and the DCP to SCP FAZ surface ratio, apart from being smaller in the control group compared with diabetics, differed between the subgroups of the study group and its size was associated with the duration of diabetes. The mean DCP FAZ surface area was smallest (502.2μm^2) in children with the shortest duration of diabetes (Group 1), larger (523.9 μm^2) in children with intermediate DM duration (Group 2) and the largest (539.7 μm^2) in patients with the longest duration of diabetes (Group 3) (**Figure 18**). The same trend was observed in the mean DCP to SCP FAZ surface area ratio which increased from 1.75 in Group 1, through 1.93 in Group 2 to 1.98 in Group 3 (**Figure 19**). In the SCP, although the FAZ surface area was smallest in the control group and largest in Group 3, with the longest DM duration, no clear stepwise increase in the FAZ surface area was noted from Group 1 to Group 3. As previously outlined, this could suggest that the DCP is affected sooner or the findings could be related to the methodology used. Nonetheless, a significant difference was shown in the difference between the DCP and SCP FAZ surface area between Group 1, i.e. children with a short duration of diabetes, and Group 2 ($p<0.03$) and Group 3 ($p<0.005$), i.e. children with a longer duration of diabetes. This implies that increased duration of diabetes may result in advancing microvascular changes even before the development of DR. To the best of my knowledge, this is the first study to report a direct relationship between DM duration and FAZ dimensions in diabetic children without diabetic retinopathy.

Despite a clear trend, no correlation was found between the FAZ parameters and duration of the diabetes, similarly to Takase et al (2015) (99) and Durbin et al (2017) (125) studies. This highlights the fact that the development of diabetic retinopathy is multifactorial. While DM duration is an important risk factor, which can influence the appearances in the microvasculature shown on OCT angiography, the disease process is also affected by other factors, which could include among others glycaemic control, genetic predisposition and lifestyle factors. Furthermore, it should be noted that inaccuracies may be present in estimated duration of DM due to a possible delay between the onset and diagnosis of the disease. The resulting risk of error cannot be mitigated, however, it could have affected the results if the DM duration were longer than deemed on the basis of the diagnosis date.

6.4. SCP and DCP FAZ Correlation

A very strong positive correlation was found between the SCP and DCP FAZ area in the study as well as control group, with r=0.7774 and r=0.815357, respectively ($p<0.05$) (**Figure 21**). To the best of my knowledge, this is the first study to report a strong correlation in these parameters in children. Bearing in mind the larger and more significant differences in the FAZ surface area in deep capillary plexus, this correlation may suggest that the changes in the DCP are followed by changes in the superficial capillary plexus. This suggests that the early microvascular changes start in the deep layers and expand more superficially. Further research is required to confirm this possibility and to gage the rate of this progression and its predictive value for prognosticating the development of DR.

6.5. FAZ parameters in relation to glycaemic control

In view of the multifactorial nature of diabetes, the correlation of FAZ parameters with BG on examination was assessed. Only a very weak correlation was found between the SCP and DCP FAZ surface areas and BG on examination (**Table 8**). The small extent of this association was confirmed by the determination coefficient, according to which FAZ parameters are affected by BG on examination in only 4% of the cases. The value of such an association is additionally very limited as the BG on examination is only a snapshot of the diabetic status and does not convey any information about the daily and long-term variations of sugar or overall diabetic control. For this purpose, HbA1c is a much more reliable indicator.

Nevertheless, no correlation was found between the FAZ and the last HbA1c either, apart from Group 1, i.e. children with the shortest duration of diabetes, where a weak negative correlation

was found between the last HbA1c and the SPC FAZ surface area (r=-0.3480) and DCP FAZ surface area (r=-0.4496). This suggests a decrease of the SCP and DCP surface areas with increasing HbA1c in the early stages of diabetes mellitus in children. However, the low determination coefficient suggests that other factors affect these parameters in at least 80% of cases. Furthermore, the size of the subgroup was relatively small (n=40) bearing in mind the variability of diabetes, which limits the external validity of these results.

Contrary to these results, Gozlan and colleagues (2017) described a positive association between the last HbA1c and the FAZ surface area in adult diabetics with varying severities of non-proliferative diabetic retinopathy. (101) This difference could be due to the methodological differences in FAZ surface area measurement – Gozlan et al (2017) used the automated software from AngioVue system (101) whereas the present study used Topcon software. Furthermore, Gozlan and colleagues (2017) examined adults with nonproliferative diabetic retinopathy, (101) in contrast to the present study looking at children without diabetic retinopathy. It is possible that the microvasculature depends differently in children and before the development of DR.

The lack of correlation between the last HbA1c and FAZ parameters for the entire study group could be due to the fact that HbA1c, although more reliable than individual BG measurements, only reflects the BG control in the last 4 months. This may not necessarily be representative of long-term diabetic control, which the microvasculature changes are a reflection of. The last HbA1c may be unreliably low or high if that period coincided with a period of sickness, stress or change of therapy. To overcome this limitation in future studies the correlation between FAZ parameters in OCTA and a cumulative HbA1c index should be assessed, e.g. using a mean HbA1c measurement. This was done by Sander B and colleagues who found a positive association between the increase in perifoveal avascualar areas and cumulative HbA1c index in diabetics by FFA. (126) Furthermore, Virk et al (2016) have shown that the variability of HbA1c was predictive of the diabetic retinopathy risk in adolescents with Type 1 diabetes. (40)

Interestingly, a subgroup analysis in the present study showed that the DCP FAZ area in diabetic children with the highest HbA1c, equal to or greater than 8.5% was significantly smaller than in those with HbA1c ≤ 7.0% and HbA1c greater than 7.0 and less than 8.5% ($p<0.006$) (**Table 12**) This finding could suggest, as previously stated, that the microvasculature changes in response to the quality of glycaemic control in children before the development of DR differ from those observed in adults. However, limitations in the measurements taken could have also affected the results in the present

study, including a degree of subjectivity in the FAZ surface measurement and the availability of only one HbA1c, as described before. Therefore, further studies are required to confirm whether the direction of the association between FAZ dimensions and HbA1c in diabetic children.

6.6. FAZ parameters in relation to age

In the present study no correlation was found between the FAZ parameters and age of children in the study or control group, which is consistent with Zhang et al (2017) observations (127) and previous studies in adults. (99,128,129)

Interestingly however, Coscas et al (2016) found a significant difference in the vessel density in healthy subjects in different age groups of adults, from the age of 20 to 60 years and older. (130) Similarly, Durbin et al (2017) reported a correlation between vessel density and age in diabetics. (125) These differences may be due to the age difference between the study participants in the present study and Coscas et al (2016) (130) and Durbin et al (2017) (125) research. In the present study children were examined. The age ranged from 6 to 18 years and the largest age difference was 12 years. In Durbin et al (2017) and Coscas et al (2016) studies, adults from 20 to 60 and more years of age were examined (125,130) and in the latter they were divided into age groups based on 20 year intervals, (130) which is larger than the maximum age difference in the present study. Therefore, it is possible that vessel density changes with age in adulthood, but it does not occur in children.

6.7. FAZ parameters in relation to anthropometric factors, family history of DM and insulin therapy

No trends or association were noted between the FAZ parameters and the nutritional status of diabetic children in the present study and obesity or being overweight was not associated with increased FAZ surface areas (**Tables 13-15**). A comparison was made between the diabetic and healthy children with a 'normal' Cole's index to eliminate the potential effect of body mass on the results, which showed increased FAZ surface area in diabetic children compared with the control group (**Table 16**). This is consistent with a meta-analysis Zhou et al (2017) who concluded that, based on the current publications, neither being overweight nor obesity were associated with an increased risk of DR. (131)

No significant differences in the FAZ parameters were shown between diabetic children with and without family history of T1DM (**Tables 17-19**). The subgroup of children who had family

history of diabetes was relatively small (n=28) which limits the generalisability of the results. However, a lack of the significant difference between these subgroups may suggest that although having a family history of T1DM increases the risk of the disease, it does not predict the risk of developing microvascular complications such as retinopathy. No supporting or contrary evidence has been found in the current literature.

The FAZ surface area in the DCP and SCP was smaller in children using insulin pumps compared with those receiving multiple daily injections, although the differences were not statistically significant (**Tables 20-22**). The lack of statistical significance could have been due to the small number of children receiving insulin injections (n=18) or due to good diabetic control in both groups – no diabetic retinopathy was noted in either group and the mean HbA1c in the injection group was only 0.6% higher than in the children using insulin pump. Nonetheless, Zabeen et al (2016) showed lower rates of diabetic retinopathy in adolescence with type 1 diabetes mellitus using insulin pumps, compared with those using multiple daily injections despite the HbA1c being only 0.1% lower in children on insulin pumps. (132) Further studies are required to ascertain whether the use of insulin pump decreases the risk of microvascular complications or changes in the retina compared with multiple daily injections even if similar diabetic control is achieved with both treatment modalities.

6.8. Choroid and retina parameters

Similar trends to those found in FAZ parameters were observed in the mean central choroid thickness, which was smallest in the control group (305.5µm) and gradually thicker in diabetics. The central choroid thickness was 309.2µm in Group 1, further increased in Group 2 (315.2µm) and the thickest in Group 3 (367.4µm) (**Figure 26**). The measurement in Group 3, in children with the longest duration of DM, particularly stood out and was statistically significantly thicker that in Group 1 ($p=0.0002$), Group 2 ($p=0.0014$) and in the control group ($p=0.0003$) Analogically, the same tendency was noted for the average choroid thickness, with 285.9µm, 291.0µm, 294.4µm and 348.0µm for the control group, Group 1, Group 2 and Group 3, respectively (**Figure 27**). The average choroid thickness in patients from Group 3 was also, statistically, significantly greater than in Group 1 ($p=0.0001$), Group 2 ($p=0.0003$) the control group ($p<0.00001$). The variability of the vasculature parameters was further depicted by the choroid to retina thickness ratio, which was smallest in the control group (1.01), slightly larger in Groups 1 and 2 (1.03) and the largest in Group 3 (1.21) (**Figure 28**). The choroid to retina thickness ratio in Group 3 was significantly

different from all the remaining groups, with the statistical significance level of p=0.0002, p=0.0014 and p=0.0001 for Group 1, Group 2 and the control group, respectively.

To the best of my knowledge, this is the first study to report increased thickness of choroid in children with diabetes mellitus. Saying and colleagues (2014) as well as Elhabashy et al (2015) found no significant difference in choroid thickness between type 1 diabetic children without diabetic retinopathy and the control group. (111,112) However, the study group sizes studies were relatively small with 41 and 30 children, which is a considerable limitation due to significant variability of diabetes as a disease. The present study comprised a considerably larger study group and the obtained results showing thicker choroid in diabetic children were statistically significant. These findings are consistent studies conducted on adult diabetics by Xu et al (2013) and Shao et al (2014), which showed increased choroid thickness in diabetic subjects. In both studies the presence and development of diabetic retinopathy were found not to be related to SFCT. (133,134) The main limitation of the Beijing study by Xu et al (2013) was performing the OCT measurements throughout the day without taking into account the diurnal variation of the parameters. This was accounted for in the present study by performing the OCT examination for all patients at the same time of day. Furthermore, the findings by Xu et al (2013) and Shao et al (2014) cannot be extrapolated to the present study due to the differences in age and race of the study group which can affect ocular physiology - both studies comprised Asian adults. (133,134) A similar study conducted in Lisbon by Tavares Ferreira et al (2017) also showed a thickening of the choroid in adult type 2 diabetic patients without diabetic retinopathy. (135) Furthermore, the increase in the choroid thickness associated with longer duration of diabetes in children shown in this study was consistent with the findings of Ferreira et al (2017) who described increased in the choroidal thickness in adult diabetics without DR after 1 year follow up. (136) The progressive nature of the choroid changes was also shown by Rewbury et al (2016) who described an increase in the subfoveal choroidal thickness with the increase in the severity of diabetic retinopathy. (137) The importance of choroid thickness was also noted by Kniggendorf et al (2016) who reported a decrease in choroid thickness in patients with diabetic macular oedema following the administration of anti-VEGF intravitreal therapy, despite the fluid not being found in the choroid. (138) Similarly, Okamoto and colleagues (2016) showed a significant reduction in choroid thickness after PRP treatment (139) and Roohipoor and colleagues (2016) reported a significant reduction in choroid thickness in eyes with proliferative diabetic retinopathy treated

with PRP and intravitreal bevacizumab at 10 months and a transient reduction in choroid thickness at 3 months compared with PRP only treatment. (140) This suggests responsiveness of the choroidal layer to retinal vascular changes. The choroid plays an integral role in the metabolic support of the retinal pigment epithelium (RPE), and outer retina. Therefore, normal choroidal vasculature is paramount for appropriate functioning of the retina. (141,142) The thickening of the choroid may be associated with choroidal swelling secondary to DM, thereby reflecting the beginning of diabetic choroidopathy. Histologically, diabetic choroidopathy is characterised by arteriosclerosis, choriocapillaris degeneration, vessel tortuosity, localised dilation or closure of capillaries, areas of ischaemia and neovascularisations, (16) which suggests that choroidal thickness could be altered in the course of diabetes. The present study and above evidence suggest that changes in the choroid be detected before the development of DR. Increased thickness could represent a regulatory attempt to increase perfusion in the presence of ischaemia. This theory is supported by Nagaoka et al (2004) study who demonstrated a decreased choroidal blood flow in diabetics, even before the development of visible DR (143) and Fryczkowski et al (1989) electron microscopy study which showed that diabetes could cause vaso-occlusion and resultant nonperfusion of the choroid and retina. (144) It could also result from the accumulation of waste at Bruch's membrane secondary to compromised choroidal blood flow, dysfunction of the photoreceptors and insufficient removal of metabolites generated by RPE cells. (145) It has also been suggested that these structural changes may correspond to the early neurodegenerative phase of DR. (136) The significant thickening of choroid and enlargement of deep capillary plexus FAZ surface area and less pronounced enlargement of the superficial capillary plexus area shown in the present study could suggest a direction of pathological vasculature changes prior to development of DR from the outermost choroid, through overlying retinal deep capillary plexus to superficial capillary plexus. The interplay between choroid and retina is further suggested by a very strong correlation between the central and average choroid thickness and the SCP FAZ surface area found in this study (correlation coefficient ranging from r=0.9315 to r=0.9726) (**Figures 29-30**). However, further research is required to confirm this possibility, to understand the significance of diabetic choroidopathy and its role as a predictive factor for disease evolution and treatment response.

Contrary, several studies, Esmaeelpour et al (2011 and 2012), (146,147) Querques et al (2012), (148) and Vujosevic et al (2012) (149) reported contradictory results, i.e. choroidal thinning in diabetics regardless of disease stage, even in patients without DR. (146-149) However, all of these studies

examined adults, which greatly limits the comparison with the present study as the choroid thickness is known to decrease with age. (150-152) Furthermore, their study sizes were relatively small with 15, 21, and 22 diabetic patients without DR, respectively. (146-149) Furthermore, Esmaeelpour et al (2011 and 2012) and Querques et al (2012) studies investigated type 2 diabetics, (146-148) unlike the present study. The Vujoseric et al (2012) study included both, type 1 and type 2 diabetics, (149) which can lead to a greater variability of the results. Gupta et al (2017) found significantly thinner choroidal thickness in Indian adults with diabetes compared with controls. (153) Similarly to the above mentioned study, the comparability of Gupta et al (2017) results with the present study is limited due to large differences in the study group, such as age and ethnicity of the participants. (153) Interestingly however, Gupta and colleagues (2017) noted an increase in choroidal thickness in subjects with diabetic retinopathy compared with diabetics without DR, (153) which supports the involvement of the choroid in the disease process. Tan and colleagues (2016) reported no significant difference in the choroidal thickness between diabetics and controls. (154) However, the size of their study group was also relatively small, 19 patients, and it was not specified what kind of diabetes they had. Furthermore, racial differences should be taken into account as the study was performed in Singapore. Importantly, none of the above studies took the diurnal variability of the measured parameters into the account, which is a significant limitation. Tavares Ferreira and colleagues (2017) suggested that differences in the reported behaviour of choroid parameters may result from their variability in the course of diabetes. They suggested that an initial increase in thickness could constitute an early phase of diabetic choroidopathy, which could be followed by atrophy of choroidal tissue leading to thinning and subsequent stabilisation compatible with greater vessel resistance and vascular remodelling. (135) In view of the disparities further large population studies are required to evaluate choroid involvement in diabetes prior to the development of DR in children as well as adults taking into account DR presence and severity and patient's ethnicity.

No significant differences were noted in the retinal thickness between diabetics and healthy children (**Tables 35-36**), which is consistent with Dimitrova et al (2017) study. (100) The lack of such a difference together with the significant enlargement of the FAZ surface area in the deep capillary plexus found on OCT Angiography may suggest that retinal vascular alterations precede retinal structural alterations thereby indicating a causative role of circulatory alterations in the retina to the development of DR. This is further suggested by a strong negative correlation found between

the DCP FAZ surface area and the retina central thickness in diabetic children in the present study (**Figure 31**), which implies thinning of central retina with increasing DCP FAZ surface area. Further research is required to test this hypothesis and to determine the microvascular sequelae in the retinal vasculature occurring prior to the development of DR.

In the study group a weak positive correlation was noted between the retina average thickness and choroid average and central thickness, with r=0.3126 and r=0.2625, respectively (**Table 37**). In the individual analysis of the subgroups a weak correlation (r=0.4003, $p<0.05$) between the retina average thickness and choroid average thickness was only found in Group 1. These findings suggest an interdependence of these vascular layers. Possible mechanism of such interaction have been described above, however, further research is required to verify these hypotheses.

6.9. Choroid and retina parameters in relation to DM duration

In addition to significant choroid thickening in diabetic children with the longest duration of diabetes, a weak positive correlation was found between the DM duration and the central choroid thickness (r=0.2721), the average choroid thickness (r=0.2938) and the choroid to retina thickness ratio (r=0.2666) (**Table 41**). However, this was verified with the determination coefficient, which showed that the choroid parameters depend on the DM duration in only less than 9% of cases. Similarly, a study by Tavares Ferreira and colleagues did not show a significant linear correlation between the DM duration of choroid thickness. This suggests that, analogically to the FAZ parameters, the choroid thickness is partially influenced by the duration of DM, however, it is also greatly affected by other factors.

6.10. Choroid and retina parameters in relation to age

In the study group a weak correlation was noted between the age and all choroid and retina thickness parameters except for central retinal thickness (**Table 39**) The determination coefficients were less than 7% for all the parameters, which means that they depend on the age in only less than 7% of cases and in the remaining 93% of cases, on different factors. The association of the choroid thickness with age was shown in previous studies (136,151,152) and choroid is known to be thicker in children than in adults. No correlation between the above parameters and age was noted in the control group (**Table 40**) The lack of correlation in the control group in this study could be due to the relatively small number of children in the control group (n=32). The weak correlation of age and choroid thickness in diabetic children and lack of such correlation in the control group

could also be due to a small age difference between the children – maximum 12 years of age. The thinning of choroid occurring later in adulthood will therefore not be present in such a cohort.

6.11. Choroid and retina parameters in relation to glycaemic control

In the present study no correlation was found between the choroid thickness and BG on examination or last HbA1c. The latter is consistent with Tavares Ferreira et al (2017) observations. (135) Interestingly, the mean central and average choroid was thinnest in children with HbA1c equal to or greater than 8.5% (**Table 45**), although the differences were not statistically significant. As previously described, BG on examination or the last HbA1c measurement are not representative of long-term diabetic control and may lead to biased results. Therefore, similar studies should be conducted in the future using other indices of diabetic control, such as cumulative HbA1c index, to reliably determine the effect of diabetic control on choroid and retina thickness.

6.12. Choroid and retina parameters in relation to anthropometric factors, family history of T1DM and insulin therapy

A statistically significant difference was noted in the central choroid thickness between the mildly and moderately malnourished subgroups (p=0.0346), with a thicker central choroid thickness in the moderately malnourished group (354.8µm). (**Table 46**) Analogically, a significant difference was noted between these group with regards to the average choroid thickness (p=0.0417) and the choroid to retina thickness ratio (p=0.0476), both parameters being higher in the moderately malnourished group (**Tables 47&50**). The central and average choroid was thickest in the moderately malnourished group. Yilmaz et al (2015) reported thinning of the choroid with increasing body mass index in adults from 18 to 40 years old, (155) which is consistent with the trend shown in this study. Previous studies have shown an association between higher BMIs and obesity and narrower retinal arteriolar, wider venular calibers and thinner choroid thickness in adults as well as children. (156-158) A vasodilator molecule, nitric oxide, has been found to be decreased in obesity and to result in impaired dilation of the vasculature. (159) In addition, raised levels if vasoconstrictor molecules including endothelin and angiotensin-II have been associated with increased BMI. (160-161) Yilmaz and colleagues hypothesized that decreased choroid thickness in patients with higher BMI may be due to the alteration of the microvasculature and the balance of vasoconstrictor and vasodilator molecules in the choroid secondary to the obesity. (155) However, this hypothesis cannot be verified on the basis of the present study due to small subgroup sizes based on the Cole's

index as well as absence of a clear trend in this study. Furthermore, the BMI index is not appropriate for use in children, which further limits the comparability of the studies.

Analogically to FAZ parameters, no significant differences were found between patients with and without a family history of T1DM with regards to the choroid and retia thickness parameters (**Tables 52-56**). This may suggest that whilst a positive family history increases the risk of developing T1DM, it may not increase the risk or microvascular complications. Nonetheless, further research is required to verify this possibility.

No significant differences were shown with regards to the choroid and retina parameters between the patients treated with insulin pump and insulin pens (**Tables 57-61**), although the choroid was slightly thicker in patients using insulin pumps. In view of the relative small number of children on multiple daily injections in this study (n=26) and a considerably higher mean HbA1c in children on injection therapy compared with those using insulin pump, further studies are required to reliably determine whether the type of therapy is associated with changes in choroid or retina parameters. Notably, however, the type of insulin therapy can only affect these parameters indirectly by the resulting diabetic control.

6.13. Genders differences in retinal microvasculature

Significant differences were noted in SCP and DCP FAZ surface areas between genders. In the study group the FAZ surface area was smaller in boys compared with girls is both superficial (p=0.0006) and deep capillary plexuses (p=0.0010) (**Figure 22**). The same gender difference was found in the control group (**Table 27**). These findings are consistent with Zhang et al (2016) study which examined Chinese children aged 8-16 years old (127) as well as previous studies on adults. (129) (128,162) This is, however, the first study, to the best of my knowledge, to confirm this gender difference in European children. Similarly, Coscas et al (2016) found a higher retinal vascular density in women than in men after 60 years of age and attributed it to late vascular aging in females. (130) Nonetheless, the results of the present study and Zhang et al (2016) observations showing differences in FAZ parameters in childhood, (127) as well as the presence of the same trend in the control group in the present study point towards a physiological gender difference rather than an age related phenomenon. Gender differences were also identified with regards to the central retina thickness, was greater in boys in diabetic and healthy children, the former being statistically significant. Similarly to the FAZ parameters, the presence of this discrepancy in both, study and control group, suggests a likely physiological difference. In view of this, it is important that

different norms be used clinically for boys and girls regardless of diabetic status. However, larger population studies are required to reliably determine the effect of sex on FAZ and retina thickness parameters.

6.14. Study limitations

The present study has several limitations. Firstly, the diabetes duration was estimated based on the date on diagnosis, which could have led to underestimating its duration. Although this potential error could not be avoided, it could have biased the results. Secondly, the last HbA1c measurement which was used as a marker of diabetic control reflects the BG fluctuations in the last few months and not long-term diabetic control. Thirdly, the FAZ surface area measurement was based on manual contouring of FAZ borders. Although additional measures were taken to ensure accuracy, including using Topcon's deep capillary plexus vessel enhancement algorithm and Angio-B function, the measurements were prone to subjectivity. Notably, however, the alternative automated algorithm for FAZ surface area measurement available in Angio Vue OCT Angiography system is not free of error. Furthermore, the choroid thickness was determined based on an SD-OCT image rather than EDI which could have given more detailed information. In addition, hydration status, which could affect the choroid thickness, was not take into account. However, all children were in good health and were euvolaemic clinically. Moreover, the choice of the eye for structural OCT and OCTA was not random – instead, it was based on the quality of the images. As none of the children had any evidence of diabetic retinopathy or asymmetry in other clinical findings on examination, it was decided that the choice of an eye based on image quality was justified in order to reduce the measurement error caused by poor quality images. As a result, a similar number of left and right eye examinations was included. Lastly, axial length was not measured and, hence, the choroid measurements were not stratified for it. Nonetheless, the present study did not include children with a high refractive error and therefore, the differences in axial lengths were unlikely to have significantly affected the results.

7. CONCLUSIONS

- OCT Angiography is a non-invasive imaging technology allowing a detailed evaluation of the retinal microvasculature in the proximity of the foveal avascular zone in healthy and diabetic children.

- OCTA is suitable for use in children in different age groups. The prerequisites include an ability to cooperate during the examination by looking in a specific direction and refraining from blinking for a short period, which is necessary to obtain good quality images. This study showed that OCTA can be indicated in diabetic children without clinical features of diabetic retinopathy in order to visualise early retinal changes which can precede the development of DR.

- Lack of significant correlation between the retinal changes identified by OCTA and the duration of diabetes, biochemical diabetic parameters and anthropometric factors highlights the multifactorial nature of microvascular changes in diabetes. Nonetheless, the significantly larger DCP FAZ surface area in diabetics compared with healthy children and its notable increase with increasing DM duration, suggest that the deep capillary plexus is the most susceptible retinal layer and that the microvascular changes which can later lead to the development of DR may originate in this layer.

- Changes occur at microvascular level before the development of diabetic retinopathy which can be visualised by means of OCT and OCTA. The significant thickening of the choroid and enlargement of DCP FAZ surface area and less pronounced enlargement of the SCP FAZ surface area as well as a very strong correlation between the central and average choroid thickness and the SCP FAZ surface shown in the present study could suggest a direction of pathological vasculature changes prior to development of DR from the outermost choroid, through overlying retinal deep capillary plexus to superficial capillary plexus. Early detection of such changes by means of OCT and OCTA may be beneficial for the management of diabetics by enabling prevention or delay of onset of diabetic retinopathy. However, prospective studies are required to determine the predictive role of FAZ and choroid parameters in the development of DR.

8. ABSTRACT

Introduction

Diabetic retinopathy (DR), the most common microvascular complication of diabetes, is the leading cause of blindness in working-age adults in the developed countries. The duration of diabetes is known to be one of the biggest risk factors for the development of DR, which makes type 1 diabetic children a high risk group for developing DR in their adulthood. OCT Angiography (OCTA) is a non-invasive imaging method which has proven effective for retinal microcirculation assessment in adult diabetics. Recent studies using OCTA in adult diabetics have shown changes in the foveal avascular one (FAZ) area prior to the development of diabetic retinopathy (DR) and increase in FAZ area with progressing DR severity. The purpose of this study was to evaluate the retinal and choroidal microvasculature in children with diabetes (DM) using OCTA and structural OCT.

Methodology

Children (aged 6-18 years) with type 1 diabetes and no DR and age-matched controls were examined using Topcon OCTA structural OCT. Children with pre-existing vitreoretinal disease were excluded. The FAZ area in superficial (SCP) and deep capillary plexus (DCP) was measured on OCTA. The choroid and retinal thickness was measured using the structural OCT. The OCTA examination was successfully preformed on 112 diabetic and 30 healthy children, whereas the structural OCT assessment included 121 diabetic children and 32 controls. For a subanalysis the study group was divided into 3 subgroups depending on DM duration Group 1: less than 5 years, Group 2: 5-10 years, Group 3: more than 10 years. Data was collected on DM duration, biochemical diabetic parameters and anthropometric factors. Student's t-test and ANOVA variance analysis were used for comparison of two and several unpaired groups, respectively and Pearson's linear correlation coefficient for correlation analysis. The statistical analysis was completed using Statistica software.

Results

The mean DCP FAZ surface area in the study group, 520.4μm^2 (SD 160.0μm^2), was significantly larger than in the control group, 408.6μm^2 (SD 114.9μm^2) (p=0.0005). The mean SCP FAZ area in the study group, 302.7μm^2 (SD 119.2μm^2), was also larger than in the control group, 284.4μm^2 (SD 123.2μm^2), however, not significantly (p=0.46). Analogically, the mean DCP to SCP FAZ surface area ratio in the study group, 1.88 (SD 0.68), was significantly greater than in the control group, 1.58 (SD 0.48)

(p=0.0232). The difference between the DCP and SCP FAZ surface area in the study group, 217.6µm^2 (SD 100.8µm^2) was significantly larger than in the control group, 124.2µm^2 (SD 72.8µm^2) (p<0.0001). The mean DCP FAZ increased with DM duration from 502.2µm^2 (SD 137.8µm^2) in Group 1 to 523.9µm^2 (SD 159.2µm^2) in Group 2 and 539.7µm^2 (SD 189.1µm^2) in Group 3. Significant differences were found between the control group and Group 1 (p=0.0120), Group 2 (p=0.0019) and Group 3 (p=0.0011). No significant differences between subgroups or trends were found with regards to the SCP FAZ. The mean DCP to SCP FAZ area ratio increased gradually with DM duration from 1.75 (SD 0.62) in Group 1 to 1.93 (SD 0.60) in Group 2 and 1.98 (SD 0.83) in Group 3. Significant differences were found between the control group and Group 2 (p=0.0210) and Group 3 (p=0.0169). Furthermore, the difference between DCP and SCP FAZ areas in the control group was also significantly smaller than in Group 1 (p<0.006), Group 2 (p<0.0001) and Group 3 (p<0.0001) and differences were noted within study group with Group 1 differing significantly from Group 2 (p<0.03) and Group 3 (p<0.05).

The central and average choroid thickness in diabetic children was noticeably thicker compared with controls, although the difference was not statistically significant. A gradual thickening of the choroid was observed on a subgroup level with increasing DM duration. The central choroid thickness increased from 305.5µm (SD 61.7µm), to 309.2µm (SD 70.1µm) in Group 1, 315.2µm (SD 64.3µm) in Group 2 and 367.4µm (SD 66.0µm) in Group 3. Statistically, the mean central choroid thickness in diabetic children from Group 3 was significantly thicker that in Group 1 (p=0.0002), Group 2 (p=0.0014) and in the control group (p=0.0003). Similarly, the average choroid thickness increased from 285.9µm (SD 51.1µm) in the control group, to 291.0µm (SD 62.5µm) in Group 1, 294.4µm (SD 56.7µm) in Group 2 and 348.0µm (SD 58.3µm) in Group 3. The average choroid thickness in patients from Group 3 was also, significantly larger than in Group 1 (p=0.0001), Group 2 (p=0.0003) the control group (p<0.00001). The choroid to retina thickness ratio was lowest in the control group, 1.01 (SD 0.17) and highest in Group 3, 1.21 (SD 0.2). No significant differences or trends were noted between the subgroups with regards to the retina thickness. The choroid to retina thickness ratio in Group 3 was significantly different from all the remaining groups, with the statistical significance level of p=0.0002, p=0.0014 and p=0.0001 for Group 1, Group 2 and the control group, respectively.

A very strong positive correlation was found between the SCP and DCP FAZ surface areas in the study and control group, with r=0.7774 and r=0.815357, respectively (p<0.05). No linear correlation

was found between FAZ parameters or choroid and retina thickness and DM duration, blood glucose level on examination or the last HbA1c. Neither the FAZ parameters nor the choroid or retina thickness were shown to be affected by the body mass index, presence of family history of T1DM or type of insulin therapy.

The DCP FAZ area in boys was significantly smaller than in girls in diabetics (p=0.0010) and healthy children (p=0.0302), with 474.0μm^2 versus 572.0μm^2 and 381.6μm^2 versus 482.8μm^2 in diabetic and healthy children, respectively. In diabetics, the SCP FAZ surface area was significantly smaller in boys (266.7μm^2) compared with girls (342.9μm^2) (p=0.0006), analogically to healthy children (p=0.0870). The central retina thickness was greater in boys in diabetic and healthy children, the former being statistically significant, with 254.1μm and 240.2μm for diabetic boys and girls, respectively (p=0.0001).

Conclusion

OCTA is suitable for use in children in different age groups. Changes occur in microvasculature of diabetic children prior to the development of DR, including increase in FAZ surface area, particularly in the deep capillary plexus, and in choroid thickness, which appear to progress with increasing DM duration. Lack of significant correlation between retinal changes identified by OCTA and the DM duration, biochemical diabetic parameters and anthropometric factors highlight the multifactorial nature of microvascular changes in diabetes. Nonetheless, the DCP is probably the most susceptible retinal layer and the microvascular changes in DR may originate there. These findings could suggest a direction of pathological vasculature changes prior to development of DR from the outermost choroid, through overlying retinal deep capillary plexus to superficial capillary plexus. However, further studies are required to confirm this and to determine the predictive role of FAZ and choroid parameters in the development of DR. Considerable differences were found in FAZ area and retinal thickness between genders in diabetic and healthy children, likely representing physiological differences. This highlights the importance of using different clinical norms for boys and girls regardless of the diabetic status.

9. STRESZCZENIE

Wstęp

Retinopatia cukrzycowa, będąca najpowszechniejszym powikłaniem mikronaczyniowym w cukrzycy, jest główną przyczyną utraty wzroku u osób dorosłych w wieku produkcyjnym w krajach rozwiniętych. Wiadomo, iż jednym z najważniejszych czynników ryzyka powstania retinopatii jest czas trwania choroby cukrzycowej. W związku z tym dzieci chorujące na cukrzycę typu 1 stanowią grupę wysokiego ryzyka w kontekście wykształcenia się retinopatii w okresie dorosłości. Angiografia OCT (Angio-OCT, OCTA) to nieinwazyjna metoda o potwierdzonej skuteczności w zakresie oceny mikrokrążenia siatkówkowego u osób dorosłych chorujących na cukrzycę. Niedawne badania z wykorzystaniem metody Angio-OCT przeprowadzone na pacjentach dorosłych, wykazały zmiany w obszarze strefy beznaczyniowej dołka (FAZ), do jakich dochodzi przed wystąpieniem retinopatii cukrzycowej. Ponadto wykazały one powiększanie się strefy FAZ wraz z postępem retinopatii. Celem niniejszego badania była ocena struktury mikronaczyniowej siatkówki i naczyniówki u chorujących na cukrzycę dzieci przy pomocy badania angiograficznego Angio-OCT oraz tomografii strukturalnej OCT.

Metodologia

Badanie Angio-OCT oraz tomografię strukturalną OCT na urządzeniu Topcon przeprowadzono na dzieciach w wieku 6-18 lat, chorujących na cukrzycę typu 1, lecz nie chorujących na retinopatię. Grupę kontrolną stanowili ich zdrowi rówieśnicy. Z badania wykluczono dzieci, u których już wcześniej wystąpiły schorzenia witreoretinalne. Metodą Angio-OCT dokonano pomiaru powierzchni strefy FAZ w splocie powierzchownym oraz głębokim, z kolei przy pomocy tomografii strukturalnej OCT mierzono grubość naczyniówki i siatkówki. Badanie Angio-OCT pomyślnie przeprowadzono na 112 dzieciach chorych oraz 30 dzieciach zdrowych, natomiast tomografię strukturalną OCT wykonano na 121 dzieciach chorych oraz 32 dzieciach z grupy kontrolnej. Na potrzeby dodatkowej analizy grupę badawczą podzielono na 3 podgrupy w zależności od czasu trwania choroby cukrzycowej: Grupa 1 – do 5 lat; Grupa 2: 5-10 lat; Grupa 3: ponad 10 lat. Zbierano dane na temat czasu trwania choroby, biochemicznych parametrów diabetologicznych oraz parametrów antropometrycznych. Porównania dwóch grup lub większej liczby niesparowanych przeprowadzono odpowiednio przy pomocy testu t-Studenta lub analizy wariancji ANOVA. Analizy korelacji dokonano w oparciu o współczynnik korelacji liniowej Pearsona. Analizę statystyczną wykonano przy pomocy programu Statistica.

Wyniki

Średnia powierzchnia strefy FAZ w splocie głębokim w grupie badanej wyniosła 520,4 μm^2 (OS 160,0 μm^2) i była istotnie większa niż w grupie kontrolnej (408,6 μm^2, OS 114,9 μm^2, p=0,0005). Średnia powierzchnia strefy FAZ w splocie powierzchownym w grupie badanej (302,7μm^2, OS 119,2 μm^2) również była większa niż w grupie kontrolnej (284,4 μm^2, OS 123,2 μm^2), choć w tym wypadku różnica nie była statystycznie istotna (p=0,46). Analogicznie, średni stosunek powierzchni strefy FAZ w splocie głębokim do jej powierzchni w splocie powierzchownym, wynoszący w grupie badanej 1,88 (OS 0,68) był istotnie większy niż w grupie kontrolnej, gdzie wyniósł 1,58 (OS 0,48) (p=0,0232). Różnica pomiędzy powierzchnią strefy FAZ w splocie powierzchownym i głębokim wyniosła w grupie badanej 217,6 μm^2 (OS 100,8μm^2) i była istotnie większa niż w grupie kontrolnej (124,2 μm^2, OS 72,8 μm^2) (p<0,0001). Średnia powierzchnia strefy FAZ w splocie głębokim rosła w miarę wydłużania się czasu trwania choroby, tj. od 502,2 μm^2 (OS 137,8 μm^2) w Grupie 1 do 523,9 μm^2 (OS 159,2 μm^2) w Grupie 2 oraz 539,7 μm^2 (OS 189,1μm^2) w Grupie 3. Stwierdzono istotne różnice pomiędzy grupą kontrolną a Grupą 1 (p=0,0120), Grupą 2 (p=0,0019) oraz Grupą 3 (p=0,0011). Nie stwierdzono natomiast istotnych różnic pomiędzy podgrupami, ani też trendów w zakresie strefy FAZ w splocie powierzchownym. Średni stosunek powierzchni strefy FAZ w splocie głębokim i powierzchownym rósł stopniowo w miarę wydłużania się czasu trwania choroby, tj. od 1,75 (OS 0,62) w Grupie 1 do 1,93 (SD 0,60) w Grupie 2 oraz 1,98 (OS 0,83) w Grupie 3. Stwierdzono istotne różnice pomiędzy grupą kontrolną a Grupą 2 (p=0,0210) oraz Grupą 3 (p=0,0169). Ponadto, różnica pomiędzy powierzchnią strefy FAZ w obydwu splotach była w grupie kontrolnej istotnie mniejsza niż w Grupie 1 (p<0,006), w Grupie 2 (p<0,0001) oraz w Grupie 3 (p<0,0001). Odnotowano także różnice w obrębie grupy badanej, gdyż Grupa 1 różniła się istotnie od Grupy 2 (p<0,03) oraz Grupy 3 (p<0,05).

Grubość centralnej części naczyniówki oraz jej grubość średnia u dzieci z cukrzycą była zauważalnie większa niż w grupie kontrolnej, choć różnica nie była tu statystycznie istotna. Na poziomie podgrup zaobserwowano stopniowy wzrost grubości naczyniówki w miarę wydłużania się czasu trwania choroby cukrzycowej. Grubość naczyniówki w części centralnej rosła z poziomu 305,5 µm (OS 61,7 µm) do 309,2 µm (OS 70,1 µm) w Grupie 1, 315,2 µm (OS 64,3 µm) w Grupie 2 oraz 367,4 µm (OS 66,0 µm) w Grupie 3. W ujęciu statystycznym, grubość centralnej części naczyniówki u dzieci chorych z Grupy 3 była istotnie większa niż u dzieci z Grupy 1 (p=0,0002), Grupy 2 (p=0,0014) oraz grupy kontrolnej (p=0,0003). Także średnia grubość naczyniówki rosła z poziomu 285,9 µm (OS 51,1 µm) w grupie kontrolnej do 291,0 µm (OS 62,5 µm) w Grupie 1, 294,4µm (OS 56,7 µm) w Grupie 2

oraz 348,0 µm (OS 58,3µm) w Grupie 3. Średnia grubość naczyniówki u pacjentów z Grupy 3 była także istotnie większa niż w Grupie 1 (p=0,0001), w Grupie 2 (p=0,0003) oraz w grupie kontrolnej (p<0,00001). Stosunek grubości naczyniówki i siatkówki był najniższy w grupie kontrolnej i wyniósł 1,01 (OS 0,17), natomiast najwyższy był w Grupie 3 (1,21, OS 0,2). Nie stwierdzono istotnych różnic ani trendów pomiędzy podgrupami w odniesieniu do grubości siatkówki. Stosunek grubości naczyniówki i siatkówki w Grupie 3 różnił się istotnie od wartości obserwowanych we wszystkich pozostałych grupach, przy poziomach istotności statystycznej wynoszących p=0,0002, p=0,0014 oraz p=0,0001 odpowiednio dla Grupy 1, Grupy 2 oraz grupy kontrolnej.

Stwierdzono bardzo silną korelację pomiędzy powierzchniami stref FAZ w splocie powierzchownym i głębokim w grupie badanej, a ich odpowiednikami w grupie kontrolnej (odpowiednio r=0,7774 oraz r=0,815357, p<0,05). Nie stwierdzono korelacji liniowej pomiędzy parametrami strefy FAZ bądź grubością naczyniówki i siatkówki a czasem trwania choroby cukrzycowej, poziomem glukozy we krwi w dniu badania bądź ostatnim wynikiem HbA1c. Ani parametry strefy FAZ, ani też grubość naczyniówki bądź siatkówki nie wydają się związane z indeksem masy ciała, z historią zachorowań na cukrzycę typu 1 w rodzinie bądź z rodzajem terapii insulinowej.

Powierzchnia strefy FAZ w splocie głębokim u chłopców była istotnie mniejsza niż u dziewcząt zarówno wśród dzieci chorych (p=0,0010), jak i zdrowych (p=0,0302): 474,0 μm^2 wobec 572.0μm^2 w przypadku chłopców oraz 381,6 μm^2 wobec 482,8 μm^2 wśród dziewcząt. Powierzchnia strefy FAZ w splocie powierzchownym w grupie dzieci chorych była istotnie mniejsza wśród chłopców (266,7μm^2) niż u dziewcząt (342,9 μm^2) (p=0,0006), podobnie jak w przypadku dzieci zdrowych (p=0,0870). Grubość siatkówki w części centralnej była większa u chłopców zarówno z grupy badanej, jak i kontrolnej. W grupie badanej różnica ta była istotna statystycznie. W przypadku chłopców z grupy badanej wyniosła ona 254,1µm, natomiast wśród dziewcząt z tej samej grupy wyniosła 240,2 µm (p=0,0001).

Wnioski

Metoda Angio-OCT może być stosowana u dzieci w różnym wieku. Zmiany w obrębie struktur mikronaczyniowych u dzieci z cukrzycą zachodzą przed wystąpieniem retinopatii i dotyczą powierzchni strefy FAZ (zwłaszcza w splocie głębokim) oraz grubości naczyniówki, która zdaje się rosnąć w miarę wydłużania się czasu trwania choroby. Brak istotnej korelacji pomiędzy zmianami w siatkówce widocznymi w badaniu Angio-OCT a czasem trwania choroby, biochemicznymi

parametrami diabetologicznymi oraz cechami antropometrycznymi wskazuje na wieloczynnikowy charakter zmian mikronaczyniowych w cukrzycy. Tym niemniej, najbardziej podatną warstwą siatkówki prawdopodobnie jest splot głęboki i właśnie w jego obrębie zmiany mogą wystąpić najwcześniej. Obserwacje te mogą wskazywać na to, że patologiczne zmiany naczyniowe poprzedzające wystąpienie retinopatii następują w kierunku od zewnątrz (tj. od naczyniówki, poprzez powlekający siatkówkę splot głęboki, ku splotowi powierzchownemu). Konieczne są jednak dalsze badania, które potwierdzą to przypuszczenie i określą wartość predykcyjną parametrów naczyniówki oraz strefy FAZ w rozwoju retinopatii cukrzycowej. W badaniu zaobserwowano znaczne różnice w powierzchni strefy FAZ oraz grubości siatkówki pomiędzy chłopcami i dziewczętami, zarówno wśród dzieci chorych, jak i w grupie kontrolnej. Różnice te są zapewne odzwierciedleniem różnic fizjologicznych. Obserwacja ta podkreśla znaczenie stosowania różnych norm klinicznych dla chłopców i dla dziewcząt, bez względu na występowanie u nich cukrzycy.

10. BIBLIOGRAPHY

1. International Diabetes Federation. IDF diabetes atlas. [Online].; 2009 [cited 2017 June 22]. Available from: http://www.diabetesatlas.org/

2. Cukrzyca Polska. [Online]. [cited 2017 July 09]. Available from: http://cukrzycapolska.pl/cukrzyca/statystyki/

3. Bowling B. Kanski's Clinical Ophthalmology. A Systematic Approach. 8th ed.: Elsevier; 2015.

4. Pieczynski J, Bandurska-Stankiewicz E, Wiatr-Bykowska D, Rutkowska J. Cukrzycowa choroba oczu. Diabetologia Doświadczalna i Kliniczna. 2010; 10(1): p. 1-10.

5. AAO PPP Retina/Vitreous Panel, Hoskins Center for Quality Eye Care. American Academy of Ophthalmology. Guidelines. Diabetic Retinopathy PPP - Updated 2016. [Online].; 2016 [cited 2017 Jun 23]. Available from: https://www.aao.org/preferred-practice-pattern/diabetic-retinopathy-ppp-updated-2017

6. Bunce C, Wormald R. Leading causes of certification for blindness and partial sight in England & Wales. BMC Public Health. 2006 Mar; 6: p. 58.

7. TADDS - Tool for the assessment of diabetic retinopathy. [World Health Organisation].; 2015 [cited 2017 July 09]. Available from: http://www.who.int/blindness/publications/TADDS_ENG.pdf?ua=1

8. Mohamed Q, Ross A, Chu C. Diabetic retinopathy (treatment). BMJ Clin Evid. 2011 May.

9. Klein R, Klein B, Moss S. The Wisconsin epidemiologic study of diabetic retinopathy: an update. Aust NZ J Ophthalmol. 1990 Feb; 18(1): p. 19–22.

10. Mohamed Q, Gillies M, Wong T. Management of Diabetic Retinopathy: A Systematic Review. JAMA. 2007 Aug; 298(8): p. 902-916.

11. Evans J, Rooney C, Ashwood F, et al. Blindness and partial sight in England and Wales: April 1990–March 1991. Health Trends. 1996; 28: p. 5-12.

12. Kawalec P, Pilc A. Koszty leczenia retinopatii cukrzycowej w Polsce (na podstawie danych za 2002 rok). Okulistyka. 2003;(3).

13. Kagan V, Shvedova A, Novikov K, Kozlov Y. Light-induced free radical oxidation of membrane lipids in photoreceptors of frog retina. Biochimica et Biophysica Acta—Biomembranes. 1973 Nov; 330(1): p. 76–79.

14. Li C, Miao X, Li F, Wang S, et al. Oxidative Stress-Related Mechanisms and Antioxidant Therapy in Diabetic Retinopathy. Oxid Med Cell Longev. 2017 Feb.

15. Kim J, Kim C, Lee Y, Jo K, et al. Methylglyoxal induces hyperpermeability of the blood-retinal barrier via the loss of tight junction proteins and the activation of matrix metalloproteinases. Graefe's Archive for Clinical and Experimental Ophthalmology. 2012; 250(5): p. 691–697.

16. Gołębiewska J. Retinopatia cukrzycowa. In Hautz W, Gołębiewska J, editors. OCT i Angio-OCT w schorzeniach tylnego odcinak gałki ocznej. Warszawa: Medipage; 2015. p. 44-58.

17. Giacco F, Brownlee M. Oxidative stress and diabetic complications. Circulation Research. 2010 Oct; 107(9): p. 1058–1070.

18. Hartnett M, Stratton R, Browne R, Rosner B, et al. Serum markers of oxidative stress and severity of diabetic retinopathy. Diabetes Care. 2000 Feb; 23(2): p. 234–240.

19. Ferrara N, Davis-Smyth T. The biology of vascular endothelial growth factor. Endocr Rev. 1997 Feb; 18(1): p. 4–25.

20. Papadopoulos N, Martin J, Ruan Q, Rafique A, et al. Binding and neutralization of vascular endothelial growth factor (VEGF) and related ligands by VEGF Trap, ranibizumab and bevacizumab. Angiogenesis. 2012 Jun; 15(2): p. 171–185.

21. Patil B, Puri P. Medical retina. In Sundaram V, Barsam A, Alwitry A, Khaw P. Training in Ophthalmology, the essential clinical curriculum.: Oxford University Press; 2009.

22. Wong T, Cheung C, Larsen M, Sharma S, Simó R. Diabetic retinopathy. Nature Reviews Disease Primers. 2016 Mar; 2.

23. Association TEM. American Academy of Ophthalmology. International Clinical Diabetic Retinopathy Severity Scale. ; 2002.

24. Diabetes Control and Complications Trial Research Group, Nathan DM, Genuth S, Lachin J, Cleary P, et al. The effect of intensive treatment of diabetes on the development and progression of long-term complications in insulin-dependent diabetes mellitus. Engl J Med. 1993 Sep; 329(14): p. 977–986.

25. Writing Team for the Diabetes Control and Complications Trial/Epidemiology of Diabetes Interventions and Complications Research Group. Effect of intensive therapy on the microvascular complications of type 1 diabetes mellitus. JAMA. 2002 May; 287(19): p. 2563–2569.

26. UK Prospective Diabetes Study (UKPDS) Group. Intensive blood-glucose control with sulphonylureas or insulin compared with conventional treatment and risk of complications in patients with type 2 diabetes (UKPDS 33). Lancet. 1998 Aug; 352(9178): p. 837–853.

27. UK Prospective Diabetes Study (UKPDS) Group. Tight blood pressure control and risk of macrovascular and microvascular complications in type 2 diabetes: UKPDS 38. BMJ. 1998 Sep; 317(7160): p. 703–713.

28. ACCORD Eye Study Group, Chew E, Ambrosius W, Davis M, al. e. Effects of medical therapies on retinopathy progression in type 2 diabetes. N Engl J Med. 2010 Jul; 363(3): p. 233–244.

29. Wong T, Klein R, Klein B. In The epidemiology and risk factors of diabetic retinopathy. New York: Oxford Press; 2009.

30. Beetham W. Visual prognosis of proliferating diabetic retinopathy. Br J Ophthalmol. 1963 Oct; ;47: p. 611–619.

31. Deckert T, Simonsen S, Poulsen J. Prognosis of proliferative retinopathy in juvenile diabetes. Diabetes. 1967 Oct; 16(10): p. 728–733.

32. Caird F, Burditt A, Draper G. Diabetic retinopathy: a further study of prognosis for vision. Diabetes. 1968 Mar; 17(3): p. 121–123.

33. Keel S, Itsiopoulos C, Koklanis K, Vukicevic M, et al. Prevalence and risk factors for diabetic retinopathy in a hospital-based population of Australian children and adolescents with type 1 diabetes. J Pediatr Endocrinol Metab. 2016 Oct; 29(10): p. 1135-1142.

34. Dhillon N, Karthikeyan A, Castle A, Dodson P, et al. Natural history of retinopathy in children and young people with type 1 diabetes. Eye (Lond). 2016 Jul; 30(7): p. 987-91.

35. de Abreu J, Silva R, Cunha-Vaz J. The blood-retinal barrier in diabetes during puberty. Arch Ophthalmol. 1994 Oct; 112(10): p. 1334-8.

36. Scanlon PH, Stratton IM, Bachmann MO, Jones C, Leese GP, Four Nations Diabetic Retinopathy Screening Study Group. Risk of diabetic retinopathy at first screen in children at 12 and 13 years of age. Diabet Med. 2016 Dec; 33(12): p. 1655-1658.

37. Salardi S, Porta M, Maltoni G, Rubbi F, et al. Infant and toddler type 1 diabetes: complications after 20 years' duration. Diabetes Care. 2012 Apr; 35(4): p. 829-33.

38. Downie E, Craig M, Hing S, Cusumano J, et al. Continued reduction in the prevalence of retinopathy in adolescents with type 1 diabetes: role of insulin therapy and glycemic control. Diabetes Care. 2011 Nov; 34(11): p. 2368-73.

39. White M, Sabin M, Magnussen C, O'Connell M, et al. Long term risk of severe retinopathy in childhood-onset type 1 diabetes: a data linkage study. Med J Aust. 2017 May; 206(9): p. 398-401.

40. Virk S, Donaghue K, Cho Y, Benitez-Aguirre P, et al. Association Between HbA1c Variability and Risk of Microvascular Complications in Adolescents With Type 1 Diabetes. J Clin Endocrinol Metab. Sep 2016; 101(9): p. 3257-63.

41. Patrick J, Tyler M. Fundus photography overview. Ophthalmic Photography: Retinal Photography, Angiography, and Electronic Imaging. 2nd ed. New York: Butterworth-Heinemann Medical; 2001.

42. Witmer M, Kiss S. The clinical utility of ultra-wide-field imaging. Rev Ophthalmol. 2013 Mar-Apr; 58(2): p. 143-54.

43. Li H, Hubbard L, Danis R, Esquivel A, et al. Monoscopic versus stereoscopic retinal photography for grading diabetic retinopathy severity. Invest Ophthalmol Vis Sci. 2010 Jun; 51(6): p. 3184–92.

44. Salz D, Witkin A. Imaging in Diabetic Retinopathy. Middle East Afr J Ophthalmol. 2015 Apr-Jun; 22(2): p. 145–150.

45. Coleman D, Silverman R, Lizzi F, Rondeau M. Ultrasonography of the Eye and Orbit. 2nd ed. Philadelphia: Lippincott Williams and Wilkins; 2006.

46. Novotny HR, Alvis DL. A method of photographing fluorescence in circulating blood in the human retina. Circulation. 1961 Jul; 24: p. 82-6.

47. Ciardella A, Brown D. Wide field imaging. In A. A, editor. Fundus Fluorescein and Indocyanine Green Angiography: A Textbook and Atlas. New York: Slack Inc; 2007. p. 79–83.

48. Friberg T, Gupta A, Yu J, Huang L, et al. Ultra wide angle fluorescein angiographic imaging: A comparison to conventional digital acquisition systems. Ophthalmic Surg Lasers Imaging. 2008 Jul-Aug; 39(4): p. 304–11.

49. Norton E, Gutman F. Diabetic retinopathy studied by fluorescein angiography. Ophthalmologica. 1965; 150(1): p. 5-17.

50. Di Antonio L, Mastropasqua L. OCT Angiography Examination of Foveal Avascular Zone. In Lumbroso B, Huand D, Chen C, Jia Y, Rispoli M, Romano A, et al. Clinical OCT Angiography Atlas.: Jaypee; 2015. p. 137-141.

51. Bresnick G, Condit R, Syrjala S, Palta M, et al. Abnormalities of the foveal avascular zone in diabetic retinopathy. Arch Ophthalmol. 1984 Sep; 102(9): p. 1286-93.

52. Zheng Y, Gandhi J, Stangos A, Campa C, et al. Automated segmentation of foveal avascular zone in fundus fluorescein angiography. Invest Ophthalmol Vis Sci. 2010 Jul; 51(7): p. 3653-9.

53. Mansour A, Schachat A, Bodiford G, Haymond R. Foveal avascular zone in diabetes mellitus. Retina. 1993; 13(2): p. 125-8.

54. Bresnick G, Condit R, Syrjala S, Palta M, et al. Abnormalities of the foveal avascular zone in diabetic retinopathy. Arch Ophthalmol. 1984 Sep; 102(9): p. 1286-93.

55. Arend O, Wolf S, Jung F, Bertram B, et al. Retinal microcirculation in patients with diabetes mellitus: dynamic and morphological analysis of perifoveal capillary network. Br J Ophthalmol. 1991 Sep; 75(9): p. 514-8.

56. Conrath J, Giorgi R, Raccah D, Ridings B. Foveal avascular zone in diabetic retinopathy: quantitative vs qualitative assessment. Eye (Lond). 2005 Mar; 19(3): p. 322-6.

57. Kwiterovich K, Maguire M, Murphy R, Schachat A, et al. Frequency of adverse systemic reactions after fluorescein angiography. Results of a prospective study. Ophthalmology. 1991 Jul; 89(7): p. 1139–42.

58. Fineschi V, Monasterolo G, Rosi R, Turillazzi E. Fatal anaphylactic shock during a fluorescein angiography. Forensic Sci Int. 1999 Mar; 100(1-2): p. 137–42.

59. Berkow J, Flower R, Orth D, Kelley J. Fluorescein and Indocyanine Green Angiography. 2nd ed. San Francisco: American Academy of Ophthalmology; 1997.

60. Early Treatment Diabetic Retinopathy Study Research Group. Photocoagulation for diabetic macular edema. Early Treatment Diabetic Retinopathy Study report number 1. Arch Ophthalmol. 1985 Dec; 103(12): p. 1796–806.

61. The Diabetic Retinopathy Study Research Group. Photocoagulation treatment of proliferative diabetic retinopathy: A short report of long range results. Diabetic Retinopathy Study (DRS) Report Number 4. Proceedings of the 10th Congress of the International Diabetes Federation. 1979.

62. Huang D, Swanson E, Lin C, Schuman J, et al. Optical coherence tomography. Science. 1991 Nov; 254(5035): p. 1178-81.

63. Hee M, Izatt J, Swanson E, Huang D, et al. Optical coherence tomography of the human retina. Arch Ophthalmol. 1995 Mar; 113(3): p. 325-32.

64. Izatt J, Hee M, Swanson E, Lin C, et al. Micrometer-scale resolution imaging of the anterior eye in vivo with optical coherence tomography. Arch Ophthalmol. 1994 Dec; 112(12): p. 1584-9.

65. Gołębiewska J. Rys Historyczny. In Hautz W, Gołębiewska J, editors. OCT i Angio-OCT w schorzeniach tylnego odcinka gałki ocznej. Warszawa: Medipage; 2015. p. 3-4.

66. Kęcik T, Kasprzak J, Kęcik D, et al. Obraz prawidłowej siatkówki w badaniu metodą optycznej koherentnej tomografii. Okulistyka. 1998; 1: p. 3-5.

67. Kasprzak J, Kęcik D, Kęcik T, et al. Metoda skanningu optycznego w badaniach dna oczu. Okulistyka. 1998; 1: p. 17-19.

68. Kowalczyk A, Wojtkowski M. Tomografia optyczna. Postępy Fizyki. 2002;: p. 172-175.

69. Chen F, Chen S. Optical coherence tomography. In Sundaram V, Barsam A, Alwitry A, Khaw PT. Training in Opthalmology, the essential clinical curriculum. Oxford: Oxford University Press.; 2009.

70. Gołębiewska J. Optyczna Koherentna Tomografia. In Hautz W, Gołębiewska J. OCT i Angio-OCT w schorzeniach tylnego odcinka gałki ocznej. Warszawa: Medipage; 2015. p. 5-6.

71. Hou R, Le T, Murgu S, Chen Z, Brenner M. Recent advances in optical coherence tomography for the diagnoses of lung disorders. Expert Rev Respir Med. 2011 Oct; 5(5): p. 711-24.

72. Tatham A. Review of Ophthalmology.; 2014 [cited 2017 June 27]. Available from: https://www.reviewofophthalmology.com/CMSDocuments/2014/3/rp0314_topconi.pdf

73. Lau T, Wong I, Iu L, Chhablani J, et al. En-face optical coherence tomography in the diagnosis and management of age-related macular degeneration and polypoidal choroidal vasculopathy. Indian J Ophthalmol. 2015 May; 63(5): p. 378–383.

74. Wang R, Jacques S, Ma Z, Hurst S, et al. Three dimensional optical angiography. Opt Express. 2007 Apr; 15(7): p. 4083-97.

75. Grulkowski I, Górczynska I, Szkulmowski M, Szlag D, et al. Scanning protocols dedicated to smart velocity ranging in spectral OCT. Opt Express. 2009 Dec; 17(26): p. 23736-54.

76. Yu L, Chen Z. Doppler variance imaging for three-dimensional retina and choroid angiography. J Biomed Opt. 2010 Jan-Feb; 15(1): p. 016029.

77. Makita S, Jaillon F, Yamanari M, Miura M, Yasuno Y. Comprehensive in vivo micro-vascular imaging of the human eye by dual-beam-scan Doppler optical coherence angiography. Opt Express. 2011 Jan; 19(2): p. 1271-83.

78. Zotter S, Pircher M, Torzicky T, Bonesi M, et al. Visualization of microvasculature by dual-beam phase-resolved Doppler optical coherence tomography. Opt Express. 2011 Jan; 19(2): p. 1217-27.

79. Braaf B, Vermeer K, Vienola K, de Boer J. Angiography of the retina and the choroid with phase-resolved OCT using interval-optimized backstitched B-scans. Opt Express. 2012 Aug; 20(18): p. 20516-34.

80. Huang D, Jia Y, Gao S. Principles of Optical Coherence Tomography. In Lumbroso B, Huang D, Souied E, Rispoli M, editors. Practical Handbook of OCT Angiography.: Jaypee; 2016. p. 1-5.

81. Mariampillai A, Standish B, Moriyama E, Khurana M, et al. Speckle variance detection of microvasculature using swept-source optical coherence tomography. Opt Lett. 2008 Jul; 33(13): p. 1530-2.

82. Motaghiannezam R, Fraser S. Logarithmic intensity and speckle-based motion contrast methods for human retinal vasculature visualization using swept source optical coherence tomography. Biomed Opt Express. 2012 Mar; 3(3): p. 503-21.

83. Fingler J, Zawadzki R, Werner J, Schwartz D, Fraser S. Volumetric microvascular imaging of human retina using optical coherence tomography with a novel motion contrast technique. Opt Express. 2009 Nov; 17(24): p. 22190-200.

84. Liu G, Lin A, Tromberg B, Chen Z. A comparison of Doppler optical coherence tomography methods. Biomed Opt Express. 2012 Oct; 3(10): p. 2669-80.

85. Jia Y, Tan O, Tokayer J, Potsaid B, et al. Split-spectrum amplitude-decorrelation angiography with optical coherence tomography. Opt Express. 2012 Feb; 20(4): p. 4710-25.

86. Tam J, Tiruveedhula P, Roorda A. Characterization of single-file flow through human retinal parafoveal capillaries using an adaptive optics scanning laser ophthalmoscope. Biomed Opt Express. 2011 Mar; 2(4): p. 781-93.

87. Riva C, Petrig B. Blue field entoptic phenomenon and blood velocity in the retinal capillaries. J Opt Soc Am. 1980 Oct; 70(10): p. 1234-8.

88. Topcon. Topcon. [Online].; 2017 [cited 2017 Sep 11]. Available from: http://www.topcon-medical.eu/eu/products/382-dri-oct-triton-swept-source-oct.html#images .

89. Lumbroso B, Huang D, Chen C, Jia Y, et al. Clinical OCT Angiography Atlas. 1st ed.: Yaypee; 2015.

90. Turgut B. Optical Coherence Tomography Angiography – A General View. European Ophthalmic Review. 2016; 10(1): p. 39–42.

91. Wylęgała A, Teper S, Dobrowolski D, Wylęgała E. Optical coherence angiography: A review. Medicine (Baltimore). 2016 Oct; 95(41): p. e4907.

92. Practical Handbook of OCT Angiography. Lumbroso, B; Huang, D; Souied, E; Rispoli, M. ed.: Yaypee; 2016.

93. Hautz W, Gołębiewska J, editors. OCT i Angio-OCT w schorzeniach tylnego odcinka gałki ocznej. Warszawa: Medipage; 2015.

94. De Oliveira P, Berger A, Chow D. Optical coherence tomography angiography in chorioretinal disorders. Can J Ophthalmol. 2017 Feb; 52(1): p. 125-136.

95. Huang D, Jia Y, Gao S. Interpretation of Optical Coherence Tomography Angiography. In Lumbroso B, Huang D, Souied E, Rispoli M, editors. Practical Handbook of OCT Angiography.: Yaypee; 2016. p. 6-15.

96. Lumbroso B, Huang D, Souied E, Rispoli M. Practical Handbook of OCT Angiography. 1st ed. Lumbroso B, Huang D, Souied E, Rispoli M, editors.: Jaypee; 2016.

97. Savastano M, Rispoli M, Lumbroso B. Diabetic retinopathy and optical coherence tomography angiography. In Lumbroso B, Huang D, Souied E, Rispoli MB. Practical Handbook of OCT Angiography.: Yaypee; 2016. p. 28-32.

98. de Barros Garcia J, Isaac D, Avila M. Diabetic retinopathy and OCT angiography: clinical findings and future perspectives. Int J Retina Vitreous. 2017 Mar; 3: p. 14.

99. Takase N, Nozaki M, Kato A, Ozeki H, et al. Enlargement of foveal avascular zone in diabetic eyes evaluated by en face optical coherence tomography angiography. Retina. 2015 Nov; 35(11): p. 2377-83.

100. Dimitrova G, Chihara E, Takahashi H, Amano H, Okazaki K. Quantitative Retinal Optical Coherence Tomography Angiography in Patients With Diabetes Without Diabetic Retinopathy. Invest Ophthalmol Vis Sci. 2017 Jan; 58(1): p. 190-196.

101. Gozlan J, Ingrand P, Lichtwitz O, Cazet-Supervielle A, et al. Retinal microvascular alterations related to diabetes assessed by optical coherence tomography angiography: A cross-sectional analysis. Medicine (Baltimore). 2017 April; 96(15): p. e6427.

102. Carnevali A, Sacconi R, Corbelli E, Tomasso L, et al. Optical coherence tomography angiography analysis of retinal vascular plexuses and choriocapillaris in patients with type 1 diabetes without diabetic retinopathy. Acta Diabetol. 2017 Jul; 54(7): p. 695-702.

103. Hwang T, Gao S, Liu L, Lauer A, et al. Automated Quantification of Capillary Nonperfusion Using Optical Coherence Tomography Angiography in Diabetic Retinopathy. JAMA Ophthalmol. 2016 Apr; 134(4): p. 367-73.

104. Durbin M, An L, Shemonski N, Soares M, et al. Quantification of Retinal Microvascular Density in Optical Coherence Tomographic Angiography Images in Diabetic Retinopathy. JAMA Ophthalmol. 2017 Apr; 135(4): p. 370-376.

105. Simonett J, Scarinci F, Picconi F, Giorno P, et al. Early microvascular retinal changes in optical coherence tomography angiography in patients with type 1 diabetes mellitus. Acta Ophthalmol. 2017 Jul; 54(7): p. 695-702.

106. Agemy SA, Scripsema NK, Shah CM, Chui T, et al. Retinal vascular perfusion density mapping using optical coherence tomography angiography in normals and diabetic retinopathy patients. Retina. 2015 Nov; 35(11): p. 2353-63.

107. Sambhav K, Abu-Amero K, Chalam K. Deep capillary macular perfusion indices obtained with OCT angiography correlate with degree of nonproliferative diabetic retinopathy. Eur J Ophthalmol. 2017 Mar.

108. Ishibazawa A, Nagaoka T, Yokota H, Takahashi A, et al. Characteristics of Retinal Neovascularization in Proliferative Diabetic Retinopathy Imaged by Optical Coherence Tomography Angiography. Invest Ophthalmol Vis Sci. 2016 Nov; 57(14): p. 6247-6255.

109. Krawitz B, Mo S, Geyman L, Agemy S, et al. Acircularity index and axis ratio of the foveal avascular zone in diabetic eyes and healthy controls measured by optical coherence tomography angiography. Vision Res. 2017 Feb.

110. Yilmaz I, Ocak O, Yilmaz B, Inal A, et al. Comparison of quantitative measurement of foveal avascular zone and macular vessel density in eyes of children with amblyopia and healthy controls: an optical coherence tomography angiography study. J AAPOS. 2017 Jun; 21(3): p. 224–228.

111. Sayin N, Kara N, Pirhan D, Vural A, et al. Evaluation of subfoveal choroidal thickness in children with type 1 diabetes mellitus: an EDI-OCT study. Semin Ophthalmol. 2014 Jan; 29(1): p. 27-31.

112. Elhabashy S, Elbarbary N, Nageb K, Mohammed M. Can optical coherence tomography predict early retinal microvascular pathology in type 1 diabetic adolescents without minimal diabetic retinopathy? A single-centre study. J Pediatr Endocrinol Metab. 2015 Jan; 28(1-2): p. 139-46.

113. Farias L, Lavinsky D, Schneider W, Guimarães L, et al. Choroidal thickness in patients with diabetes and microalbuminuria. Ophthalmology. 2014 Oct; 121(10): p. 2071-3.

114. Radzikowski A, Wielowiejska A. Ocena stanu odżywienia dzieci. In P. A, editor. Gastroenterologia dziecięca.: Wydawnictwo Czelej; 2014 r.

115. Instytut "Pomnik-Centrum Zdrowia Dziecka". [Online]. [cited 2017 May 2]. Available from: http://www.czd.pl/index.php?option=com_content&view=article&id=1717&Itemid=538 .

116. Zhang K, Ferreyra H, Grob S, et al. Diabetic retinopathy: genetics and etiologic mechanisms. In Ryan SJ, Sadda SR, Hinton DR, editor. Retina. London: Elsevier Saunders; 2013. p. 925–939.

117. Di G, Weihong Y, Xiao Z, Zhikun Y, et al. A morphological study of the foveal avascular zone in patients with diabetes mellitus using optical coherence tomography angiography. Graefes Arch Clin Exp Ophthalmol. 2016 May; 254(5): p. 873-9.

118. de Carlo T, Chin A, Bonini Filho M, Adhi M, et al. Detection of microvascular changes in eyes of patients with diabetes but no clinical diabetic retinopathy using optical coherence tomography angiography. Retina. 2015 Nov; 35(11): p. 2364-70.

119. Hasegawa N, Nozaki M, Takase N, Yoshida M, Ogura Y. New insights into microaneurysms in the deep capillary plexus detected by optical coherence tomography angiography in diabetic macular edema. Invest Ophthalmol Vis Sci. 2016 Jul; 57(9): p. OCT348–OCT355.

120. Ishibazawa A, Nagaoka T, Takahashi A, Omae T, et al. Optical coherence tomography angiography in diabetic retinopathy: a prospective pilot study. Am J Ophthalmol. 2015 Jul; 160(1): p. 35–44.

121. Couturier A, Mané V, Bonnin S, Erginay A, et al. Capillary plexus anomalies in diabetic retinopathy on optical coherence tomography angiography. Retina. 2015 Nov; 35(11): p. 2384–2391.

122. Suzuki N, Hirano Y, Tomiyasu T, Esaki Y, et al. Retinal hemodynamics seen on optical coherence tomography angiography before and after treatment of retinal vein occlusion. Invest Ophthalmol Vis Sci. 2016 Oct; 57(13): p. 5681-5687.

123. Miyamoto K, Ogura Y. Pathogenetic potential of leukocytes in diabetic retinopathy. Semin Ophthalmol. 1999 Dec; 14(4): p. 233–239.

124. Gill A, Cole E, Novais E, Louzada R, et al. Visualization of changes in the foveal avascular zone in both observed and treated diabetic macular edema using optical coherence tomography angiography. Int J Retina Vitreous. 2017 Jun; 3: p. 19.

125. Durbin M, An L, Shemonski N, Soares M, et al. Quantification of Retinal Microvascular Density in Optical Coherence Tomographic Angiography Images in Diabetic Retinopathy. JAMA Ophthalmol. 2017 Apr; 135(4): p. 370-376.

126. Sander B, Larsen M, Engler C, Lund-Andersen H, Parving H. Early changes in diabetic retinopathy: capillary loss and blood-retina barrier permeability in relation to metabolic control. Acta Ophthalmolo (Copenh). 1994 Oct; 72(5): p. 553-9.

127. Zhang Z, Huang X, Meng X, Chen T, et al. In vivo assessment of macula in eyes of healthy children 8 to 16 years old using optical coherence tomography angiography. Sci Rep. 2017 Aug; 7(1): p. 8936.

128. Samara W, Say E, Khoo C, Higgins T, et al. Correlation of foveal avascular zone size with foveal morphology in normal eyes using optical tomography angiography. Retina. 2015 Nov; 35(11): p. 2188-95.

129. Tan C, Lim L, Chow V, Chay I, et al. Optical Coherence Tomography Angiography Evaluation of the Parafoveal Vasculature and Its Relationship With Ocular Factors. Invest Ophthalmol Vis Sci. 2016 Jul; 57(9): p. OCT224-34.

130. Coscas F, Sellam A, Glacet-Bernard A, Jung C, et al. Normative Data for Vascular Density in Superficial and Deep Capillary Plexuses of Healthy Adults Assessed by Optical Coherence Tomography Angiography. Invest Ophthalmol Vis Sci. 2016 Jul; 57(9): p. OCT211-23.

131. Zhou Y, Zhang Y, Shi K, Wang C. Body mass index and risk of diabetic retinopathy: A meta-analysis and systematic review. Medicine (Baltimore). 2017 Jun; 96(22): p. e6754.

132. Zabeen B, Craig M, Virk S, Pryke A, et al. Insulin pump therapy is associated with lower rates of retinopathy and peripheral nerve abnormality. PLoS One. Apr 2016; 11(4): p. e0153033.

133. Xu J, Xu L, Du K, Shao L, et al. Subfoveal choroidal thickness in diabetes and diabetic retinopathy. Ophthalmology. 2013 Oct; 120(10): p. 2023-8.

134. Shao L, Wang Y, Xu J, Chen C, et al. Subfoveal choroidal thickness of Chinese aged over 50 years and patients with diabetes mellitus and glaucoma. [Article in Chinese]. Zhonghua Yan Ke Za Zhi. 2014 Jun; 50(6): p. 414-20.

135. Tavares Ferreira J, Vicente A, Proença R, Santos B, et al. Choroidal thickness in diabetic patients without diabetic retinopathy. Retina. 2017 Mar; 0: p. 1–10.

136. Tavares Ferreira J, Proença R, Alves M, Dias-Santos A, et al. Retina and Choroid of Diabetic Patients Without Observed Retinal Vascular Changes: A Longitudinal Study. Am J Ophthalmol. 2017 Apr; 176: p. 15-25.

137. Rewbury R, Want A, Varughese R, Chong V. Subfoveal choroidal thickness in patients with diabetic retinopathy and diabetic macular oedema. Eye (Lond). 2016 Dec; 30(12): p. 1568-1572.

138. Kniggendorf V, Novais E, Kniggendorf S, Xavier C, et al. Effect of intravitreal anti-VEGF on choroidal thickness in patients with diabetic macular edema using spectral domain OCT. Arq Bras Oftalmol. 2016 May-Jun; 79(3): p. 155-8.

139. Okamoto M, Matsuura T, Ogata N. Effects of panretinal photocoagulation on choroidal thickness and choroidal blood flow in patients with servere nonproliferative diabetic retinopathy. Retina. 2016 Apr; 36(4): p. 805-11.

140. Roohipoor R, Sharifian E, Ghassemi F, Riazi-Esfahani M, et al. Choroidal thickness changes in proliferative diabetic retinopathy treated with panretinal photocoagulation versus panretinal photocoagulation with intravitreal bevacizumab. Retina. 2016 Oct; 36(10): p. 1997-2005.

141. McCourt E, Cadena B, Barnett C, Ciardella A, et al. Measurement of subfoveal choroidal thickness using spectral domain optical coherence tomography. Ophthalmic Surg Lasers Imaging. 2010 Nov-Dec; 41(Suppl): p. S28-33.

142. Tan C, Cheong K, Lim L, Li K. Topographic variation of choroidal and retinal thicknesses at the macula in healthy adults. Br J Ophthalmol. 2014 Mar; 98(3): p. 339-44.

143. Nagaoka T, Kitaya N, Sugawara R, Yokota H, et al. Alteration of choroidal circulation in the foveal region in patients with type 2 diabetes. Br J Ophthalmol. 2004 Aug; 88(8): p. 1060-3.

144. Fryczkowski A, Hodes B, Walker J. Diabetic choroidal and iris vasculature scanning electron microscopy findings. Int Ophthalmol. 1989 Jul; 13(4): p. 269-79.

145. Cao J, McLeod S, Merges C, Lutty G. Choriocapillaris degeneration and related pathologic changes in human diabetic eyes. Arch Ophthalmol. 1998 May; 116(5): p. 589-97.

146. Esmaeelpour M, Považay B, Hermann B, Hofer B, et al. Mapping choroidal and retinal thickness variation in type 2 diabetes using three-dimensional 1060-nm optical coherence tomography. Invest Ophthalmol Vis Sci. 2011 Jul; 52(8): p. 5311-6.

147. Esmaeelpour M, Brunner S, Ansari-Shahrezaei S, Nemetz S, et al. Choroidal thinning in diabetes type 1 detected by 3-dimensional 1060 nm optical coherence tomography. Invest Ophthalmol Vis Sci. 2012 Oct; 53(11): p. 6803-9.

148. Querques G, Lattanzio R, Querques L, Del Turco C, et al. Enhanced depth imaging optical coherence tomography in type 2 diabetes. Invest Ophthalmol Vis Sci. 2012 Sep; 53(10): p. 6017-24.

149. Vujosevic S, Martini F, Cavarzeran F, Pilotto E, Midena E. Macular and peripapillary choroidal thickness in diabetic patients. Retina. 2012; 32(9): p. 1781-90.

150. Michalewski J, Michalewska Z, Nawrocka Z, Bednarski M, Nawrocki J. Correlation of choroidal thickness and volume measurements with axial length and age using swept source optical coherence tomography and optical low-coherence reflectometry. Biomed Res Int. 2014; 2014: p. 639160.

151. Margolis R, Spaide R. A pilot study of enhanced depth imaging optical coherence tomography of the choroid in normal eyes. Am J Ophthalmol. 2009 May; 147(5): p. 811-5.

152. Wakatsuki Y, Shinojima A, Kawamura A, Yuzawa M. Correlation of Aging and Segmental Choroidal Thickness Measurement using Swept Source Optical Coherence Tomography in Healthy Eyes. PLoS One. 2015 Dec; 10(12): p. e0144156.

153. Gupta P, Thakku S, Sabanayagam C, Tan G, et al. Characterisation of choroidal morphological and vascular features in diabetes and diabetic retinopathy. Br J Ophthalmol. 2017 Aug; 101(8): p. 1038-1044.

154. Tan K, Laude A, Yip V, Loo E, et al. Choroidal vascularity index - a novel optical coherence tomography parameter for disease monitoring in diabetes mellitus? Acta Ophthalmol. 2016 Nov; 94(7): p. e612-e616.

155. Yilmaz I, Ozkaya A, Kocamaz M, Ahmet S, et al. Correlation of choroidal thickness and body mass index. Retina. 2015 Oct; 35(10): p. 2085-90.

156. Boillot A, Zoungas S, Mitchell P, Klein R, et al. Obesity and the microvasculature: a systematic review and meta-analysis. PLoS One. 2013; 8(2): p. e52708.

157. Shankar A, Sabanayagam C, Klein B, Klein R. Retinal microvascular changes and the risk of developing obesity: population-based cohort study. Microcirculation. 2011 Nov; 18(8): p. 655-62.

158. Erşan I, Battal F, Aylanç H, Kara S, et al. Noninvasive assessment of the retina and the choroid using enhanced-depth imaging optical coherence tomography shows microvascular impairments in childhood obesity. J AAPOS. 2016 Feb; 20(1): p. 58-62.

159. Iantorno M, Campia U, Di Daniele N, Nistico S, et al. Gut hormones and endothelial dysfunction in patients with obesity and diabetes. Int J Immunopathol Pharmacol. 2014 Jul-Sep; 27(3): p. 433-6.

160. Baretella O, Chung S, Barton M, Xu A, Vanhoutte P. Obesity and heterozygous endothelial overexpression of prepro-endothelin-1 modulate responsiveness of mouse main and segmental renal arteries to vasoconstrictor agents. Life Sci. 2014 Nov; 118(2): p. 206-12.

161. Kamide K. Role of renin-angiotensin-aldosterone system in metabolic syndrome and obesity-related hypertension. Curr Hypertens Rev. 2014 Aug.

162. Yu J, Jiang C, Wang X, Zhu L, et al. Macular perfusion in healthy Chinese: an optical coherence tomography angiogram study. Invest Ophthalmol Vis Sci. 2015 May; 56(5): p. 3212-7.

11. APPENDIX

11.1. Agreement of the Ethical Committee

UNIWERSYTET MEDYCZNY IM. KAROLA MARCINKOWSKIEGO W POZNANIU

KOMISJA BIOETYCZNA PRZY UNIWERSYTECIE MEDYCZNYM
IM. KAROLA MARCINKOWSKIEGO W POZNANIU

Collegium Maius
ul. Fredry 10
61-701Poznań

tel. (+48 61) 854 62 51, 854 60 60
fax. (+48 61) 854 61 07
www.bioetyka.ump.edu.pl

Uchwała nr 303/16

Na podstawie przepisów Ustawy z dnia 5 grudnia 1996 r. o zawodach lekarza i lekarza dentysty (Dz. U. 2011, Nr 277, poz. 1634 z późn. zm.); Rozporządzenia Ministra Zdrowia i Opieki Społecznej z dnia 11 maja 1999r. w sprawie szczegółowych zasad powoływania i finansowania oraz trybu działania komisji bioetycznych (Dz. U. Nr 47, poz.480); Ustawy z dnia 6 września 2001r. Prawo farmaceutyczne (Dz. U. 2008 Nr 45, poz. 271 z późn. zm.); Rozporządzenia Ministra Finansów z dnia 30 kwietnia 2004r. w sprawie obowiązkowego ubezpieczenia odpowiedzialności cywilnej badacza i sponsora (Dz. U. 2004 nr 101, poz. 1034 z późn. zm.); Rozporządzenia Ministra Finansów z dnia 18 maja 2005r. zmieniające rozporządzenie w sprawie obowiązkowego ubezpieczenia odpowiedzialności cywilnej badacza i sponsora (Dz. U. Nr 101, poz. 845); Rozporządzenia Ministra Zdrowia z dnia 30 kwietnia 2004r. w sprawie sposobu prowadzenia badań klinicznych z udziałem małoletnich (Dz. U. 2004 Nr 104, poz. 1108); Rozporządzenia Ministra Zdrowia z dnia 30 kwietnia 2004r. w sprawie zgłaszania niespodziewanego ciężkiego niepożądanego działania produktu leczniczego (Dz. U. Nr 104, poz. 1107); Rozporządzenie Ministra Zdrowia z dnia 15 listopada 2010 r. w sprawie wzorów wniosków przedkładanych w związku z badaniem klinicznym, wysokości opłat za złożenie wniosków oraz sprawozdania końcowego z wykonania badania klinicznego (Dz. U. 2010r. nr 222 poz. 1453, z późn. zm.); Ustawy z dnia 20 maja 2010 r. o wyrobach medycznych (Dz. U. 2010r. nr 107 poz. 679, z późn. zm.); Rozporządzenie Ministra Finansów z dnia 6 października 2010 r. w sprawie obowiązkowego ubezpieczenia odpowiedzialności cywilnej sponsora i badacza klinicznego w związku z prowadzeniem badania klinicznego wyrobów (Dz. U. 2010, Nr 194 poz. 1290);Ustawa z dnia 18 marca 2011 r. o Urzędzie Rejestracji Produktów Leczniczych, Wyrobów Medycznych i Produktów Biobójczych (Dz.U. 2011 nr 82 poz. 451);Rozporządzenie Ministra Zdrowia z dnia 2 maja 2012r. w sprawie Dobrej Praktyki Klinicznej (Dz. U. 2012, poz. 489);Rozporządzenie Ministra Zdrowia z dnia 2 maja 2012r. w sprawie wzorów dokumentów przedkładanych w związku z badaniem klinicznym produktu leczniczego oraz w sprawie wysokości i sposobu uiszczania opłat za złożenie wniosku o rozpoczęcie badania klinicznego (Dz. U. 2012, Nr 0 poz. 491); w oparciu o Deklarację Helsińską - Zasady Etycznego Postępowania w Eksperymencie Medycznym z Udziałem Ludzi oraz przepisy ICH GCP.

Komisja Bioetyczna, na posiedzeniu w dniu **03 marca 2016 r.**

rozpatrzyła wniosek dotyczący prowadzenia badań naukowych.

Kierownik projektu:
dr hab. n. med. Marcin Stopa

Miejsce prowadzenia badań:
Katedra Optometrii i Biologii Układu Wzrokowego
Uniwersytetu Medycznego w Poznaniu

Główny badacz: **lek. med. Magdalena Niestrata-Ortiz**
Członkowie zespołu badawczego: **dr hab. n. med. Marcin Stopa**
prof. dr hab. med. Krystyna Pecold

Temat badań:
„Ocena patologicznych zmian siatkówki i jej naczyń w przebiegu cukrzycy typu I u dzieci za pomocą angiografii optycznej koherentnej tomografii".

Komisja wydała uchwałę o pozytywnym zaopiniowaniu tego wniosku

Przewodniczący Komisji
prof. dr hab. med. Paweł Chęciński